Intersection Graphs of Pseudosegments

vorgelegt von
Dipl.-Math. Cornelia Dangelmayr
aus Reutlingen

vom Fachbereich Mathematik und Informatik
der Freien Universität Berlin
zur Erlangung des akademischen Grades

Doktor der Naturwissenschaften
– Dr. rer. nat. –

genehmigte Dissertation

Berichterstatter: Prof. Dr. Martin Aigner
Prof. Dr. Stefan Felsner

Tag der wissenschaftlichen Aussprache
15. Januar 2010

Berlin 2010

Contents

Chapter 1

Introduction

In this thesis we consider intersection graphs of Jordan curves in the Euclidean plane, for short *string graphs*. String graphs were introduced in 1966 by Sinden [63] in connection with electrical networks. Independently, in 1976, Ehrlich et al. [20] investigated string graphs from a theoretical point of view. They observed that the graph resulting from subdividing each edge of the complete graph on five vertices is not a string graph. Furthermore, they proved that intersection graphs of straight line segments, known as *segment graphs*, form a proper subset of string graphs, and they investigated the complexity of the k-colorability problem of segment graphs. Since then, string graphs and segment graphs have been widely studied, both, for practical and theoretical reasons.

The starting point of our investigations on string and segment graphs was the following conjecture stated by Scheinerman in 1984:

Conjecture 1.1. ([61]) Every planar graph is a segment graph.

This conjecture was strengthened by a conjecture of West from 1991 stated next:

Conjecture 1.2. ([68]) Every planar graph has a segment representation where the segments are of at most four directions.

Conjecture 1.1 was confirmed in 2009 by Chalopin and Gonçalves [8]. Before, many interesting results for subclasses of planar graphs [13, 14, 15, 39] had been found and, in this context, intersection graphs of *pseudosegments*, for short *pseudosegment graphs*, had gained further interest [9]. The notion of a set of pseudosegments is similar to the notion of an *arrangement of pseudolines*; the latter was introduced in 1926 by Levi [48] as a generalization of *arrangements of straight lines*. In 1956, Ringel showed that there are simple arrangements of pseudolines that are not isomorphic to arrangements of straight lines [56]. This at hand, Kratochvil and Matoušek [47] showed that there are pseudosegment graphs which are not segment graphs.

Motivated by Conjecture 1.1 and 1.2, and by the natural connection of pseudosegment graphs with pseudoline arrangements, we investigated graph-theoretic properties of pseudosegment graphs. All graphs considered are finite.

First, we give a short outline of the contents of this thesis. This is followed by two introductory chapters which conclude in a detailed overview of our results. Then we present our investigations on pseudosegment graphs.

1.1 Outline

In Chapter 2 we give the basic definitions and concepts needed to introduce the field of intersection graph theory in Chapter 3. In this context, we present string graphs and implicit subclasses of string graphs, in particular pseudosegment and segment graphs. Then we consider further subclasses of string graph as *planar*, *chordal* and *cocomparability graphs*. These graphs are then analyzed in view of pseudosegment, and sometimes even segment representations. Take into account that every pseudosegment graph has a pseudosegment representation that consists of polygonal arcs as every such representation constitutes a plane graph.

In Chapter 4 we consider planar graphs and segment graphs. Section 4.1 contains our contribution to Conjecture 1.2. Together with Bodirsky and Kára we show that every *series-parallel graph*- a graph that does not contain a subdivision of K_4- has a segment representation with segments of at most three directions [4].

In Subsection 4.3 we use the dual graph of a pseudoline arrangement to construct a pseudosegment graph that is a segment graph if and only if the chosen pseudoline arrangement is isomorphic to a straight line arrangement.

In Chapter 5 we consider chordal graphs in view of pseudosegment representations, and show in Section 5.1 that every *path graph* is a pseudosegment graph.

In Section 5.2 and 5.4 we present two families of chordal graphs that are not pseudosegment graphs. At this we use a planarity argument in the first case, and in the second case we apply a Ramsey argument. These graphs show, in addition, that chordal graphs that are pseudosegment graphs are not induced by many "treelike" subtrees.

The proof of the first case makes use of a partition of a pseudosegment representation into an arrangement of pseudosegments and a certain set of disjoint Jordan arcs. The crucial argument then results from an upper bound on the size of the latter set depending on the size of the arrangement.

This leads to further investigations on Jordan arcs, namely on k-*segments*, contained in arrangements of pseudosegments and pseudolines. These include an upper bound on the number of k-segments and on the number of edges in the $(\leq k)$-*zone* of a pseudoline in a pseudoline arrangement.

The results of Chapter 5 are joint work with Felsner and Trotter, and can also be found in [11] and [12].

Finally, in Chapter 6, we determine cocomparability graphs that are pseudosegment graphs. Among these are *interval graphs*, *point-interval graphs* and two further subclasses of *trapezoid graphs*.

Danksagung

Im Rahmen meiner Doktorarbeit habe ich vielseitig Unterstützung erfahren, für die ich mich aufrichtig bedanken möchte.

Zu allererst gilt mein Dank Prof. Dr. Martin Aigner, der mich in die mathematische Welt der Berliner Universitäten eingeführt, sich auf meine Interessen eingelassen und mir die Möglichkeit gegeben hat, meiner Forschung nachzugehen und diese Dissertation auszuarbeiten. Durch seine Unterstützung und auch durch die Einbindung in die Graduiertenkollegien „Combinatorics, Geometry and Computation“ und „Methods for Discrete Structures“ der Berliner Universitäten hat meine Arbeit wichtige Impulse und Weichenstellungen erhalten.

Während der letzten fünf Jahre war ich Mitglied der Arbeitsgruppe „Diskrete Mathematik“ des Mathematischen Instituts der FU Berlin. Hier am Institut konnte ich in menschlich angenehmer Umgebung arbeiten, viele anregende Angebote nutzen und hatte die Möglichkeit, an für mich und meine Arbeit relevanten Schulen und Konferenzen teilzunehmen. Bei allen, die hierzu beigetragen haben, insbesondere Prof. Dr. Ralph-Hardo Schulz, möchte ich mich herzlich bedanken.

Prof. Dr. Stefan Felsner hat mich mit den Problemen und Methoden der kombinatorischen Geometrie vertraut gemacht. Sein anhaltendes Interesse an meiner Thematik, sein Verständnis und seine vielfältige Unterstützung haben entscheidend zum Gelingen dieser Arbeit beigetragen; die meisten meiner Ergebnisse sind in Zusammenarbeit mit ihm entstanden. Für all das möchte ich mich ganz besonders bedanken.

Andreas Paffenholz, Axel Werner, Sarah Kappes und Wiebke Höhn haben mir in mancher Hinsicht geholfen, etwa durch Diskussionen, bei formalen Fragen, durch Korrektur lesen, und nicht zuletzt als Freunde: Auch Ihnen vielen Dank.

Während der Zeit meiner Doktorarbeit ist mir meine Familie stets zur Seite gestanden und hat mir den Rücken gestärkt. Diese Erfahrung, sowie das Verständnis und Vertrauen meines Mannes waren und sind für mich von unschätzbarem Wert. Für all das bin ich Ihnen sehr verbunden.
Und auch für die Feierabende, die dank meines Mannes und meines Sohnes die nötige Erholung geboten haben.

Chapter 2

Preliminaries

Combinatorial geometry is a mixture of principles from fields like topology, graph theory, number theory, and other disciplines. Intersection graph theory is an interesting field that is part of this area. The following sections will introduce the basic terms and definitions that are used throughout this thesis. More specific definitions are given where they belong to, in order to keep this chapter succinct and the different chapters coherent.

2.1 Curves in the plane

In the following we present objects like planar curves and segments classically considered in topology and analytic geometry. Our work and investigations on these objects differs considerably from the classical point of view on them as we are mainly interested in the intersection relation within a finite set of certain curves. Thus, we will focus on the notions needed in our context. They are taken mainly from [24, 35, 50].

If not stated differently we consider the Euclidean plane $\mathbb{R}^2$, equipped with a coordinate system and the standard metric; the coordinate axes are denoted by X_1 and X_2.

A *homeomorphism* of the plane is a continuous bijection φ such that the inverse function φ^{-1} is continuous again.

A *planar curve* γ is the image of a continuous function φ from an interval $I \subseteq \mathbb{R}$ to $\mathbb{R}^2$. If φ is injective, then we say that γ is a *Jordan curve*, a *simple curve* or a *string*.

2.1.1 Straight lines (segments) and pseudolines (pseudosegments)

If φ is a linear function from $\mathbb{R}$ to $\mathbb{R}^2$, the image γ of φ is called a *(straight) line*. Recall that two lines are either parallel, that is they are either disjoint or they are the same, or they cross.

If we omit the linearity of φ, we obtain a natural generalization of straight lines. So let $\mathcal{J}$ be a family of Jordan curves which tend to infinity in either direction. If, additionally, every pair of Jordan curves of $\mathcal{J}$ has at most one point of intersection where the two curves cross, then we call $\mathcal{J}$ a *partial arrangement of pseudolines*. If every pair of curves of a partial arrangement $\mathcal{J}$ has a unique crossing point, we call $\mathcal{J}$ an *arrangement of pseudolines* and denote it by $\mathcal{L}$. Note that in general, Jordan curves may intersect differently to straight lines as sketched in Figure 2.1.

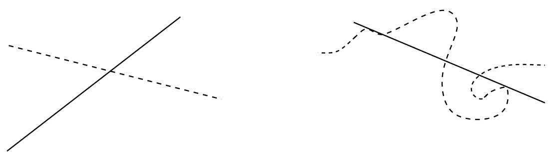

Figure 2.1: On the left-hand side two straight lines cross, and on the right-hand side two Jordan curves cross, touch and overlap.

If $I = [A, B] \subset \mathbb{R}$ and φ is an injective function from $\mathbb{R}$ to $\mathbb{R}^2$, we say that γ is a *Jordan arc* or a *simple arc*. If $\varphi(A) = \varphi(B)$, we say that γ is *closed*, otherwise it is *open*. A fundamental result in topology is the following theorem, known as the *Jordan Curve Theorem*.

Theorem 2.1. ([65]) Every closed Jordan arc partitions the plane into two connected components, one bounded, the other unbounded. □

A *(straight line) segment* is a connected subset of a line that is bounded by two different points of the line. If the points $P, Q \in \mathbb{R}^2$ bound segment s, then P and Q are called *endpoints* of s and we write $s = [P, Q]$.

If l is a line with $s \subset l$, then l is called the *supporting line* of s. We call two segments parallel if their supporting lines are parallel. If two parallel segments share more than an endpoint, they overlap. If two segments intersect in an endpoint of one of them and are disjoint otherwise, they touch. If two non-parallel segments intersect in an interior point of either segment, they cross.

We are interested in a generalization of segments similar to the one of straight lines by pseudolines. So let $\mathcal{J}$ be a family of Jordan arcs such that every pair of Jordan arcs of $\mathcal{J}$ has at most one point of intersection where they cross or touch. Then we call $\mathcal{J}$ a *set of pseudosegments*. If in addition no intersection point of elements of $\mathcal{J}$ is an endpoint of a Jordan arc of $\mathcal{J}$, then we call $\mathcal{J}$ a *partial arrangement of pseudosegments*. If every pair of Jordan arcs of a partial arrangement $\mathcal{J}$ has a unique crossing point, we call $\mathcal{J}$ an *arrangement of pseudosegments* and denote it by $\mathcal{S}$. Note that every set of pseudosegments can be changed into a partial arrangement without changing the intersection relations by slightly perturbing intersection points.

A *polygonal arc* is a Jordan arc composed of finitely many line segments such that each segment starts at the endpoint of the previous one and no point appears in more than one segment except for common endpoints of consecutive segments. If the endpoints of a polygonal arc are the same, we call the curve a *polygon*. In this case we call the segments the *sides*, and the common points the *corners* of the polygon.

A subset $C \subset \mathbb{R}^2$ is *convex* if for every two points $X, Y \in C$, the whole segment $s = [X, Y]$ is contained in C. The *convex hull* of a subset $C \subset \mathbb{R}^2$, denoted $\mathrm{conv}(C)$, is the intersection of all convex sets in $\mathbb{R}^2$ containing C.

2.1.2 Arrangements in the Euclidean plane

An arrangement of pseudolines (pseudosegments) is called *simple* if no three pseudolines (pseudosegments) have a point in common.

An arrangement of pseudolines (pseudosegments) partitions the plane into *cells* of dimension 0, 1 and 2. The intersection points of the pseudolines (pseudosegments) are the 0-dimensional cells, they are called *vertices* of the arrangement. The maximal connected components of the pseudolines (pseudosegments) obtained from removing the vertices from the plane are the 1-dimensional cells and are called the *edges* of the arrangement. The maximal connected components of the plane obtained from removing the arrangement from the plane are the 2-dimensional cells, called the *faces* of the arrangement. This cell decomposition is called the *induced cell complex*. Note that the edges and faces of a pseudoline arrangement are either bounded or unbounded.

Given an arrangement, we say that a vertex (edge) is *adjacent* to an edge respectively a face (to a face) if the vertex lies on the boundary of the edge, respectively the face (of the face). Then $\bar{f}$ denotes the union of f and all vertices and edges adjacent to f, in other words, the *closure* of f. We say that an edge of an arrangement is *adjacent* to a pseudoline (pseudosegment) of the arrangement if it is adjacent to a vertex of the pseudoline (pseudosegment).

A *k-segment* of an arrangement $\mathcal{L}$ of pseudolines (pseudosegments) is a Jordan arc that crosses exactly k different edges of $\mathcal{L}$ such that no two of these edges belong to the same pseudoline (pseudosegment) of $\mathcal{L}$ and no edge of $\mathcal{L}$ is intersected more than once. Two k-segments p and p' are *(combinatorially) equivalent* if p and p' intersect the same set of edges of the arrangement in the same order or in reversed orders. A set of different k-segments of an arrangement is *contained* in the arrangement.

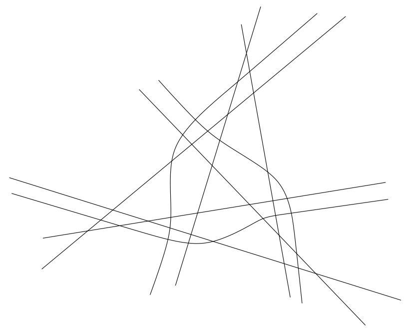

Figure 2.2: An arrangement of pseudosegments that is not isomorphic to an arrangement of straight lines.

Two arrangements of pseudolines (pseudosegments) are *isomorphic* if and only if there is an incidence and dimension preserving isomorphism between the induced cell complexes. If an arrangement of pseudolines (pseudosegments) is isomorphic to an arrangement of straight lines (straight line segments), then we call this arrangement *stretchable*. Figure 2.2 gives an example of a nonstretchable arrangement of nine pseudolines [37].

For $n \in \mathbb{N}$ let $\mathcal{L}_n$ ($\mathcal{S}_n$) be an arrangement of n pseudolines (pseudosegments). Let f be an unbounded face of $\mathcal{L}_n$ and denote the unbounded face of $\mathcal{L}_n$ that is separated from f by all pseudolines of $\mathcal{L}_n$ as the *antipodal face* $\bar{f}$ of f. The pair $(\mathcal{L}_n, f)$ is then called a *marked arrangement*. A *sweep* of $(\mathcal{L}_n, f)$ is a sequence of arcs $c_0, c_1, ..., c_r$ such that each arc has the same endpoints $X \in f$ and $\bar{X} \in \bar{f}$ and the following holds:

- None of the arcs contains a vertex of $\mathcal{L}_n$.
- Each arc has exactly one point of intersection with each line $p \in \mathcal{L}_n$.
- Any two arcs c_i, c_j are interiorly disjoint.
- For any two consecutive arcs c_i, c_{i+1} of the sequence there is exactly one vertex of $\mathcal{L}_n$ between them, that is in the interior of the closed arc $c_i \cup c_{i+1}$.
- Every vertex of the arrangement lies between a unique pair of consecutive arcs, hence, the interior of the closed arc $c_0 \cup c_r$ contains all vertices of $\mathcal{L}_n$.

In [34] it is shown, that every pseudoline arrangement is isomorphic to a *wiring diagram*, that is an arrangement of piecewise linear curves, of so called *wires*. To see this, take a sweep of $\mathcal{L}_n$ and label the pseudolines of $\mathcal{L}_n$ from $1, ..., n$ according to the order in which c_0 intersects them between f and $\bar{f}$. Then, at $x_1 = 0$, we start drawing n parallel horizontal lines labeled $1, ..., n$ from above to below. For $i \in \{1, ..., r\}$, we twist lines j, k at $x_1 = i$ if the vertex defined by the intersection of pseudolines j and k lies within the interior of $c_{i-1} \cup c_i$. The resulting set of polygonal arcs is a representation of $\mathcal{L}_n$ as wiring diagram.

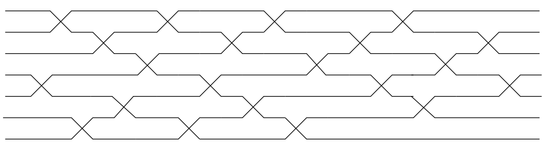

Figure 2.3: A wiring diagram is a pseudoline arrangement that consists of polygonal arcs called "wires" [35].

Let $\mathcal{L}$ be an arrangement of pseudolines and $p \in \mathcal{L}$ be a pseudoline of $\mathcal{L}$. The *zone* $Z(p)$ of p in $\mathcal{L}$ is the set of vertices, edges and faces of $\mathcal{L}$ that are not separated from p by any pseudoline $q \in \mathcal{L}$. In other words, an edge of $\mathcal{L}$ belongs to the zone $Z(p)$ of p in $\mathcal{L}$ if there is a 2-segment of $\mathcal{L}$ that intersects this edge and an edge of p. Then a vertex (face) of $\mathcal{L}$ belongs to $Z(p)$ if the vertex (face) is adjacent to an edge of $Z(p)$.

The *complexity* of the zone $Z(p)$ is the number of vertices, edges and faces of $Z(p)$. A famous result of combinatorial geometry is a linear upper bound on the complexity of the zone of an arbitrary line in a straight line arrangement.

Theorem 2.2. ([1]) The complexity of the zone of a straight line in an arrangement of n straight lines in the plane is bounded by $6(n-1) \in O(n)$. □

2.2 Partially ordered sets

The following definitions are taken mainly from [23]. The set X considered in the sequel is a finite set.

A *(strict) partial ordering* $<$ on a (finite) set X is a binary relation such that

- $x \not< x$, that is $<$ is irreflexive, and
- if $x < y$ and $y < z$, then $x < z$, that is $<$ is transitive.

Then, we call $P = (X, <)$ a *partially ordered set* or *poset*, and X the *ground set* of P. Furthermore, we say that $x, y \in X$ are *comparable* in P if $x < y$ or $y < x$; otherwise x and y are *incomparable* in P. A set of pairwise comparable elements of X is called a *chain* of P.

A poset $P = (X, <)$ is a *linear order* if for every two elements $x, y \in X$ it holds that either $x < y$ or $y < x$ in P. Then there exists a function φ that assigns each element of X to a point on the real line such that $x < y$ in P if and only if $\varphi(x) < \varphi(y)$ in $\mathbb{R}$.

A poset $P = (X, <)$ is an *interval order* if there is a function φ assigning each point $x \in X$ to a closed interval $I_x = [l_x, r_x]$ of the real line so that $x < y$ in P if and only if $r_x < l_y$ in $\mathbb{R}$.

Now let $P = (X, <_P)$ and $Q = (X, <_Q)$ be partial orders on the same ground set X. We call Q an *extension* of P if for all $x, y \in X$ with $x <_P y$, we have $x <_Q y$ as well. If Q is a linear order, then Q is called a *linear extension* of P. If Q is an interval order, then Q is called an *interval extension* of P.

We say that a family of linear extensions (interval extensions) $\{Q_1, ..Q_t\}$ of P is a *realizer* (an *interval realizer*) of P if $<_P = <_{Q_1} \cap .. \cap <_{Q_t}$. The *dimension* $\dim(P)$ (the *interval dimension* $\mathrm{idim}(P)$) of $(X, <_P)$ is defined as the least positive integer t for which there exists a family of t linear extensions (of t interval extensions) of P that is a realizer (an interval realizer) of P.

2.3 Graphs

The present section is supposed to provide the basic graph theoretic definitions and concepts used in the following chapters. From the many books about graph theory we have chosen [2, 16, 53, 69] as references. Note that we only consider finite sets

A *graph* $G = (V(G), E(G))$ consists of a non-empty *vertex set* $V(G)$, an *edge set* $E(G)$ and a relation that associates with each edge two vertices called *endpoints* of the edge. A graph is *finite* if its vertex and edge set are finite.

A *loop* is an edge whose endpoints are equal. *Multiple edges* are edges having the same pair of endpoints. A graph without loops or multiple edges is called *simple*. In this case $E(G)$ can be considered as a set of unordered pairs of $V(G)$, that is $E(G) \subseteq \binom{V(G)}{2}$.

If not stated differently, the graphs considered from now on are simple and finite. Note that we sometimes write $G = (V, E)$ instead of $G = (V(G), E(G))$.

An edge $e \in E(G)$ with endpoints $u, v \in V(G)$ is denoted $e = uv$ or $e = \{u, v\}$ and u and v are called *incident* to edge uv. In addition, we say that u and v are *adjacent* and call them *neighbors*. For every vertex $u \in V(G)$ we denote the set of neighbors of u in G by $N_G(u)$. With this we define the *degree* of u in G as $d_G(u) := |N_G(u)|$.

The *complement* $\bar{G}$ of G is the simple graph with vertex set $V(\bar{G}) = V(G)$ and edge set $E(\bar{G}) = \binom{V(G)}{2} \setminus E(G)$.

Let G and H be two graphs. An *isomorphism from G to H* is a bijection φ from $V(G)$ to $V(H)$ such that $uv \in E(G)$ if and only if $\varphi(u)\varphi(v) \in E(H)$. Then we say that G is *isomorphic* to H, denoted as $G \cong H$.

2.3.1 Basic concepts

Let G and H be two graphs. Then H is a *subgraph* of G if $V(H) \subseteq V(G)$ and $E(H) \subseteq E(G) \cap \binom{V(H)}{2}$. A subgraph H of G is called an *induced* subgraph of G if $E(H) = E(G) \cap \binom{V(H)}{2}$. A subgraph H of G is called a *spanning* subgraph of G if $V(H) = V(G)$.

The subgraph obtained from G by deleting edge e (vertex v) or a set of edges M (vertices S) of G is denoted as $G - e$ ($G - v$) and $G - M$ ($G - S$) respectively.

If H is a subgraph of G or is isomorphic to a subgraph of G, then we say that H is *contained* in G. Graph G is called H*-free* if it does not contain a subgraph isomorphic to H.

An *independent* in a graph G is a set of pairwise nonadjacent vertices of G, a *clique* a set of pairwise adjacent vertices. If all vertices of G are pairwise adjacent, G is called a *complete graph*. A complete graph on n vertices is denoted by K_n.

We say that a graph G is *bipartite* if $V(G)$ is the union of two disjoint (possibly empty) sets that induce independent sets of G; they are called the *partite sets* of G. A bipartite graph is a *complete bipartite graph*, if every vertex of one partite set is adjacent to every vertex of the other partite set. If the partite sets consist of n and m vertices, we denote the respective complete bipartite graph by $K_{n,m}$.

A k*-coloring* of a graph G is a labeling $\varphi : V(G) \to S$, where $|S| = k$. The labels are the *colors*, the vertices of one color form a *color class*. A k-coloring is *proper* if adjacent vertices have different colors. A graph is k*-colorable* if it has a proper k-coloring. The *chromatic number* $\chi(G)$ is the least k such that G is k-colorable. A natural lower bound of the chromatic number of a graph G is the maximal size of a clique contained in G, that is the *clique number* $\omega(G)$.

A *path* is a graph whose vertices can be ordered such that two vertices are adjacent if they are consecutive in the ordering. If P is a path and $(v_1, v_2, .., v_n)$ the ordered set of vertices of P, we say that P is a v_1v_n*-path* that connects v_1 and v_n, denoted by $P(v_1, v_n)$. Two paths $P(v_1, v_n)$ and $P(u_1, u_m)$ are called *independent* or *internally disjoint* if $P(v_1, v_n)$ does not contain a vertex of $\{u_2, ..., u_{m-1}\}$ and $P(u_1, u_m)$ does not contain a vertex of $\{v_2, ..., v_{n-1}\}$.

If we add edge v_nv_1 to $P(v_1, v_n)$ we obtain a *cycle* C. More precisely, a *cycle* is a graph whose vertices can be placed around a circle so that two vertices are adjacent if they appear consecutively along the circle. Similar to paths, we often denote a cycle by the cyclic sequence of its vertices, for example $(v_1, ..., v_n, v_1)$. In this case, C is also called an n*-cycle*, denoted C_n. A graph that does not contain a cycle is called *acyclic*. A graph that does not contain a 3-cycle is sometimes called triangle-free.

A graph G is *connected* if it contains an u, v-path for every pair u, v of vertices of G. The *connectivity* of G, written $\kappa(G)$, is the minimum size of a vertex set S such that $G - S$ is disconnected or has only one vertex. We say that a graph is *k-connected* if its connectivity is at least k.

Theorem 2.3. A graph G is k-connected if and only if for every two vertices u, v of G there are k different, pairwise internally disjoint u, v-paths in G. □

A *maximal connected subgraph* of G, for short a *component* of G, is a subgraph of G that is not contained in any other connected subgraph of G.

A *separating set* or *vertex cut* of a graph G is a set $S \subset V(G)$ such that $G - S$ has at least one component more than G. A *cut-vertex* is a separating set that consists of exactly one vertex. A maximal connected subgraph H of G that has no cut-vertex of H is a *block*. If G itself is connected and has no cut-vertex, then G is a block.

A *tree* is a connected acyclic graph, a *forest* a graph whose maximal connected components are trees. A vertex of a tree T that has degree one is called a *leaf* of T.

A *caterpillar* is a tree in which a single path, called the *spine*, is incident to every edge. Then, the vertices of the caterpillar that are not on the spine are exactly the leaves of the caterpillar.

The *distance* $d_G(u, v)$ of two vertices u, v of a graph $G = (V(G), E(G))$ is the least length of a path of G connecting u and v. The *diameter* $\operatorname{diam}(G)$ of G is defined as $\max\{d_G(u, v) \mid u, v \in V(G)\}$.

2.3.2 Planar graphs

A *drawing* of a graph G is a function φ defined on $V(G) \cup E(G)$ that assigns each vertex $v \in V(G)$ to a point $\varphi(v)$ in the plane such that the images $\varphi(u)$ and $\varphi(v)$ of different vertices $u, v \in V(G)$ are distinct, and each edge $e = uv \in E(G)$ to a Jordan arc with endpoints $\varphi(u)$ and $\varphi(v)$. A drawing is a *straight line drawing* if every Jordan arc representing an edge is a straight line segment.

A common point of $\varphi(e)$ and $\varphi(e')$ of different edges e and e', that is no endpoint, is called a crossing. A graph is *planar* if it has a drawing without crossings. A drawing φ without crossings is called a *planar embedding* of the respective graph.

Lemma 2.4. If G is a planar graph, then G has a planar embedding such that all edges are polygonal arcs.

A *plane graph* $H = (G, \varphi)$ is a particular planar embedding φ of a planar graph G. The vertices of H are the images of the vertices of G, that is points in the plane. The edges of H are the images of the edges of G. As a consequence of Lemma 2.4, we can always choose these as polygonal arcs.

The maximal connected components of the plane obtained from removing the embedding H from the plane are called *faces* $F(H)$ of H.

In addition to the vertex-edge-incidence in a graph, we say that a vertex (an edge) of a plane graph H is *incident* to face of H if the vertex (edge) lies on the boundary of the face. Then we say that two plane graphs H and H' are *(combinatorially) isomorphic* if there are isomorphisms $\varphi_V : V(H) \to V(H')$, $\varphi_E : E(H) \to E(H')$ and $\varphi_F : F(H) \to F(H')$ preserving the vertex-edge-, vertex-face- and edge-face-incidences.

Every plane graph is related to a particular, not necessarily simple, plane graph, its *dual graph*. If G is an arbitrary plane graph, the *dual graph* G^* of G is the plane graph whose vertices correspond to the faces of G. The edges of G^* correspond to the edges of G as follows: if e is an edge of G incident to faces f and f' of G, then the endpoints of the *dual edge* $e^* \in E(G^*)$ are the elements $f, f' \in V(G^*)$. Note that $(G^*)^* = G$ if and only if G is connected.

The definition of the dual graph involves a *natural (planar) embedding* of G^* into G. Here each vertex $f \in V(G^*)$ is assigned to a point of the interior of the face it represents and each edge $e^* = ff' \in E(G^*)$ to a polygonal arc with endpoints f and f'. Each such arc can be chosen such that it intersects the edge of G it is dual to at most once and is disjoint from any other vertex or edge of G.

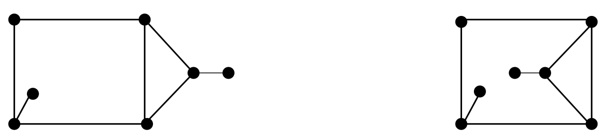

Figure 2.4: Two planar embeddings of a planar graph with nonisomorphic dual graphs.

In general, a planar graph can have planar drawings with combinatorially nonisomorphic dual graphs. The following result of Whitney shows that this is not the case if G is 3-connected.

Theorem 2.5. A planar graph G has a unique dual graph if and only if G is 3-connected. Moreover the dual graph is a simple graph in this case. $\square$

A *subdivision* of an edge uv of a graph G is the operation of replacing uv in G by the path (u, w, v) with a new vertex w. We say that G is a *subdivision* of H if G can be obtained from H by successive subdivisions of edges. We say that G is the *complete subdivision* of H if G is obtained from H by subdividing each edge of H exactly once.

Theorem 2.6. A graph is planar if and only if it does not contain a subdivision of K_5 or $K_{3,3}$. $\square$

The relation between the numbers of vertices, edges and faces of a planar graph are is given by *Euler's Formula*, stated next.

Theorem 2.7. If a plane graph has exactly n vertices, e edges and f faces, then $n - e + f = 2$. $\square$

If a plane graph has exactly n vertices, e edges, f faces and consists of k components, then Euler's Formula can be generalized to $n - e + f = k + 1$.

A *maximal planar graph* is a simple planar graph that is not a spanning subgraph of another planar graph. A *triangulation* is a simple plane graph where every face boundary is a 3-cycle. A triangulation is 4-connected if it does not contain a separating 3-cycle.

As we are dealing with finite graphs, every plane graph has one unbounded face, called the *outer face*. With respect to this we sometimes refer to the vertices and edges that lie on the boundary of the outer face as *outer vertices* and *outer edges*. Accordingly the vertices and edges that do not lie on the boundary of the outer face are called *inner vertices* and *inner edges*. Then a graph is *outerplanar* if it has an embedding where every vertex is an outer vertex. An *outerplane graph* is an embedding of an outerplanar graph where all vertices lie on the outer face.

2.3.3 Chordal graphs

A *chord* of a path or a cycle is an edge between non-consecutive vertices of the path or the cycle respectively. A graph is *chordal* if it does not contain any induced subgraph that is an n-cycle with $n \geq 4$.

Chordal graphs can be characterized differently by *perfect elimination orderings*. To define this term let $G = (V(G), E(G))$ be a graph and let $\sigma = [v_1, ..., v_n]$ be an ordering of the vertices $V(G)$. We call a vertex v_i of G *simplicial* if the subgraph induced by $N_G(v_i)$ is a clique. We denote the subgraph of G that is induced by the vertices $\{v_i, ..., v_n\}$ by G_i. Then σ is called a *perfect elimination ordering* of G if v_i is a simplicial vertex in G_i for all $i \in \{1, ..., n\}$.

Theorem 2.8 ([26])**.** A graph is chordal if and only if it has a perfect elimination ordering. □

2.3.4 Comparability graphs

A *directed graph* or *digraph* D is a triple consisting of a vertex set $V(D)$, an edge set $E(D)$ and a function assigning each edge to an ordered pair of vertices. Note that in the case of digraphs we allow multiple edges. Often, an edge (u, v) of a digraph is called an *arc* from u to v.

An *orientation* of a graph G is a digraph D obtained from G by choosing an orientation (x, y) or (y, x) for each edge $xy \in E(G)$. An *oriented graph* is an orientation of a simple graph. A *transitive orientation* of a graph G is an orientation D such that whenever (x, y) and (y, z) are arcs of D, there is also an edge xz in G such that (x, z) is an arc of D.

Any poset $P = (X, <)$ naturally induces a *comparability graph* G. Here, G has X as vertex set and an edge for every pair of elements of X that are comparable in P. The complement of G is called the *cocomparability graph* of P.

2.4 COMPLEXITY

This section provides an introduction to algorithms and complexity in order to supply the terms and concepts used here. To this end we will follow the informal outlines given in [40] and [62]. For a more comprehensive and complete treatment of the topic we recommend [27].

2.4.1 Order of growth

Let $T(n)$ be a positive function depending on $n \in \mathbb{N}$. Let $\varphi(n)$ be a further nonnegative function on n.

A function $T(n)$ is *order* $\varphi(n)$, or $T(n)$ is $O(\varphi(n))$, if there exist constants $c > 0$ and $n_0 \geq 0$ such that for all $n \geq n_0$ it holds that $T(n) \leq c \cdot \varphi(n)$. In this case we say that $T(n)$ is asymptotically upper bounded by $\varphi(n)$.

We say that $T(n)$ is $\Omega(\varphi(n))$ if there exist constants $c > 0$ and $n_0 \geq 0$ such that for all $n \geq n_0$ it holds that $T(n) \geq c \cdot \varphi(n)$. Then we say that $T(n)$ is asymptotically lower bounded by $\varphi(n)$.

If $\varphi(n)$ is the "right" bound for $T(n)$, that is $T(n)$ is $O(\varphi(n))$ and $T(n)$ is $\Omega(\varphi(n))$, then we say that $T(n)$ is $\theta(\varphi(n))$.

We say that $T(n)$ is $o(\varphi(n))$ if for all $c > 0$ there exists a constant $n_0 \geq 0$ such that for all $n \geq n_0$ it holds that $T(n) \leq c \cdot \varphi(n)$.

2.4.2 Algorithms and computational problems

A *computational problem* can be viewed as an (infinite) collection of instances together with a set of solutions for every instance. Classical examples are *decision problems* and *optimization problems*. Here a decision problem is a question in some formal system with a yes-or-no answer that depends on the values of some input parameters. An optimization problem asks for the "best possible" solution among the set of all feasible solutions. It can be easily transformed to a decision problem.

An *algorithm* can be seen as a finite set of instructions that perform operations on certain data. These include elementary arithmetic operations like addition, multiplication, and comparison, and others derived from these. An algorithm is designed to solve a certain computational problem. The *input* of the algorithm are the instances of the problem and give the initial data. When the algorithm stops, the *output* will be found in prescribed locations of the data set.

The data may consist of numbers, letters and other symbols and is usually stored as a finite string of 0's and 1's. The size of the data is the total length of the respective strings. While the set of instructions constituting the algorithm is finite and fixed, the size of the data set may vary and will depend on the size of the input.

Algorithms are analyzed and evaluated by the amount of time and space they use depending on the input size n. To do so one assumes that an elementary operation takes constant time. Then the *running time* of an algorithm is the maximal number of elementary operations that are performed to solve a certain computational problem using the algorithm for any instance.

2.4.3 P and NP

A *polynomial-time algorithm* is an algorithm whose running time is bounded by a polynomial in the input size n; in other words there is a $k \in \mathbb{N}$ and a polynomial n^k such that the algorithm solves every instance of the problem in $O(n^k)$ time. We say that a problem is *polynomial-time solvable* or is *solvable in polynomial time*, if it can be solved by a polynomial-time algorithm.

For many computational problems there is no polynomial-time algorithm known, but also no proof that such an algorithm does not exist. This motivates the definition of so called *complexity classes*, consisting of problems that are "comparably difficult".

The collection of all decision problems that are polynomial-time solvable is denoted by *P*. The collection of all decision problems for which each input with positive answer can be confirmed by a polynomial-time algorithm is denoted by *NP*. Trivially P $\subset$ NP.

Two more complexity classes are *NP-hard* and *NP-complete* defined using the following *polynomial reduction*. Given two problems A and B, we say that A is *polynomially reducible* to B if there exists a polynomial-time algorithm which transforms any instance $a \in A$ into an instance $b \in B$, such that the answer to b is yes if and only if the answer to a is yes. Then we say that a decision problem is *NP-hard* if every problem of NP is polynomially reducible to it. A decision problem is called *NP-complete* if it is NP-hard and in NP.

CHAPTER 3

INTERSECTION GRAPHS

The study of intersection graphs was motivated both by theoretical and practical reason. Besides being a necessary and important tool to model real world problems, they provide an interesting graph-theoretic structure enriched by their own specific concepts. Since 1980, when Golumbic wrote his classic book on intersection graphs [31], many researchers have worked in this field, and lately several books have appeared covering more recent research in this area.

In this chapter we will introduce the field of intersection graph theory, give examples like chordal graphs and cocomparability graphs and present intersection graphs of strings. We will name relevant results and address the issue of some computational problems. Finally, being equipped with the necessary terms, we will give a detailed overview of our results.

3.1 BASIC DEFINITIONS AND EXAMPLES

The following definitions are taken mainly from [51]. This book is a good reference for further reading on intersection graph theory and cites many interesting references, also on recent topics. Further definitions and results come from [7, 32] if not stated differently.

Let $\mathcal{F} = \{S_1, ..., S_n\}$ be a family of sets or graphs. The *intersection graph* of $\mathcal{F}$, denoted $\Omega(\mathcal{F})$, is the graph having $\mathcal{F}$ as vertex set with S_i adjacent to S_j if and only if $i \neq j$ and $S_i \cap S_j \neq \emptyset$. The family $\mathcal{F}$ will be referred to as *intersection representation* of $\Omega(\mathcal{F})$. Note that $\mathcal{F}$ is a multiset.

Theorem 3.1. ([49]) Every graph is an intersection graph. $\square$

To illustrate this result, let $G = (V, E)$ be a graph. For every $v \in V$ set

$S_v := \{vw \mid vw \in E\}$. Then G is isomorphic to the intersection graph $\Omega(\mathcal{F})$ with $\mathcal{F} = \{S_v \mid v \in V\}$.

3.1.1 Intersection classes

The topic becomes interesting when we pose restrictions on the graph G and the family $\mathcal{F}$. So let $\mathcal{G}$ be a set of graphs and $\sum$ be a set of sets.

If every graph $G \in \mathcal{G}$ is isomorphic to the intersection graph $\Omega(\mathcal{F})$ of some family $\mathcal{F} \subset \sum$ and, vice versa each intersection graph $\Omega(\mathcal{F})$ of a family $\mathcal{F} \subset \sum$ is isomorphic to some graph $G \in \mathcal{G}$, then we say that $\mathcal{G}$ is *isomorphic* to $\Omega(\sum)$.

If there is a set of sets $\sum$ for a set of graphs $\mathcal{G}$ such that $\mathcal{G}$ is isomorphic to $\Omega(\sum)$ we say that $\mathcal{G}$ is an *intersection class*.

A set $\mathcal{G}$ of graphs is *closed under induced subgraphs* if $G' \in \mathcal{G}$ whenever G' is an induced subgraph of some $G \in \mathcal{G}$. To see that every intersection class is closed under induced subgraphs let $\mathcal{G}$ be an intersection class that is isomorphic to $\Omega(\sum)$ and let $G = (V, E)$ be an element of $\mathcal{G}$. Furthermore let $\mathcal{F} \in \sum$ be a family of sets representing G with $v \in V$ represented by $S_v \in \mathcal{F}$. Then every subgraph $G' \subset G$ induced by $V' \subseteq V$ can be represented by the family $\mathcal{F}' = \{S_w \mid w \in V'\} \subseteq \mathcal{F}$, that is $G' \cong \Omega(\mathcal{F}')$.

3.1.2 Intersection graphs of subgraphs of a graph

The family of sets used to illustrate Theorem 3.1 preludes a special type of intersection graphs, namely *vertex intersection graphs of subgraphs of a graph*.

A well known example are *vertex intersection graphs of subtrees of a tree*, for short *tree graphs*. More precisely, a graph $G = (V(G), E(G))$ is a *tree graph* if there exists a tree $T = (V(T), E(T))$, a set $\mathcal{T}$ of subtrees of T and a mapping φ from $V(G)$ to $\mathcal{T}$ with $\varphi(v) = T_v \in \mathcal{T}$ such that $vw \in E(G)$ whenever $T_v \cap T_w \neq \emptyset$. The pair $(T, \mathcal{T})$ is a *tree representation* of G.

In [28, 66] it is shown that the class of tree graphs is the class of chordal graphs. Another characterization of chordal graphs [26, 64] yields a polynomial-time recognition algorithm for chordal graphs. To state the respective

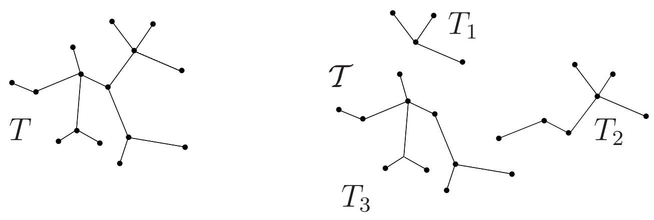

Figure 3.1: A tree T and three subtrees of T such that the tree graph G with tree representation $(T, \{T_1, T_2, T_3\})$ is a path.

result, we need to introduce a further notion. Let G be a graph. Initially all vertices are unnumbered and have counters set to zero. Choose an unnumbered vertex with largest counter , give it the next number, and add 1 to all the counters of its neighbors. Continue doing this until all the vertices have been numbered, say $(v_1, ..., v_n)$. Then this ordering is called a maximum cardinality search ordering, for short an *MCS ordering.* Recalling the definition of a perfect elimination ordering from Chapter 2 we come to formulating the mentioned characterization.

Theorem 3.2 ([26],[64]). The following conditions are equivalent:

(i) G is a chordal graph.

(ii) G has a perfect elimination ordering.

(iii) The reversal of any MCS ordering of G is a perfect elimination ordering of G. □

In the literature, chordal graphs are also called triangulated graphs [3] and rigid-circuit graphs [57]. They have been intensively studied since the late 1960's, have applications to biology, computing and matrix theory and further characterizations.

A well studied subclass of chordal graphs are *path graphs.* More precisely, a graph $G = (V(G), E(G))$ is a *path graph* if there exists a tree $T = (V(T), E(T))$, a set $\mathcal{P}$ of paths in T and a mapping φ from $V(G)$ to $\mathcal{P}$ with $\varphi(v) = P_v \in \mathcal{P}$ such that $vw \in E(G)$ if and only if $P_v \cap P_w \neq \emptyset$. Such a pair $(T, \mathcal{P})$ is said to be a *path representation* of G .

Path graphs have been introduced in [29] where also a characterization and a recognition algorithm are given. Since then path graphs have been studied continuously. In [54] some applications and many references can be found.

A further and rather famous subclass of chordal graphs are *interval graphs*. They were maybe the first graphs considered in the context of intersection graphs. In accordance with the characterization of chordal graphs as tree graphs, interval graphs are *vertex intersection graphs of subpaths of a path*. Interval graphs were first mentioned in 1957 [38] and were already characterized in 1962 [5]. They have been intensively studied [30, 26, 5] and can be recognized in linear time [6]. As indicated in the term "interval" they correspond to a further type of intersection graph, namely to "geometric intersection graphs".

3.1.3 Intersection graphs of convex subsets of the plane

An interval graph can be defined equivalently as an intersection graph of a family of finite closed intervals of the real line. The family of intervals is then called an *interval representation* of the respective interval graph.

The fact that intervals are the convex subsets of $\mathbb{R}$ led to considering intersection graphs of convex subsets of $\mathbb{R}^2$. In [17] it is shown that every chordal graph is the intersection graph of convex subsets of $\mathbb{R}^2$. A further example of intersection graphs in $\mathbb{R}^2$ are planar graphs. Using Koebe's circle packing theorem we can represent each planar graph as the intersection graph of a set of circles whose interiors are disjoint, in other words by touching disks [42].

For $d \geq 2$, intersection graphs of geometric objects like hyperplanes, d-dimensional boxes and balls of $\mathbb{R}^d$ are studied. Among others, it is shown that every graph is the intersection graph of convex subsets of $\mathbb{R}^3$ [67].

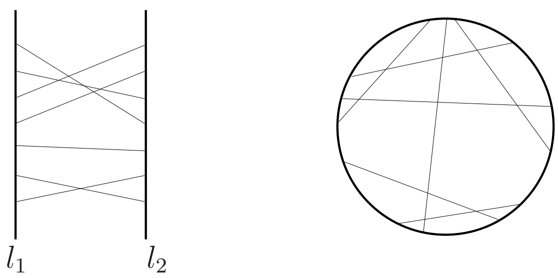

Figure 3.2: An intersection representation of a permutation graph on the left-hand side, and of a circle graph on the right-hand side.

Another interesting type of intersection graphs in the plane are intersection graphs of segments spanned between two parallel lines; an example is given in the left part of Figure 3.2. They are known as *permutation graphs* which is motivated by the following observation.

Let $G = (V, E)$ be a permutation graph with n vertices and $\mathcal{S}$ a set of segments spanned between two parallel lines l_1 and l_2 such that $G \cong \Omega(\mathcal{S})$. Then, the endpoints of the segments of $\mathcal{S}$ on line l_1 induce a linear ordering L_1 and the endpoints on l_2 a linear ordering L_2 of the vertices of G. Assume that the points on l_1 are ordered $(1, ..., n)$, then there is a permutation π that gives the ordering L_2 so that the edges of G are the pairs $\{i, j\}$ with $i < j$ and $\pi(j) < \pi(i)$.

A *circle graph* is a generalization of a permutation graph and can be defined as an intersection graph of chords of a circle. An example of a *circle representation* of a circle graph is given on the right-hand side of Figure 3.2.

3.1.4 Cocomparability graphs

Recall the latter observation about permutation graphs. Recall that the intersection of linear orderings on $[n]$ gives a partial ordering on the set $[n]$. Thus, every permutation graph is the cocomparability graph of a poset of dimension at most two. If we reverse the order of the elements in one of the orderings, we see that every permutation graph is also a comparability graph.

Theorem 3.3 ([21, 19])**.** The following conditions are equivalent for a graph $G = (V, E)$:

(i) G is a permutation graph.

(ii) G is both a comparability graph and a cocomparability graph of a poset $P = (V, <_P)$.

(iii) $\dim(V, <_P) = 2$. □

Cocomparability graphs have been characterized in [33] as intersection graphs of function diagrams.

Theorem 3.4 ([33])**.** A graph is a cocomparability graph if and only if it is the intersection graph of a set of curves in $\mathbb{R}^2$ where each curve is the image of a continuous function from $[0, 1]$ to $\mathbb{R}$. □

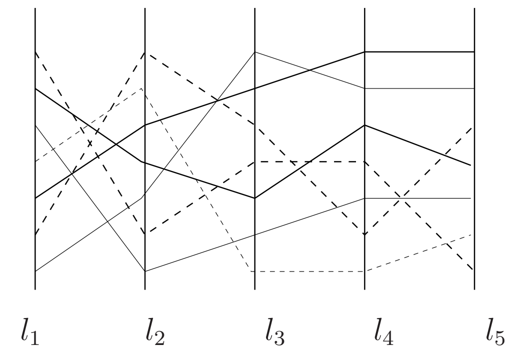

Figure 3.3: A realizer of a poset induces a representation of the corresponding cocomparability graph as an intersection graph of polygonal arcs.

To illustrate Theorem 3.4 let $G = (V(G), E(G))$ be a cocomparability graph. Then $\bar{G}$, its complement, is the comparability graph of some poset P with ground set $V(G)$. Let $\mathcal{R} = \{L_1, ..., L_k\}$ be a realizer of P. As in the case of permutation graphs embed the linear orders of $\mathcal{R}$ onto k different parallel lines $l_1, ..., l_k$ in the plane. Then connect every pair of points on two consecutive lines that correspond to the same element of $V(G)$ by a straight line segment. The concatenation of the respective segments yields a polygonal arc for each element of $V(G)$. Now it is easy to see that the set of polygonal arcs is a representation of the cocomparability graph G of poset P as intersection graph of Jordan arcs fulfilling the conditions of Theorem 3.4.

If we embed an interval realizer of a given poset in the way just mentioned and connect every pair of left, respectively right endpoints of intervals on two consecutive lines by segments, we obtain an intersection graph of so called *ribbons*.

In the case of cocomparability graphs of interval dimension two, the resulting ribbons are trapezoids, thus the respective intersection graphs are called *trapezoid graphs*. In the case of cocomparability graphs of interval dimension one, we are left with an intersection graph of intervals, that is an interval graph.

3.2 String graphs

We are mainly interested in intersection graphs of Jordan curves in the plane, which are known as *string graphs*. String graphs were introduced independently in 1966 in [63] and in 1976 in [20]. Since then they have been widely studied.

In the following sections we will review graphs that are not string graphs, present subclasses of the class of string graphs and name the most famous complexity results.

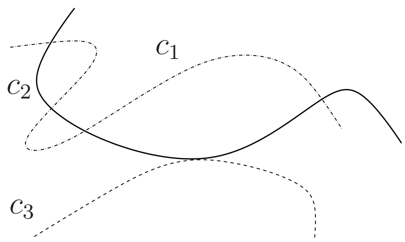

Figure 3.4: The graph $\Omega(\{c_1, c_2, c_3\})$ is a path on three vertices.

3.2.1 Graphs that are not string graphs

Already in [20], graphs are determined that are not string graphs. Here they observed that the complete subdivision of K_5, and thus of any nonplanar graph, is not a string graph.

To see this, let $G = (V, E)$ be an arbitrary nonplanar graph and assume that there is a *string representation* $\mathcal{G}$ of the complete subdivision $\hat{G}$ of G. The strings of $\mathcal{G}$ can be partitioned into the set $\mathcal{S}_V$ representing the elements of $V(G)$ and $\mathcal{S}_E$ representing the elements of $V(\hat{G}) \backslash V(G)$, that is the elements of $E(G)$. Now we can contract each string p_v of $\mathcal{S}_V$ to a point without creating any new intersections except for the ones of strings representing the elements of $N_{\hat{G}}(v)$; these will meet in a point now. The resulting configuration then contains a planar embedding of G which is a contradiction to the assumption that G is nonplanar. Thus, the complete subdivision of any nonplanar graph is not a string graph.

3.2.2 Implicit subclasses of string graphs

Natural and rather interesting subclasses of the class of string graphs arise by posing restrictions on the properties and the intersection behavior of the

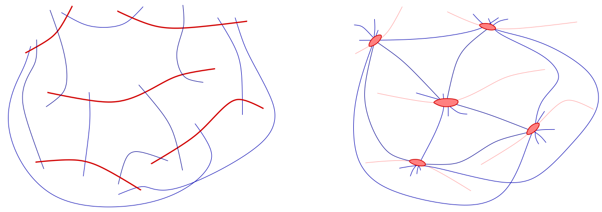

Figure 3.5: A pseudosegment representation of any subgraph of the complete subdivision of K_5 induces a planar embedding of the respective subgraph.

Jordan curves. In the following we will mostly be interested in string representations where no three strings have a point in common. Such a string representation is called a *simple* string representation and can be achieved from an arbitrary string representation by adequately perturbing the multiple intersection points.

As shown in [55, 59], every string graph has a string representation where the number of intersection points is finite. Thus, when dealing with a string graph we can always assume that we are given a string representation with Jordan curves of finite-length, hence Jordan arcs. In [46], the authors consider string representations where the number of intersections of any pair of strings is bounded and touching points are excluded. These additional properties yield the following subclasses of string graphs.

Let $G = (V, E)$ be a string graph. If G has a simple string representation $\mathcal{S}$ such that every common point of a pair of strings of $\mathcal{S}$ is a crossing of these strings, then we say that $\mathcal{S}$ is a *cross representation* of G and G is a *cross graph*.

If G has a cross representation $\mathcal{S}$ and the number of intersection points of any two strings of $\mathcal{S}$ is bounded by k, then we say that $\mathcal{S}$ is a *k-cross representation* of G and G is a *k-cross graph*.

3.2.3 Further subclasses of string graphs

Theorem 3.4 of [33] implies that cocomparability graphs are string graphs. An example of a string representation of a cocomparability graph resulting from a realizer is given in Figure 3.3.

Maybe the most famous subclass of string graphs are planar graphs; this was already shown in [20]. To see this let $G = (V(G), E(G))$ be a planar graph and $\{C_v \mid v \in V(G)\}$ the set of disks resulting from Koebe's touching disks representation. Let S_v be the boundary of C_v for every $v \in V(G)$. As S_v is a simple curve, the set $\mathcal{S} = \{S_v \mid v \in V(G)\}$ is a string representation of G.

If we want the intersection points to be crossings, we set s_v as the circle that results from augmenting the radius of S_v by some $\epsilon > 0$ so that G is the intersection graph of the set $\mathcal{S}' = \{s_v \mid v \in V(G)\}$. If we want the strings to be open curves, we simply delete a point of each S_v that is not contained in any other curve of $\mathcal{S}$ or of s_v of $\mathcal{S}'$ respectively, and obtain a string representation of G with open curves. This operation is sketched on the left-hand side of Figure 3.6.

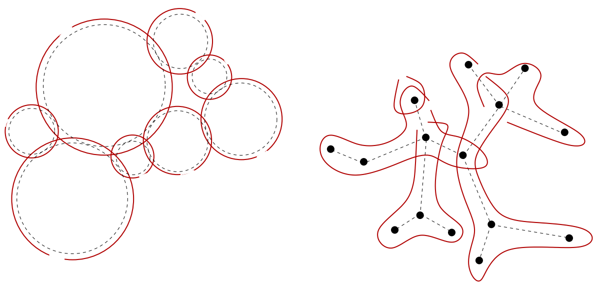

Figure 3.6: String representations of a planar and a chordal graph obtained from a representation by touching disks and a tree representation respectively.

A further interesting subclass of the class of string graphs is the class of chordal graphs. Recall that every chordal graph is a vertex intersection graph of subtrees of a tree. If we embed a tree representation of a chordal graph into the plane, we can locally replace every subtree by an open curve, obtained from a walk around the respective subtree. These curves can be modified in such a way that two curves intersect if and only if the corresponding subtrees intersect. See the right-hand side of Figure 3.6 for an illustration.

3.2.4 Complexity results for string graphs

Interesting research has been conducted regarding the membership complexity of the class of string graphs and certain subclasses. The problem for string graphs was stated in 1976 [36]. It was not known to be decidable for almost thirty years. In two independent papers [55, 59] it is shown that every string graph has a string representation where the number of intersection points is bounded by an exponential in the number of strings. In [58] it is shown that the recognition problem for string graphs is in NP. In [44] it is shown that recognizing string graphs is NP-hard.

Note that for certain subclasses of string graphs like interval, chordal and permutation graphs the recognition problem is polynomially solvable.

In [43] it is shown that the independent set and clique problem are NP-complete for string graphs in general. In the case of interval, chordal and permutation graphs, the independent set and clique problems are polynomially solvable, see for example [21, 32, 43].

3.3 Pseudosegment graphs

In Figures 3.3 and 3.6 we sketched string representations of planar, chordal and cocomparability graphs. In any case we can achieve that the resulting string representation is a simple cross-representation. In the case of planar graphs we even know that they are 2-cross-graphs as there are string representations where the number of intersections of any two strings is bounded by two. So it is an obvious question to ask whether planar graphs are 1-cross-graphs.

In the literature, 1-cross-graphs have received different names each referring to a certain point of view. The one we will use here is *pseudosegment graphs*; it accounts for the fact that every pair of Jordan arcs of a 1-cross-representation intersects like a pair of straight line segments. In other words, a graph G is a *pseudosegment graph* if there is a set $\mathcal{S}$ of pseudosegments in the plane such that G is isomorphic to the intersection graph $\Omega(\mathcal{S})$ of the pseudosegments of $\mathcal{S}$; the set $\mathcal{S}$ is then a *pseudosegment representation* of G. The class of intersection graphs of pseudosegments is denoted *PSI*.

Remark: Each pseudosegment representation can easily be changed into a simple pseudosegment representation by perturbing the pseudosegments participating in a multiple intersection locally. This can be done without changing the intersection relations or augmenting the number of pairwise intersections. Thus, we do not have to care for multiple intersection points.

3.3.1 Pseudosegment graphs and intersection graphs of polygonal arcs

Let G be an arbitrary pseudosegment graph and let $\mathcal{J}$ be a set of pseudosegments such that $G \cong \Omega(\mathcal{J})$. Let $X(\mathcal{J})$ be the set of crossing points and endpoints of the elements of $\mathcal{J}$. Then $\mathcal{J}$ induces a plane graph $G(\mathcal{J})$ on $X(\mathcal{J})$. More precisely, $G(\mathcal{J})$ has an edge for every two elements of $X(\mathcal{J})$ that appear consecutive on a pseudosegment of $\mathcal{J}$. By Lemma 2.4 we know that every plane graph can be represented in such a way that the edges are polygonal arcs. This implies that G has a pseudosegment representation where the pseudosegments are polygonal arcs.

3.3.2 Graphs that are not pseudosegment graphs

Obviously not every graph is the intersection graph of some set of pseudosegments. An example of a graph that is not a pseudosegment graph is the complete subdivision of K_5 as seen in Section 3.2.1. This result leads to a further example of a graph that does not belong to PSI.

Definition 3.5. Let V be the set consisting of the union $[5] \cup \binom{[5]}{3}$. Then let $G[5,3]$ be the graph with vertex set V such that $[5]$ and $\binom{[5]}{3}$ induce independent sets and xy is an edge of $G[5,3]$ if and only if $x \in [5]$, $y \in \binom{[5]}{3}$ and $x \in y$.

Proposition 3.6. The graph $G[5,3]$ is not a pseudosegment graph.

Proof. Assume that $G[5,3]$ is a pseudosegment graph and let $\mathcal{G}$ be an arbitrary pseudosegment representation of $G[5,3]$. Then $\mathcal{G}$ can be partitioned into two sets, $P_1 = \{p_1, ..., p_5\}$ representing the elements of $[5]$ and $P_2 = \{p_{ijk} \mid \{i,j,k\} \in \binom{[5]}{3}\}$ representing the elements of $\binom{[5]}{3}$. As $\mathcal{G}$ is a pseudosegment representation of $G[5,3]$, the sets P_1 and P_2 consists of disjoint Jordan arcs and $p_l \in P_1$ intersects $p_{ijk} \in P_2$ if and only if $l \in \{i,j,k\}$. Note that the intersection points on $p_{ijk} \in P_2$ induce a linear ordering on the elements i, j and k of $[5]$.

Assume there is a pseudosegment $p_{ijk} \in P_2$ for every pair of elements p_i,p_j of P_1 such that the subset of p_{ijk} that connects p_i and p_j does not contain the intersection point with p_k. Denote this part of p_{ijk} by c_{ij}. Then the union

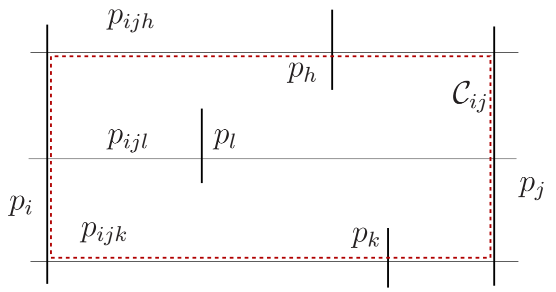

Figure 3.7: Curve $\mathcal{C}_{ij}$ prevents that a Jordan arc represents p_{klh}.

$P_1 \cup \{c_{ij} | \{i,j\} \in \binom{[5]}{2}\}$ is a pseudosegment representation of the complete subdivision of K_5. This is not possible as observed in [20].

Thus, there is a pair p_i and p_j of pseudosegments in P_1 such that the subset of p_{ijk} contains the intersection with p_k for all $k \in [5] \setminus \{ij\}$. In this case, there is a pseudosegment $p_l \in P_1 \setminus \{p_i, p_j\}$ that lies within the closed curve $\mathcal{C}_{ij}$ that is contained in the union of p_i, p_j, p_{ijk} and p_{ijh} for $\{i,j,k,l,h\} = [5]$; see Figure 3.7 for an illustration. This implies that the pseudosegment of $\mathcal{P}_2$ representing the triple $\{h,l,k\}$ has to intersect either $\mathcal{C}_{ij}$ or p_{ijl}. This contradicts the assumption that $\mathcal{G}$ is a pseudosegment representation of $G[5,3]$. As $\mathcal{G}$ was chosen arbitrarily, $G[5,3]$ is not a pseudosegment graph. $\square$

3.3.3 Implicit subclasses of pseudosegment graphs

The most natural subclass of pseudosegment graphs is the class *SEG* of *intersection graphs of segments*. Intersection graphs of segments, for short *segment graphs*, were already considered in 1976 [20] and received further interest as a result of Conjecture 1.1 from 1984:

Conjecture 1.1([61]) Every planar graph is a segment graph.

This conjecture was supported by the first results for subclasses of planar graphs, but stayed an open question until 2009, when it could be confirmed in [8]. The following further leading conjecture from 1991 is still open.

Conjecture 1.2([68]) Every planar graph has a segment representation where the segments are of at most four directions.

There are some graphs where pseudosegment representations, and sometimes even *segment representations*, are trivial or very easy to find. Examples of graphs which trivially belong not only to PSI but even to SEG are permutation graphs and circle graphs; both types of graphs are intersection graphs of segments by definition.

3.3.4 Complexity results for pseudosegment and segment graphs

The recognition problem of pseudosegment graphs is shown to be NP-complete in [45]. The recognition problem of segment graphs is NP-hard according to [46]. Interestingly, it is open whether the recognition problem of segment graphs is NP-complete. It is known, however, that a representation via segments with integer endpoints may require endpoints of size $2^{2^{\sqrt{n}}}$ [47].

In [43, 52] the complexities of optimization problems for segment graphs are analyzed. It is known that the independent set problem for segment graphs is NP-complete but the complexity of the clique problem is still not known. Nevertheless it is known that computing the chromatic number of segment graphs is NP-hard [20]

3.4 Preview

With this as background we come to give a comprehensive overview of our work on pseudosegment graphs. Keep in mind that we can always choose a pseudosegment representation consisting of polygonal arcs.

In Section 3.2.3 we considered string representations of planar, chordal and cocomparability graphs:

- a string representation of an arbitrary planar graph can be read off a touching disks representation;
- a string representation of a chordal graph can be constructed using a tree representation;
- a realizer of a poset yields a string representation of the corresponding cocomparability graph.

In each of these cases there are graphs where the so obtained string representation is not a 1-string representation, in other words it is not a pseudosegment representation. This naturally leads to the question whether all planar, chordal and cocomparability graphs are pseudosegment graphs. With respect to planar graphs the existence of segment representations was already conjectured in 1984, and was proven lately in 2009 [8]. At this, the actual question is whether there exist segment representations using segments of at most four different directions, as stated in Conjecture 1.2.

Chapter 4 deals with Conjecture 1.2 and the relation of pseudosegment and segment graphs.

In Section 4.1 we consider subclasses of planar graphs and show that every *series-parallel graph* is a segment graph. Our proof yields a segment representation of an arbitrary series-parallel graph where the segments are of at most three directions. Thus, Conjecture 1.2 is true for series-parallel graphs.

In addition, no two parallel segments share a point, so our result, furthermore, induces a proper 3-coloring of the represented series-parallel graph. The analog holds for bipartite planar and triangle-free planar graphs where proper 2- and 3-colorings result from the respective segment representations obtained in [13, 15, 39]. Note that in the proof of [8], showing that every planar graph is a segment graph, no upper bound on the number of directions used in the resulting segment representations is given. The latter proof, confirming Conjecture 1.1, will be sketched in Section 4.2.

In Section 4.3 we turn our attention to arrangements of pseudolines and straight lines to analyze the consequences of restricting pseudosegments to straight line segments. Pseudolines were introduced by Levi [48] as a generalization of straight lines. An example of a nonstretchable arrangement of pseudolines was already given in [56].

In Section 4.3.1 we construct a pseudosegment graph that captures the combinatorial structure of an arbitrary but fixed pseudoline arrangement. Then we show that this pseudosegment graph is a segment graph if and only if the chosen pseudoline arrangement is stretchable.

In Chapter 5 we consider chordal graphs with respect to pseudosegment representations.

First, in Section 5.1, we show that path graphs are pseudosegment graphs. This is not as trivial as it may seem at first glance when considering a path representation of such a graph embedded in the plane.

Subsequently we present chordal graphs that do not belong to the class of pseudosegment graphs. In Section 5.2 we introduce the family $(K_n^3)_{n\in\mathbb{N}}$ of chordal graphs. Every graph K_n^3 has the vertex set $V = V_C \cup V_I$ such that $V_C = [n]$ induces a clique on n and $V_I = \binom{[n]}{3}$ is an independent set on $\binom{n}{3}$ elements. Additionally, every vertex $\{i, j, k\}$ of V_I is adjacent to the vertices i, j and k of V_C. Assuming that there is a pseudosegment representation of K_n^3 for every $n \in \mathbb{N}$, we focus on the subset of pseudosegments that represent the clique of K_n^3; this set corresponds to an arrangement of n pseudosegments. The remaining pseudosegments are disjoint 3-segments contained in the arrangement. We then show that every arrangement of n pseudosegments can contain at most $6n^2$ disjoint 3-segments which prevents the existence of a pseudosegment representation of K_n^3 if $\binom{n}{3} > 6n^2$.

Disregarding our original objective, this partitioning leads to further questions on 3-segments contained in an arrangement of pseudosegments. If we require that the set of 3-segments contained in the arrangement is a set of pseudosegments itself, we are not able to bound the size of such a set. One problem about answering this question is that the 3-segments can bypass the pseudosegments of the arrangement at their ends.

To evade this problem we exchange the arrangement of pseudosegments by an arrangement of pseudolines. In Section 5.3 we bound not only the number of 3-segments but even of k-segments contained in a pseudoline arrangement. To this end, we introduce the $(\leq k)$-*zone* of a pseudoline in a pseudoline arrangement which generalizes the classical zone. Then we determine a linear upper bound on the number of edges in the $(\leq k)$-zone which enables us to show that the maximal size of a set of k-segments of an arbitrary arrangement of n pseudolines is $O(n^2)$. The bound on the number of edges in the $(\leq k)$-zone is of independent interest and has already found application in the work of Scharf and Scherfenberg [60].

Next, in Section 5.4, we consider the family $(S_n^3)_{n\in\mathbb{N}}$ of chordal graphs defined as follows. For every $n \in \mathbb{N}$, the graph S_n^3 has as vertex set $V = V_I' \cup V_C'$ such that $V_I' = [n]$ is an independent set of n and $V_C' = \binom{[n]}{3}$ a clique of $\binom{n}{3}$ vertices; again membership accords with adjacency between elements of V_I' and V_C'. This time we use an argument from Ramsey Theory to show that for large n, every string representation of S_n^3 contains two strings representing a pair of elements of V_C' that intersect more than once. This contradicts the existence of a pseudosegment representation of S_n^3 for large n.

Every K_n^3 has a representation as vertex intersection graphs of caterpillars of a caterpillar with maximal degree three. Every S_n^3 has a representation as vertex intersection graph of substars of a star where the substars have maximal degree three. Hence these subtrees are "close" to being paths. Recalling that every path graph is a pseudosegment graph we conclude that graphs that are chordal graphs and pseudosegment graphs cannot be induced by many treelike subtrees of a tree.

Finally, in Chapter 6 we consider cocomparability graphs of interval dimension two, better known as trapezoid graphs, and determine subclasses of trapezoid graphs that consist of pseudosegment graphs.

Interval graphs are the cocomparability graphs of posets of interval dimension one. As every interval graph is also a path graph, we know from Section 5.1 that every interval graph is a pseudosegment graph. In Section 6.1 we construct pseudosegment representations of interval graphs using interval representations of the respective graphs, that is interval realizers of the corresponding posets.

Permutation graphs are the cocomparability graphs of posets of dimension two. Using two dimensional realizers of the posets, we easily obtain not only pseudosegment but even segment representations of permutation graphs. These pseudosegment representations and the ones of interval graphs obtained in Section 6.1 will be of use when we consider further subclasses of trapezoid graphs in view of pseudosegment representations.

In Section 6.2 and 6.4 we construct pseudosegment representations of *point-interval graphs*, a generalization of permutation and interval graphs, and two more subclasses of trapezoid graphs using two dimensional interval realizers of the respective posets. It remains an open question whether every trapezoid graph is a pseudosegment graph.

Chapter 4

Segment Graphs

Segment graphs, that is intersection graphs of segments, were already considered in 1976 by Ehrlich et al. in [20], one of the first papers on string graphs. In 1984, Scheinerman conjectured that every planar graph was a segment graph.

Conjecture 1.1([61]) Every planar graph is a segment graph.

This called wide attention to segment graphs and initiated many investigations. The conjecture was supported by the first results on subclasses of planar graphs. In 1991 it was shown by de Fraysseix et al. [15] and independently by Hartman et al. [39] that every bipartite planar graph is a segment graph. In 2002, de Castro et al. [13] extended this result and showed that every triangle-free planar graph is a segment graph. The latter results strengthened Conjecture 1.2, stated by West in 1991:

Conjecture 1.2([68]) Every planar graph has a segment representation where the segments are of at most four directions.

In all three cases, the resulting segment representations consist of segments of two respectively three directions.

Further work in view of Conjecture 1.1 was conducted and, in 2005, de Fraysseix and de Mendez [14] showed that every 4-connected 3-colorable planar graph and every 4-colored planar graph without an induced C_4 using four colors is a segment graph. Finally, in 2009, Chalopin and Gonçalves confirmed Conjecture 1.1 [8]. Conjecture 1.2 remains open in general.

The first two sections of this chapter are devoted to this topic. In Section 4.1 we will present our own contribution to Conjecture 1.2; it dates back to 2005 and shows that every series-parallel graph, that is every graph that does not contain a subdivision of K_4, has a segment representation; the segment representations we obtain consist of segments that are of at most three directions.

We proceed in Section 4.2 with a sketch of the interesting though rather technical proof of the result from [8] that every planar graph is a segment graph.

During the work on Conjecture 1.1 it sometimes turned out to be useful to first construct a pseudosegment representation of the considered planar graph. To clarify the difference of pseudosegment and segment representations we consider arrangements of pseudolines and straight lines. In Section 4.3 we use a pseudoline arrangement to construct a pseudosegment graph. Our construction implies that the resulting pseudosegment graph is a segment graph if and only if the chosen pseudoline arrangement is stretchable.

4.1 Series-parallel graphs

Motivated by the fruitful work on subclasses of planar graphs as segment graphs, we investigated the class of *series-parallel graphs*. In this section, we show that every series-parallel graph is a segment graph; this is joint work with Bodirsky and Kára and can also be found in [4]. The resulting segment representations have the additional property that the segments used in the representations are of at most three directions. This confirms Conjecture 1.2 for series-parallel graphs. As, in addition, parallel segments are disjoint, every segment representation of a series-parallel graph induces a proper coloring of the respective graph with three colors, the directions.

4.1.1 Definitions

A *series-parallel network* is a graph with two distinguished vertices s and t, called the *source* and the *sink*, that is inductively defined as follows: let G_1 and G_2 be two series-parallel networks where s_1 is the source of G_1 and s_2 the source of G_2. Analogously let t_1 denote the sink of G_1 and t_2 the sink of G_2. Then G is a series-parallel network if G is either an edge between the source and the sink, or G is obtained by one of the two operations:

- G is obtained from G_1 and G_2 by identifying t_1 and s_2. The source of G is s_1 and its sink t_2. This operation is called a *serial composition*.

- G is obtained from G_1 and G_2 by identifying s_1 and s_2 and t_1 and t_2. The source of G is $s_1 = s_2$ and its sink $t_1 = t_2$. This operation is called a *parallel composition*.

These operations may give rise to multiple edges. But as the definition of intersection graphs does not account for multiple edges we only consider the underlying simple graphs.

A graph is a *series-parallel graph* if each of its 2-connected components is a series-parallel network.

Theorem 4.1. Every series-parallel graph has a segment representation.

To prove Theorem 4.1 we will first construct a segment representation $\mathcal{S}$ of an arbitrary series-parallel network N that has the following additional properties:

(P1) The segments of $\mathcal{S}$ are of at most three different directions.

(P2) No two parallel segments of $\mathcal{S}$ intersect.

(P3) The intersection point of two segments is an endpoint of at least one of them.

Note that a segment representation that fulfills properties $(P1)$,$(P2)$ and $(P3)$ is also called a *PURE-3-SEG-CONTACT-representation* [47].

Secondly we will show that any series-parallel graph G is a subgraph of some series-parallel network N. The fact that N has a segment representation $\mathcal{S}'$ fulfilling property $(P3)$ implies that G has a segment representation $\mathcal{S} \subset \mathcal{S}'$ resulting from shortening and deleting certain segments of $\mathcal{S}'$. This implies that every series-parallel graph is a segment graph.

Remark: Let us point out that properties $(P1)$ and $(P2)$ involve that the directions used induce a proper 3-coloring of the represented series-parallel graph.

4.1.2 A special segment representation of a series-parallel network

Before we come to the construction of a segment representation of a series-parallel network, we need to define some geometric terms.

Let l_1, l_2 be two different halflines that end in a common point. We call the area between l_1, l_2 with angle less than or equal to $\pi/2$ the *cone* of l_1 and l_2. We say that a cone is *bounded by segments* p_1 and p_2 if they both contain the endpoint $l_1 \cap l_2$, p_1 is contained in l_1 and p_2 and l_2 overlap. See Figure 4.1 for an illustration.

Now let C be a cone bounded by segments p_1 and p_2. If there is a segment $p_3 \subset C$ such that

- p_1, p_2 and p_3 are pairwise not parallel,
- p_3 touches p_1 and p_2 in its endpoints which are not endpoints of p_1 and p_2,

then we call C an *admissible cone* and say that p_3 *assures the admissibility of* C.

Lemma 4.2. Let G be an arbitrary series-parallel network with source s and sink t. Let C be an arbitrary admissible cone bounded by two segments p and p', and let $\bar{p}$ be an arbitrary segment assuring the admissibility of C. Then there exists a segment representation $\mathcal{S}$ of G with properties $(P1)$,$(P2)$ and $(P3)$ such that $\mathcal{S}$ is inside the triangle defined by p, p' and $\bar{p}$. Furthermore, s and t are represented by p and p', that is $p = p_s$, $p' = p_t$.

Proof. The proof is by induction on the number of vertices of G. For the induction basis assume that G is just an edge, hence, the vertices of G are just s and t. Then the bounding segments p and p' of C form a segment representation of G fulfilling properties $(P1)$,$(P2)$ and $(P3)$.

Now let G be a series-parallel network with n vertices and assume that Lemma 4.2 has been proven for graphs with at most $n-1$ vertices. Let C be an arbitrary admissible cone bounded by two segments p and p', and let $\bar{p}$ be an arbitrary segment assuring the admissibility of C. By definition, G is either a serial or a parallel composition of two series-parallel networks G_1 and G_2, each having less than n vertices. Let s_1 and s_2 be the source and t_1 and t_2 be the sink of G_1 and G_2 respectively.

(a) Assume that G is a serial composition of the series-parallel networks G_1 and G_2 with source $s = s_1$ and sink $t = t_2$. Let C_1 be a cone bounded by segments p and $\bar{p}$ and admissible by a segment p_1 contained within C

that is parallel to p'. By the induction hypothesis G_1 has a segment representation $\mathcal{S}_1$ fulfilling properties $(P1)$,$(P2)$ and $(P3)$ within C_1 such that $p = p_{s_1}$ and $\bar{p} = p_{t_1}$.

Now choose an open disk centered at the intersection of $\bar{p}$ and p' that has empty intersection with any segment of $\mathcal{S}_1$ different from $\bar{p}$. Then choose a segment p_2 in C parallel to p that lies within this disk. Let C_2 be the cone bounded by segments p' and $\bar{p}$ and admissible by segment p_2. By the induction hypothesis, G_2 has a segment representation $\mathcal{S}_2$ fulfilling properties $(P1)$,$(P2)$ and $(P3)$ within C_2 such that $p' = p_{t_2}$ and $\bar{p} = p_{s_2}$.

By the choice of p_2, $\mathcal{S}_2$ is disjoint from $\mathcal{S}_1$ except for $\bar{p}$, thus, the union $\mathcal{S}_1 \cup \mathcal{S}_2$ is a segment representation of G fulfilling properties $(P1)$,$(P2)$ and $(P3)$ within C such that $p = p_s$ and $p' = p_t$. See the right-hand side of Figure 4.1 for an illustration.

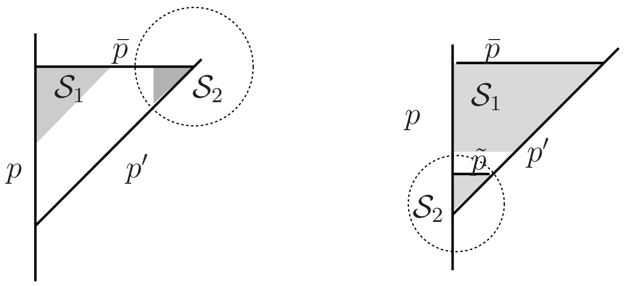

Figure 4.1: Segment representations of G after (a) a serial and (b) a parallel composition.

(b) Now assume that G is a parallel composition of the series-parallel networks G_1 and G_2 with source $s = s_1 = s_2$ and sink $t = t_1 = t_2$. By the induction hypothesis, G_1 has a segment representation fulfilling properties $(P1)$,$(P2)$ and $(P3)$ within C such that $p = p_{s_1}$ and $p' = p_{t_1}$. As before C is admissible via $\bar{p}$. We denote this segment representation by $\mathcal{S}_1$.

Now choose an open disk centered at the intersection of p and p' that has empty intersection with any segment of $\mathcal{S}_1$ different from p and p'. Then choose a segment $\tilde{p}$ in C parallel to $\bar{p}$ that lies within this disk. By the induction hypothesis there is a segment representation $\mathcal{S}_2$ of G_2 fulfilling properties $(P1)$,$(P2)$ and $(P3)$ within C such that $p = p_{s_2}$

and $p' = p_{t_2}$ and $\tilde{p}$ assures the admissibility of C. The union $\mathcal{S}_1 \cup \mathcal{S}_2$ is a segment representation of G fulfilling properties $(P1)$,$(P2)$ and $(P3)$ within C such that $p = p_s$ and $p' = p_t$. For an illustration of case (b) see the left-hand side of Figure 4.1.

□

Lemma 4.3. Let $G = (V, E)$ be a graph and let $\mathcal{S}$ be a segment representation of G that fulfills property $(P3)$. Let $G' = (V', E')$ be a subgraph of G. Then there is a segment representation $\mathcal{S}'$ of G' fulfilling property $(P3)$ that can be obtained from $\mathcal{S}$ by shortening and deleting some of the segments of $\mathcal{S}$.

Proof. Let $\mathcal{S}$ be a segment representation of G fulfilling property $(P3)$ and let p_v be the segment representing $v \in V$ in $\mathcal{S}$. In order to obtain $\mathcal{S}'$ from $\mathcal{S}$ we first delete all segments from $\mathcal{S}$ that correspond to vertices of G and not of G'. The resulting set $\bar{\mathcal{S}}$ of segments is a segment representation of the subgraph $\bar{G}$ of G that is induced by the vertices V' of G'.

Now let F be the set of edges in $\bar{G}$ and not in G'. If $F = \emptyset$, then $\bar{G} = G'$ and $\bar{\mathcal{S}}$ is a segment representation of G'. Otherwise let $e = uw$ be an edge of F. By definition, segments p_u and p_w meet in a common point and one of them, say p_u, ends there. Then we can shorten p_u so that it does not intersect p_w anymore while preserving all intersection points of p_u with other segments of $\bar{\mathcal{S}}$. If we repeat this procedure for each edge of F, we obtain a segment representation $\mathcal{S}'$ of G' that fulfills property $(P3)$. □

In the next subsection we will show how this construction can be used to represent an arbitrary series-parallel graph.

4.1.3 Series-parallel graphs and series-parallel networks

It is a well known fact that the class of series-parallel graphs is the class of graphs that do not contain a subdivision of K_4 [18]. This will be used to show that every series-parallel graph is the subgraph of some series-parallel network.

Lemma 4.4. Let G be a graph that does not contain a subdivision of K_4. Then there is a graph H such that

- G is a subgraph of H,
- H is 2-connected,
- H does not contain a subdivision of K_4.

Proof. Let $G = (V, E)$ be an arbitrary graph that does not contain a subdivision of K_4. If G has several components, then we can add edges such that the resulting graph is connected and does not contain a subdivision of K_4. So let us assume that G is connected. We then prove Lemma 4.4 by induction on the number of blocks of G.

For the induction basis we assume that G contains only one block. If G is 2-connected, Lemma 4.4 holds for $H = G$. Otherwise G is an edge. In this case we obtain H by adding a vertex and connecting it to the vertices of G, and, again, Lemma 4.4 holds.

Now assume that G consists of k blocks and Lemma 4.4 has been proven for graphs with at most $k-1$ blocks. Let B_1 and B_2 be two different blocks of G that share vertex $v \in V$. Let u_1 and u_2 be neighbors of v in B_1 and B_2 respectively. Let $G' = (V, E \cup \{u_1u_2\})$. Clearly the number of blocks of G' is one less than the number of blocks in G. If G' does not contain a subdivision of K_4, then we are done by induction.

So suppose that G' contains a subdivision S of K_4. Let $W = \{w_1, .., w_4\}$ be the vertices of degree three in S. Then there are three internally disjoint paths between w_i and w_j for every two different vertices $w_i, w_j \in W$. As there are at most two internally disjoint paths between a vertex of B_1 and a vertex of B_2 different from v in G, the vertices of W must be contained within one block of G.

Without loss of generality let W be contained in B_1. As G does not contain a subdivision of K_4, S must contain a path P that enters B_2 via v and returns to B_1 via u_1u_2. Note that we can replace the subpath of P between v and u_2 in B_2 by the edge vu_1. By this we obtain a subdivision of K_4 that is a subgraph of B_1, and thus of G as well. This contradicts the fact that G does not contain a subdivision of K_4. Thus, induction gives that there is a 2-connected graph H that does not contain a subdivision of K_4 but contains G as a subgraph. □

The previous lemma enables us to show Theorem 4.5 which is a stronger version of Theorem 4.1.

Theorem 4.5. Let $G = (V, E)$ be a series-parallel graph. Then G has a segment representation that fulfills properties $(P1)$, $(P2)$ and $(P3)$.

Proof. Given a series-parallel graph G, Lemma 4.4 implies that there exists a 2-connected graph H that contains G as a subgraph and does not contain a subdivision of K_4. Hence, H is a 2-connected series-parallel graph, and thus, H is a series-parallel network. Applying Lemma 4.2 we obtain a segment representation $\mathcal{S}'$ of H that fulfills properties $(P1)$, $(P2)$ and $(P3)$ and lies within a cone bounded by two segments p and p' and admissible by $\bar{p}$. Using Lemma 4.3 we can shorten and delete segments of $\mathcal{S}'$ such that we obtain a segment representation $\mathcal{S}$ of G fulfilling properties $(P1)$, $(P2)$ and $(P3)$. This proves Theorem 4.5 □

4.2 Planar graphs

In [8] it is shown that every planar graph is a segment graph which confirms Conjecture 1.1 from 1984.

Theorem 4.6. ([8]) Planar graphs are segment graphs.

In the following we will sketch the proof of this result. In order to give an introductory overview of the result, we will leave out most of the technical details and concentrate on the basic ideas. Note that many details and technical lemmas can be found only in the extended version of [8].

4.2.1 Overview

It suffices to prove Theorem 4.6 for triangulations as every plane graph is an induced subgraph of a triangulation. After introducing some definitions, we will present the constructive models and operations used in [8] to present an arbitrary triangulation as a segment graph. Subsequently we will sketch the proof of Theorem 4.6 from [8]; it is by induction on the number of separating 3-cycles of a triangulation.

4.2.2 Graph theoretic definitions

The following operation enables us to restrict our attention to triangulations when heading for segment representations of planar graphs.

Let G be a plane graph. Then the graph $h(G)$ is obtained from G by embedding a new vertex v_f into face f of G and connecting it to every vertex of G on the boundary of f by a new edge. This is done for every face of G. Then it follows that the graph $h(G)$ is a connected plane graph containing G as an induced subgraph, $h(h(G))$ is 2-connected and $h(h(h(G)))$ is a triangulation.

A plane graph is called a *near-triangulation* if all inner faces are triangles. An edge $uv \in E$ is an *inner chord* of a near-triangulation T if u and v are outer vertices of T and uv is an inner edge. A *W-triangulation* is a 2-connected near-triangulation containing no separating 3-cycle.

A W-triangulation T is 3-*bounded* if the boundary of the outer face of T is the union of three paths $(a_1, .., a_p)$,$(b_1, .., b_q)$ and $(c_1, .., c_r)$ that satisfy the following conditions

- $a_1 = c_r$, $b_1 = a_p$ and $c_1 = b_q$,
- the paths are not trivial, that is $p \geq 2$, $q \geq 2$ and $r \geq 2$,
- there exists no inner chord $a_i a_j$, $b_k b_l$, $c_m c_n$ with $1 < i + 1 < j \leq p$, $1 < k + 1 < l \leq q$ and $1 < m + 1 < n \leq r$.

The boundary of T will be denoted by $(a_1, .., a_p) - (b_1, .., b_q) - (c_1, .., c_r)$, see Figure 4.2 for an example.

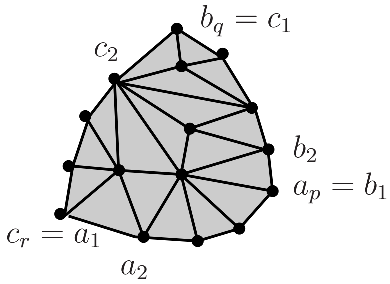

Figure 4.2: A 3-bounded W-triangulation T with boundary $(a_1, .., a_p) - (b_1, .., b_q) - (c_1, .., c_r)$.

By definition, any 4-connected triangulation is a W-triangulation. Notice that a W-triangulation has no cut-vertex and outer edges induce a cycle.

The following Lemma gives a sufficient condition for a subgraph of a W-triangulation T to be a W-triangulation.

Lemma 4.7. Let T be a W-triangulation and C a cycle of T. The subgraph of T defined by C and the edges inside C according to the embedding of T is a W-triangulation.

In the following construction, the order on the three boundary paths and their directions will be important, that is $(a_1, .., a_p) - (b_1, .., b_q) - (c_1, .., c_r)$ is different from $(b_1, .., b_q) - (c_1, .., c_r) - (a_1, .., a_p)$ and $(a_p, .., a_1) - (c_r, .., c_1) - (b_q, .., b_1)$.

4.2.3 Constructive definitions

If $\mathcal{S}$ is a set of segments where no two segments overlap, then S is called *unambiguous*. If, in addition, every endpoint of a segment of $\mathcal{S}$ belongs to exactly one segment and the intersection of any three segments is empty, then we call $\mathcal{S}$ a *model* of every graph G with $G \cong \Omega(\mathcal{S})$.

Let T be a triangulation and $\mathcal{S}$ a model of T. A *face-segment* $\bar{\boldsymbol{abc}}$ of face abc of T is a segment that intersects the segments p_a, p_b and p_c of $\mathcal{S}$ such that $\bar{\boldsymbol{abc}}$ connects the crossing point of p_a and p_b to an inner point of p_c. The endpoints of $\bar{\boldsymbol{abc}}$ are then called crossing end P and flat end Q respectively; see Figure 4.3 for an example.

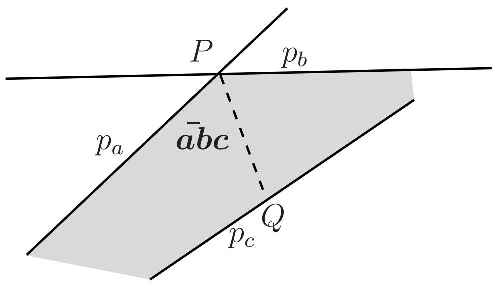

Figure 4.3: The placement of a face-segment $\bar{\boldsymbol{abc}}$

A *full model* of a triangulation T is a couple $\mathcal{M} = (\mathcal{S}, \mathcal{F})$ of segments $\mathcal{S}$ representing the vertices, and $\mathcal{F}$ representing the faces of T such that

- $\mathcal{S}$ is a model of T;

- the face-segments are non-crossing and there is a face-segment for every inner face of T;
- $\mathcal{S} \cup \mathcal{F}$ is unambiguous.

To show that any triangulation T has a segment representation, the authors of [8] construct a full model for T. It turns out to be practical to work with multiple intersection points representing subgraphs of T during the construction. Therefore the authors use so called *premodels*. To define this term, we need some more notations.

Let $\mathcal{R}$ be a set of segments. The set of *representative points* $\mathrm{Rep}_{\mathcal{R}}$ of $\mathcal{R}$ consists of the endpoints and crossing points of elements of $\mathcal{R}$. The relations between the elements of $\mathcal{R}$ and the representative points of $\mathcal{R}$ can be expressed by the *constraint graph* $\mathrm{Const}_{\mathcal{R}}$ defined as a bipartite digraph on vertex set $\mathcal{R} \cup \mathrm{Rep}_{\mathcal{R}}$. In $\mathrm{Const}_{\mathcal{R}}$ two elements $P, r \in \mathcal{R} \cup \mathrm{Rep}_{\mathcal{R}}$ are adjacent if $P \in \mathrm{Rep}_{\mathcal{R}}$ and $r \in \mathcal{R}$ such that $P \in r$. Then (P, r) is an arc of $\mathrm{Const}_{\mathcal{R}}$ if P is an endpoint of r, and otherwise (r, P) is an arc of $\mathrm{Const}_{\mathcal{R}}$.

In a premodel of T, representative points will stand for certain subgraphs of T; these are useful in view of the induction. The representative points are classified by the type of subgraph they represent, for example

- a segment end corresponds to the single vertex represented by the segment;
- a flat face-segment f corresponds to the single vertex represented by the segment at the *end* of f;
- a crossing corresponds to the edge between the vertices represented by the crossing segments.

There are five more types of subgraphs, that is a path, a fan and combinations of a path and a fan, namely fan-path-v_1-point, path-fan-v_1-point and double-fan-v_1-point; we omit the precise definition and refer to Figure 4.4 where examples of the latter three types are sketched.

Let $\mathcal{S}$ be a set of segments, $\mathcal{F}$ a set of non-crossing face-segments and φ a function that assigns a type to each representative point of $\mathcal{S} \cup \mathcal{F}$. Then the triple $\mathcal{M} = (\mathcal{S}, \mathcal{F}, \varphi)$ is a *premodel* of a near-triangulation T if the following holds

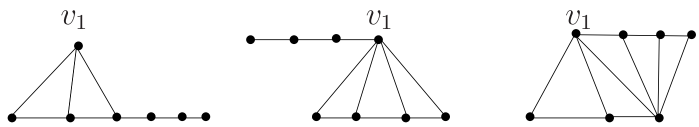

Figure 4.4: A fan-path-v_1-point, a path-fan-v_1-point and a double-fan-v_1-point

- The set $\mathcal{S} \cup \mathcal{F}$ is unambiguous and the digraph $\mathrm{Const}_{\mathcal{S}\cup\mathcal{F}}$ is acyclic;
- there is a bijection between the vertices of T and the segments of $\mathcal{S}$;
- there is an edge $ab \in E(T)$ if and only if p_a and p_b of $\mathcal{S}$ intersect in a point P such that the graph corresponding to $\varphi(P)$ contains the edge ab;
- there is a face $abc \in F(T)$ if and only if one of the following holds:
  - there exists a face-segment corresponding to abc in $\mathcal{F}$,
  - p_a, p_b and p_c intersect in a point P such that the graph corresponding to $\varphi(P)$ has an inner face abc.

It remains to state how a full model is obtained from a premodel. To this end, the authors use three operations, that is prolonging, gliding and traversing. Changing one premodel to another one by such an operation is called a *partial realization*. Note that the number of representative points of a full model is finite and bounds the number of representative points in any premodel. Then the following corollary gives that a premodel can be transformed into a full model in a finite number of steps.

Corollary 4.8. Any premodel $\mathcal{M} = (\mathcal{S}, \mathcal{F}, \varphi)$ of a near-triangulation T admits a sequence of partial realizations that yields a full model $\mathcal{M}' = (\mathcal{S}', \mathcal{F}')$ of T.

Induction on the number of separating 3-cycles of T

To show that any triangulation T admits a segment representation or, more precisely, has a full model, the authors do induction on the number k of separating 3-cycles of T. For the induction basis let T be a triangulation with outer vertices a, b, c and without separating 3-cycle. Then T is a 4-connected W-triangulation 3-bounded by $(a, b)-(b, c)-(c, a)$. Then it follows from Lemma 4.9, stated at the end of this section, that there is a premodel $\mathcal{M} = (\mathcal{S}, \mathcal{F}, \varphi)$ of T. By Corollary 4.8, any premodel can be transformed into a segment representation of the respective graph, thus the induction basis is established.

Now let $k > 0$ and assume Theorem 4.6 has been proven for triangulations with $(k-1)$ separating 3-cycles. So let T be a triangulation with k separating 3-cycles and choose (a, b, c) to be a separating 3-cycle of T such that there is no separating 3-cycle in the subgraph that lies inside (a, b, c) including a, b and c in T. Let T_2 be the subgraph of T induced by all vertices of T that lie properly inside (a, b, c). Let T_1 be the triangulation obtained from T by removing all vertices of T_2. Since the cycle (a, b, c) bounds a face of T_1, (a, b, c) is not a separating 3-cycle in T_1. Thus, T_1 has one separating 3-cycle less than T so that induction implies that there exists a full model $\mathcal{M} = (\mathcal{S}, \mathcal{F})$ of T_1. Moreover, there is a face segment $\bar{\boldsymbol{a}}\boldsymbol{cb}$ in $\mathcal{F}$ as (a, b, c) bounds an inner face of T_1.

Now consider T_2 and a vertex v of T_2. Assume v is the only vertex of T_2 adjacent to a in T. Then v is also the only vertex of T_2 adjacent to b and c in T as the subgraph of T inside (a, b, c) has no separating 3-cycle. Otherwise, each of the vertices a, b and c is adjacent to at least two vertices of T_2.

In the first case, it is easy to add a segment representing v see the left-hand side of Figure 4.5. Furthermore it is possible to add face-segments representing the triangles abv, acv and bcv to the full model of T_1 in order to obtain a full model of T. This is done by choosing a real number $\epsilon > 0$ such that the ϵ-ellipse around the face-segment $\bar{\boldsymbol{a}}\boldsymbol{bc}$ is intersected only by p_a, p_b and p_c. Within this ϵ-ellipse, p_v and the face-segments representing abv, acv and bcv can be placed.

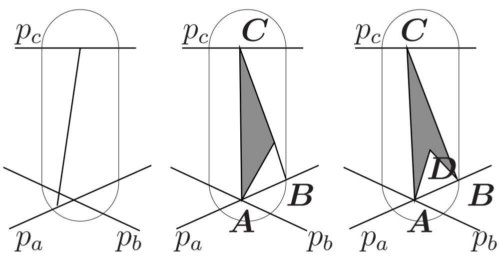

Figure 4.5: An ϵ-ellipse around the face segment $\bar{\boldsymbol{a}}\boldsymbol{bc}$ contains different premodels of T_2.

In the second case T_2 forms a 3-bounded W-triangulation. Let $(a_1, ..., a_p)$

be the path in T_2 that consists exactly of the vertices of T_2 adjacent to a. Analogously there is a path $(b_1, ..., b_q)$ and a path $(c_1, ..., c_r)$ consisting exactly of the vertices of T_2 adjacent to b and c respectively such that $a_p = b_1, b_q = c_1$ and $c_r = a_1$. As $p > 1, q > 1$ and $r > 1$, cycle $(a_1, ..., a_p, b_2, ..., b_q, c_2, ..., c_r)$ bounds T_2 so that T_2 is a W-triangulation. Furthermore, there does not exist an inner chord $a_i a_j$, $b_k b_l$ or $c_m c_n$ with $1 < i + 1 < j \leq p$, $1 < k + 1 < l \leq q$ and $1 < m + 1 < n \leq r$ as this would imply a separating 3-cycle within T'. Thus T_2 is a 3-bounded W-triangulation.

As for the induction basis, the authors use Lemma 4.9 to proceed.

Lemma 4.9. Consider a W-triangulation T, 3-bounded by $(a_1, ..., a_p) - (c_1, ..., b_q) - (c_1, ..., c_r)$.

1. If $p = 2$ for any triangle $\boldsymbol{BCD}$ there exists a premodel $\mathcal{M} = (\mathcal{S}, \mathcal{F}, \varphi)$ of T contained in $\boldsymbol{BCD}$ such that
   - $\boldsymbol{B}$ is a path-$(b_1, ..., b_q)$-point,
   - $\boldsymbol{C}$ is a path-$(c_1, ..., c_r)$-point,
   - $\boldsymbol{D}$ is a fan-a_2-$(d_1, ..., d_s, a_1)$-point with $d_1, ..., d_s$ being inner vertices of T and a face-segment incident if and only if $s = 0$.
2. If $p > 2$, for any triangle $\boldsymbol{ABC}$ there exists a point $\boldsymbol{D}$ inside $\boldsymbol{ABC}$ and a premodel $\mathcal{M} = (\mathcal{S}, \mathcal{F}, \varphi)$ of T contained in the polygon $\boldsymbol{ABCD}$ such that
   - $\boldsymbol{A}$ is a path-$(a_2, ..., a_p)$-point,
   - $\boldsymbol{B}$ is a path-$(b_1, ..., b_q)$-point,
   - $\boldsymbol{C}$ is a path-$(c_1, ..., c_r)$-point,
   - $\boldsymbol{D}$ is a crossing point of p_{a_1} and p_{a_2}.

As a consequence of Lemma 4.9 there is a premodel for T_2 that lies inside a triangle $\boldsymbol{BCD}$ if $p = 2$ and inside a polygon $\boldsymbol{ABCD}$ otherwise. This premodel of T_2 is glued into an ϵ-ellipse containing the face-segment $\bar{\boldsymbol{a}}\boldsymbol{bc}$ in the full model of T_1; the result is a premodel of T, sketched in the middle and on the right-hand side of Figure 4.5. By Corollary 4.8 this premodel can be changed into a full model of T which is a segment representation of T. This finishes the proof of Theorem 4.6.

4.3 Pseudosegment graphs and arrangements

Already in [20], one of the first papers on string graphs, the relation between pseudosegment and segment graphs is investigated. In this context, an example of a pseudosegment graph that is not a segment graph is given. In [47], a general construction of pseudosegment graphs that are not segment graphs is given in the proof of the following theorem.

Theorem 4.10. ([47]) Let $\mathcal{P}_n$ be a simple partial arrangement of n pseudolines that constitutes a pseudosegment representation of a graph G. Then there exists a pseudosegment graph G' on $O(n^2)$ vertices (and is constructible in polynomial time), containing G as an induced subgraph, with the following property:

G' is a segment graph if and only if $\mathcal{P}_n$ is stretchable.

□

With Theorem 4.11 we prove a weaker version of this result using a graph $\tilde{G}$ different from G' which naturally carries the combinatorial structure of the given pseudoline arrangement.

Theorem 4.11. Let $\mathcal{L}_n$ be a simple arrangement of n pseudolines; this arrangement constitutes a pseudosegment representation of the complete graph K_n. Then there exists a pseudosegment graph $\tilde{G}$ on $O(n^2)$ vertices, containing K_n as a subgraph, with the following property:

$\tilde{G}$ is a segment graph if and only if $\mathcal{L}_n$ is stretchable.

The proof of Theorem 4.11 consists of three parts. The first part is the definition of the graph $\tilde{G}$. This is given in Section 4.3.1. Then, in Section 4.3.2 we will show that $\mathcal{L}_n$ is stretchable, if $\tilde{G}$ is a segment graph. Finally, in Section 4.3.3 we will assume that $\mathcal{L}_n$ is stretchable and construct a segment representation of $\tilde{G}$, thus showing that $\tilde{G}$ is a segment graph.

4.3.1 From an arrangement of pseudolines to a pseudosegment graph

Before we come to the precise definition of a graph $\tilde{G}$, let us recall that the term pseudoline was introduced by Levi in [48] as a generalization of a

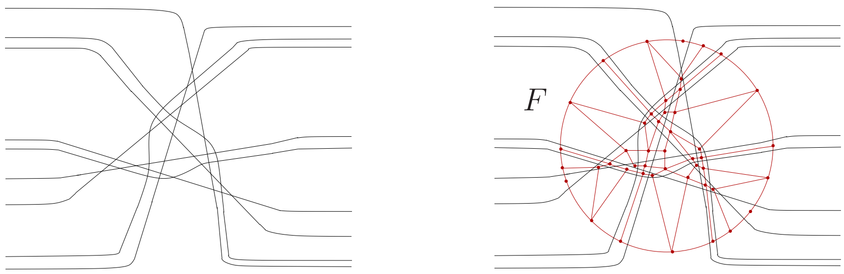

Figure 4.6: The false Pappus arrangement and its dual graph naturally embedded into it.

straight line. The *false Pappus arrangement*, sketched in Figure 4.6, is an example of a nonstretchable pseudoline arrangement.

The combinatorial structure of a pseudoline arrangement can be captured by its *dual graph*. Here, the *dual graph* of the pseudoline arrangement $\mathcal{L}$ has the faces of $\mathcal{L}$ as vertices such that two vertices f, f' of the dual graph of $\mathcal{L}$ are adjacent if and only if f and f' share an edge of $\mathcal{L}$ on their boundary. If f and f' share edge e of $\mathcal{L}$ on their boundary, then $e^* = ff'$ is an edge of the dual graph of $\mathcal{L}$ and is called the dual edge of e.

The definition of the dual graph $\bar{D}$ of $\mathcal{L}$ induces a *natural (planar) embedding* of $\bar{D}$ within $\mathcal{L}$ similar to the embedding of the dual graph of a plane graph; as an example of such an embedding consider the dual graph of the false Pappus arrangement naturally embedded into it on the right-hand side of Figure 4.6. Note that a marked pseudoline arrangement is uniquely determined by its corresponding marked dual graph [25].

Definition of a pseudosegment graph $\tilde{G}$

Now we come to the construction of a pseudosegment graph $\tilde{G}$ associated with a given pseudoline arrangement $\mathcal{L}_n$. We will construct a graph $\tilde{G}$ that contains the complete subdivision of the dual graph of $\mathcal{L}_n$ as an induced subgraph. This will allow us to transfer the question whether $\tilde{G}$ is a segment graph or not to the question whether $\mathcal{L}_n$ is stretchable or not.

Let $\mathcal{L}_n$ be an arbitrary simple arrangement of pseudolines and $\bar{D}$ a natural embedding of the dual graph of $\mathcal{L}_n$ within $\mathcal{L}_n$. Choose a circle $\mathcal{C}_{\bar{D}}$ that completely contains $\bar{D}$ and, hence, also all intersection points of elements of $\mathcal{L}_n$ in its interior. If we delete all pieces of pseudolines of $\mathcal{L}_n$ that are outside of $\mathcal{C}_{\bar{D}}$, we obtain an arrangement $\mathcal{S}_n$ of pseudosegments and an embedding of $\bar{D}$ into $\mathcal{S}_n$. We call $\mathcal{S}_n$ the arrangement of pseudosegments that is *induced* by $\mathcal{L}_n$. Note that $\mathcal{S}_n$ is stretchable if and only if $\mathcal{L}_n$ is stretchable. Now let $p_i \in \mathcal{S}_n$ be the pseudosegment that is supported by $\bar{p}_i \in \mathcal{L}_n$. We will add a vertex to $\bar{D}$ for every endpoint of every element of $\mathcal{S}_n$. To do so set $\mathcal{C}_D$ as the circle that results from augmenting the radius of circle $\mathcal{C}_{\bar{D}}$ by some $\epsilon > 0$. Then $\mathcal{S}_n \cup \bar{D}$ is completely contained in the interior of $\mathcal{C}_D$. Now we add vertices v_{i1} and v_{i2} at the intersection points of pseudoline $\bar{p}_i \in \mathcal{L}_n$ with the circumscribing circle $\mathcal{C}_D$. We denote the endpoint of p_i that is next to v_{ij} on $\bar{p}_i$, by e_{ij}, $j \in \{1, 2\}$ and call v_{ij} an *endpoint vertex*. This is done for every pseudoline of $\mathcal{L}_n$. The pieces of $\mathcal{C}_D$ between two endpoint vertices that are consecutive on $\mathcal{C}_D$ are now taken as edges between the respective vertices such that we obtain a cycle on $2n$ vertices that encloses $\mathcal{S}_n \cup \bar{D}$. For an illustration see Figure 4.7. This cycle is called the *frame*.

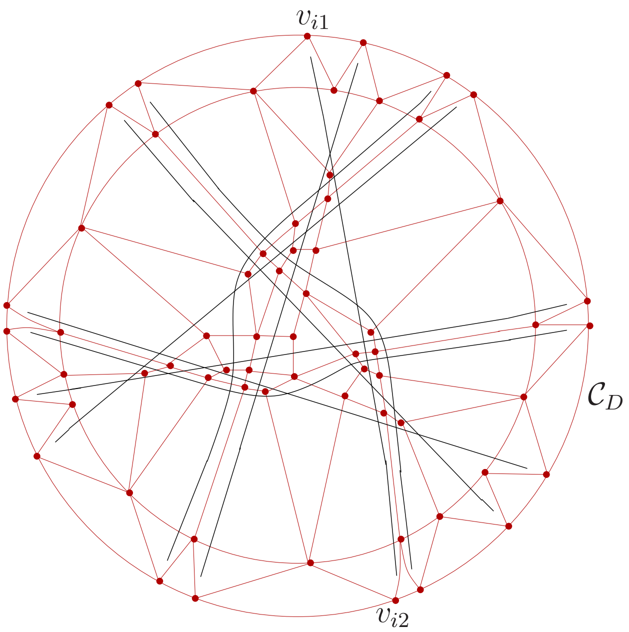

Figure 4.7: The graph D, embedded into the false Pappus arrangement, consists of $\bar{D}$ and the attached frame.

Finally we connect each vertex v_{ij} to the two vertices that correspond to the unbounded faces of $\mathcal{L}_n$ that have e_{ij} on their boundary. This can be done so that the resulting drawing is a plane graph and completes the construction of the graph D. In Figure 4.7, the plane graph D resulting from the false

Pappus arrangement, is naturally embedded into the arrangement.

We will refer to the union of $\mathcal{S}_n$ and the planar embedding of D within $\mathcal{S}_n$ that fulfills the latter condition as natural embedding of D within $\mathcal{S}_n$ and denote it by $\mathcal{S}_n^D$. Now we are ready to define $\tilde{G}$.

Definition 4.12. On the vertex set $V(\tilde{G}) = V(D) \cup E(D) \cup \{p \mid p \in \mathcal{S}_n\}$ we define the graph $\tilde{G}$ with edges $uv \in E(\tilde{G})$ if and only if in the natural embedding $\mathcal{S}_n^D$

- $u \in V(D)$, $v \in E(D)$ and v is incident to u in D or
- $u, v \in \mathcal{S}_n$ and $u \neq v$ or
- $u \in E(D)$ is the dual edge of an edge of pseudoline $\bar{v}$ of $\mathcal{L}_n$ corresponding to v of $\mathcal{S}_n$.

By definition we have that $|V(D)| = (\binom{n}{2}+n+1)+2n$ and $|E(D)| = n^2+6n$. With $\mathcal{S}_n$ we then obtain that

$$|V(\tilde{G})| = \frac{1}{2}(3n^2 + 19n + 2) \in O(n^2).$$

Lemma 4.13. The graph $\tilde{G}$ of Definition 4.12 is a pseudosegment graph.

Proof. To obtain a pseudosegment representation of $\tilde{G}$, consider the embedding of D in $\mathcal{S}_n^D$. Here, every element of $\mathcal{S}_n$ and $E(D)$ is a Jordan arc such that $p \in \mathcal{S}_n$ and $e \in E(D)$ intersect if and only if they are adjacent in $\tilde{G}$. In $\mathcal{S}_n^D$ graph D is naturally embedded into $\mathcal{S}_n$, so that p and e intersect at most once, and if they intersect, they cross.

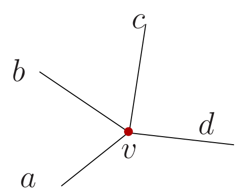

Figure 4.8: The Jordan arcs that represent the neighbors of v in $\tilde{G}$ are cyclically arranged around v in $\mathcal{S}_n^D$.

Two Jordan arcs representing edges of D intersect in their endpoints if and only if they are incident to the same vertex. These points will be extracted to Jordan arcs such that the Jordan arcs of elements of $E(D)$ do no longer intersect. This is done as follows: remove the endpoints of every Jordan arc of $\mathcal{S}_n^D$ representing an element of $E(D)$ and denote the union of the thus shortened Jordan arcs by $\mathcal{P}_2$. Let $\mathcal{P}_1$ be $\mathcal{S}_n$. Then $\mathcal{P}_1 \cup \mathcal{P}_2$ is a pseudosegment representation of the subgraph of $\tilde{G}$ induced by $\mathcal{S}_n \cup E(D)$.

Next consider an arbitrary element v of $V(D)$. In $\mathcal{S}_n^D$ vertex v is a point contained within a face or a pseudoline of $\mathcal{L}_n$. Let $E(v) \subset E(D)$ be the set of elements adjacent to v in $\tilde{G}$. The Jordan arcs of $\mathcal{P}_2$ corresponding to the elements of $E(v)$ are cyclically arranged around v in $\mathcal{S}_n^D$. Hence we can replace every point $v \in V(D)$ by a Jordan arc p_v disjoint from $\mathcal{S}_n$ such that

- p_v intersects a Jordan arc of $\mathcal{P}_2$ if and only if this Jordan arc corresponds to an element of $E(v)$,
- $\mathcal{P}_3 := \{p_v \mid v \in V(D)\}$ is a set of disjoint pseudosegments, and
- $\mathcal{P}_2 \cup \mathcal{P}_3$ is a set of pseudosegments.

Figure 4.9: Two Jordan arcs that represent vertex $v \in V(D)$ in a pseudosegment representation of $\tilde{G}$ resulting from $\mathcal{S}_n^D$.

Examples of Jordan arcs representing the elements of $V(D)$ are given in Figure 4.9. All this is possible without changing the intersection relations within $\mathcal{S}_n^D$. Then the union $\tilde{\mathcal{G}} = \mathcal{P}_1 \cup \mathcal{P}_2 \cup \mathcal{P}_3$ is a pseudosegment representation of $\tilde{G}$. An example of such a pseudosegment representation of $\tilde{G}$ is given in Figure 4.10. $\square$

4.3.2 If $\tilde{G}$ is a segment graph, then $\mathcal{L}_n$ is stretchable.

Let $\mathcal{L}_n$ be an arbitrary simple pseudoline arrangement, $\mathcal{S}_n$ the arrangement of pseudosegments induced by $\mathcal{L}_n$ and $\bar{D}$ the dual graph of $\mathcal{L}_n$. Then we construct D as in Section 4.3.1 and obtain $\tilde{G}$ from Definition 4.12. One

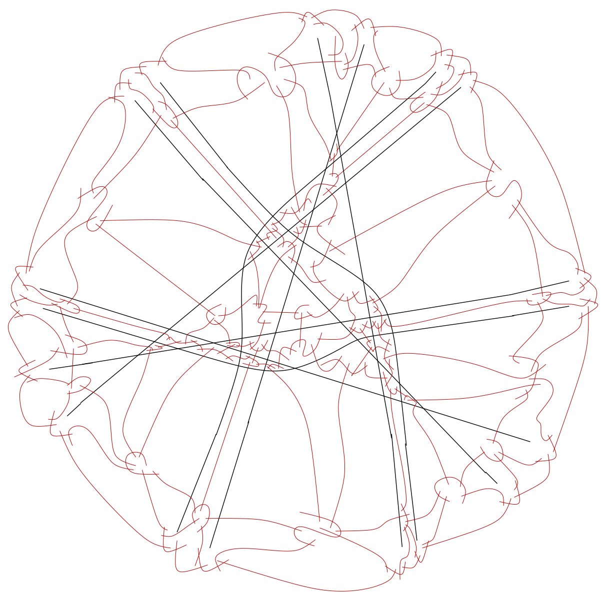

Figure 4.10: A pseudosegment representation of $\tilde{G}$, when $\tilde{G}$ is defined using the false Pappus arrangement.

implication of Theorem 4.11 is that $\mathcal{L}_n$ is stretchable, if $\tilde{G}$ is a segment graph. To prove this implication we show the contrary, stated next as Lemma 4.14.

Lemma 4.14. If $\mathcal{L}_n$ is nonstretchable, then $\tilde{G}$ is not a segment graph.

To prove Lemma 4.14 we will first show that D is a 3-connected planar graph; this implies that D has a combinatorially unique dual graph. Then we will use the definition of the pseudosegment graph $\tilde{G}$ to deduce certain conditions on the intersection behavior within an arbitrary pseudosegment representation of $\tilde{G}$. These are recorded in Lemma 4.17. They imply that the subgraph of $\tilde{G}$ induced by $\mathcal{S}_n$ represents a set of paths of the dual graph of D. The key argument to prove Lemma 4.14 is then given as Corollary 4.18.

Lemma 4.15. The graph D is a 3-connected planar graph.

In the proof of Lemma 4.15 we will use a "separating" subgraph of D defined as follows: let E_i be the set of edges of D intersected by p_i in $\mathcal{S}_n^D$. Then we call the subgraph of D induced by the endpoint vertices e_{i1}, e_{i2} and the vertices of E_i the *ladder* L_i of p_i, see Figure 4.11 for an illustration.

Proof. By construction, the embedding of D within $\mathcal{S}_n^D$ is planar. Thus, it remains to show that for all $u, v \in V(D)$ there are three different, pairwise internally disjoint u, v-paths in D. So consider an arbitrary pair of vertices f_i, f_j of $D \subset \mathcal{S}_n^D$. They either correspond to faces of $\mathcal{L}_n$ or to endpoints of pseudosegments of $\mathcal{S}_n$. As we concentrate on simple pseudoline arrangements, every bounded face of $\mathcal{L}_n$ has at least three edges of $\mathcal{L}_n$ on its boundary and every unbounded face at least two. If f_i corresponds to a face of $\mathcal{L}_n$, choose p_i to be a pseudosegment that contributes an edge to the boundary of f_i. If f_i represents an endpoint of pseudosegment q of $\mathcal{S}_n$, set $p_i = q$. Then choose p_j in the same way with the additional condition that p_j is different from p_i.

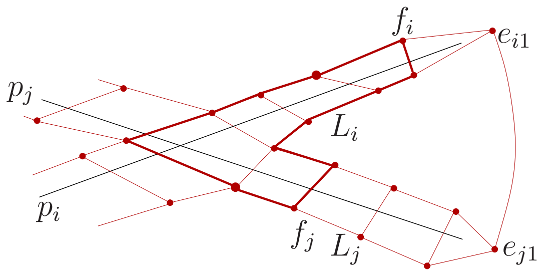

Figure 4.11: Every pair of vertices of D is connected by at least two disjoint paths.

Recall that every pair of pseudosegments of $\mathcal{S}_n$ intersects. Hence, there are $f_i f_j$-paths in D within $L_i \cup L_j$, as sketched in Figure 4.11. Let $P^1(f_i, f_j)$ be a shortest $f_i f_j$-path within $L_i \cup L_j$.

By the definition of a ladder, there is a further $f_i f_j$-path within $L_i \cup L_j$ that is internally disjoint from $P^1(f_i, f_j)$ and does not have an endpoint vertex as interior vertex. Let $P^2(f_i, f_j)$ be such an $f_i f_j$-path with the minimum number of edges. The existence of $P^1(f_i, f_j)$ and $P^2(f_i, f_j)$ implies that D is 2-connected.

Now consider the frame of D, that is the cycle of D that consists of endpoint vertices. If f_i is the endpoint vertex of pseudosegment p_i, assume f_i to be e_{i1}. Otherwise choose e_{i1} to be the endpoint of p_i such that p_j does not cross p_i between f_i and e_{i1}. In the same way determine e_{j1} for f_j. Recall that the degree of every vertex of D is at least three. Then f_i can be connected to e_{i1} by a path $P(f_i, e_{i1})$, which is internally disjoint from $P^1(f_i, f_j)$ and $P^2(f_i, f_j)$. An analog path, denoted by $P(f_j, e_{j1})$, exists for f_j. The vertices e_{i1} and e_{j1} lie on the frame which does not contain any vertex of $\bar{D}$. Hence, they can be connected by at least one path $P(e_{i1}, e_{j1})$, consisting only of endpoint vertices. The union of $P(f_1, e_{i1})$, $P(e_{i1}, e_{j1})$ and $P(e_{j1}, f_j)$ is an f_i, f_j-path that is internally disjoint from $P^1(f_i, f_j)$ and $P^2(f_i, f_j)$. As f_i and f_j were chosen arbitrarily, every pair of vertices of D can be connected by at least three different internally disjoint paths, hence D is 3-connected. □

Lemma 4.15 together with Theorem 2.5 implies that D has a combinatorially unique dual graph.

Now let $\mathcal{G}$ be an arbitrary but fixed pseudosegment representation of $\tilde{G}$. As in the proof of Lemma 4.13, let $\mathcal{P}_1$, $\mathcal{P}_2$ and $\mathcal{P}_3$ be the pseudosegments of $\mathcal{G}$ representing $\mathcal{S}_n$, $E(D)$ and $V(D)$ respectively. For every $p_i \in \mathcal{S}_n$ let $g_i \in \mathcal{P}_1$ be the pseudosegment representing p_i. Furthermore set $\mathcal{E}_i \subset \mathcal{P}_2$ as the set of pseudosegments representing the elements of E_i, that is the elements of $E(D)$ adjacent to p_i. Note that we can order each set $\mathcal{E}_i$ according to the order in which g_i intersects the elements of $\mathcal{E}_i$ in $\mathcal{G}$, say $\bar{\mathcal{E}}_i := (q_{i1}, ..., q_{in})$. This order induces a linear order on the respective set E_i, called the *intersection order* of E_i with respect to $\mathcal{G}$. We say that elements q_{i1} and q_{in} contribute to the outer and elements $q_{i2}, ..., q_{i(n-1)}$ to the inner intersections of g_i. Let us denote the vertex of the endpoint of $p_i \in \mathcal{S}_n$ that is next to q_{i1} by e_{i1}, and the one next to q_{in} by e_{i2}.

Analogously, pseudosegment $q_{ij} \in \mathcal{E}_i$ induces an intersection order on the elements it intersects so that each q_{ij} has exactly two outer and one inner intersection.

Observation 4.16. Let $\mathcal{G}$ be an arbitrary pseudosegment representation of $\tilde{G}$. Every element of $\mathcal{P}_2 \subset \mathcal{G}$ has exactly two intersections with two different elements of $\mathcal{P}_3 \subset \mathcal{G}$ and no intersection with any other element of $\mathcal{P}_2$ nor with any element of $\mathcal{P}_1 \subset \mathcal{G}$. For every element $q \in \mathcal{P}_2$, let us denote the part of q that connects the two intersection points with elements of $\mathcal{P}_3$ as *edge segment* b of q.

As no element of $\mathcal{P}_3$ intersects any element of $\mathcal{P}_1$, we can contract the pseudosegments of $\mathcal{P}_3$ to points. This contraction can be carried out without changing any intersection relation between an element of $\mathcal{P}_1$ and an element of $\mathcal{P}_2 \cup \mathcal{P}_3$. Thus, we obtain a planar embedding $D_{\mathcal{G}}$ of D from $\mathcal{P}_2 \cup \mathcal{P}_3$ naturally embedded within $\mathcal{P}_1$; note that there possibly remain pending ends of elements of $\mathcal{P}_2$.

Lemma 4.17. Let $\mathcal{G}$ be an arbitrary pseudosegment representation of $\tilde{G}$. Let $g_i \in \mathcal{P}_1 \subset \mathcal{G}$ and $q_{ij} \in \bar{\mathcal{E}}_i$, $\bar{\mathcal{E}}_i \subset \mathcal{P}_2 \subset \mathcal{G}$. If q_{ij} contributes to an inner intersection of g_i, then g_i contributes to an inner intersection of q_{ij}.

Proof. Let $\mathcal{G}$ be an arbitrary pseudosegment representation of $\tilde{G}$ consisting of $\mathcal{P}_1$, $\mathcal{P}_2$ and $\mathcal{P}_3$. Consider a pseudosegment $g_i \in \mathcal{P}_1$. Then g_i contributes to an inner intersection of pseudosegment q_{ij} if and only if the intersection of g_i and pseudosegment q_{ij} takes place within the edge segment b_{ij}.

We will prove Lemma 4.17 by contradiction, so assume that g_i intersects a pending end r of q_{ij} for a $j \in \{2, ..., n-1\}$. Consider the embedding $D_{\mathcal{G}}$ of D within $\mathcal{P}_1$, obtained as described in Observation 4.16. For every $i \in [n]$ there is a $k \in [n]\backslash\{i\}$ such that b_{ij} is an edge of ladder L_k in $D_{\mathcal{G}}$. Then there is a path $P_{L_k}(e_{k1}, e_{k2}) \subset L_k$ that contains b_{ij} and does not contain any edge of $D_{\mathcal{G}}$ that is an edge of E_k. Now set $P_{fr}(e_{k1}, e_{k2})$ as the subpath of the frame of $D_{\mathcal{G}}$ that contains e_{i1}. The latter path $P_{fr}(e_{k1}, e_{k2})$ together with $P_{L_k}(e_{k1}, e_{k2})$ is a closed curve $\mathcal{C}_r$ embedded within $\mathcal{P}_1$. An example of such a curve is depicted in Figure 4.12.

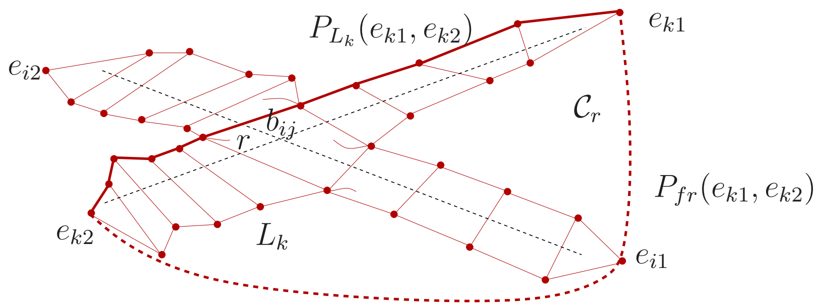

Figure 4.12: The pending end r of q_{ij} lies either inside or outside of $\mathcal{C}_r$, and, thus, g_i lies either inside or outside of $\mathcal{C}_r$.

Note that the pending end r of q_{ij} lies either inside or outside the cycle $\mathcal{C}_r$. Moreover, $q_{i,1}, .., q_{i,j-1}$ lie outside and $q_{i,j+1}, ..., q_{i,n}$ inside $\mathcal{C}_r$. Recall that g_i intersects $q_{i,1}, ..., q_{i,n}$ as it represents p_i; thus g_i has to intersect $\mathcal{C}_r$. The only part of $\mathcal{C}_r$ that can be intersected by g_i is b_{ij}. As g_i intersects r, it cannot intersect b_{ij} as we are given a pseudosegment representation. Hence g_i has to lie within one of the regions defined by $\mathcal{C}_r$. But then it either does not intersect $q_{i,1}, .., q_{i,j-1}$ or $q_{i,j+1}, ..., q_{i,n}$. In either case g_i does not represent p_i so that $\mathcal{G}$ is not a pseudosegment representation. Thus, g_i has to intersect the edge segments of $q_{i2}, ..., q_{i(n-1)}$ in order to represent p_i. Hence, if q_{ij} is a pseudosegment contributing to an inner intersection of g_i, then g_i contributes to an inner intersections of q_{ij}. □

Lemma 4.15 together with Lemma 4.17 gives the key argument to prove Lemma 4.14.

Corollary 4.18. Let $\mathcal{G}$ be an arbitrary pseudosegment representation of $\tilde{G}$ with $\mathcal{P}_1 \subset \mathcal{G}$ representing the elements of $\mathcal{S}_n$. Then $\mathcal{P}_1$ is isomorphic to $\mathcal{S}_n$. □

Proof. Recall the pseudosegment representation $\tilde{\mathcal{G}}$ of $\tilde{G}$ resulting from $\mathcal{S}_n^D$ in the proof of Lemma 4.13. For $p_i \in \mathcal{S}_n$ let $\bar{E}_i = (e_{i1}, ..., e_{in})$ denote the elements of E_i ordered according to the intersection order induced by p_i with respect to $\tilde{\mathcal{G}}$. Let e^*_{ij} be the dual edge of e_{ij}. As D is the dual graph of $\mathcal{L}_n$ and D^* is the dual graph of D, it holds that the edges $e^*_{i1}, ..., e^*_{in}$ of D^* induce the chordless path $P^*_i = (e^*_{i1}, ..., e^*_{in}) \subset D^*$. Thus, pseudosegment $p_i \subset \tilde{\mathcal{G}}$ can be seen as a natural embedding of P^*_i into $D \subset \tilde{\mathcal{G}}$.

Now consider an arbitrary pseudosegment representation $\mathcal{G}$ of $\tilde{G}$. Let $g_i \in \mathcal{P}_1$ be the pseudosegment of $\mathcal{G}$ representing p_i and let $\bar{\mathcal{E}}_i$ be the pseudosegments of $\mathcal{G}$ representing the elements of E_i given in the intersection order with respect to $\mathcal{G}$. Let $D_{\mathcal{G}}$ be the planar embedding of D contained within $\mathcal{G}$ as obtained in Observation 4.16. With Lemma 4.15 we know that D^* is combinatorially unique, so that edges $e^*_{i1}, ..., e^*_{in} \in E(D^*_{\mathcal{G}})$ induce the chordless path $P^*_i = (e^*_{i1}, ..., e^*_{in})$. Hence, $\bar{\mathcal{E}}_i = (q_{i1}, ..., q_{in})$ such that q_{ij} represents either e_{ij} or $e_{i(n-j+1)}$. As a consequence of Lemma 4.17, g_i contains a natural embedding of the path $P(e^*_{i2}, e^*_{i,(n-1)}) \subset P^*_i$ within $D_{\mathcal{G}}$. Thus, the uniqueness of D^* induces an incidence and dimension preserving isomorphism between $\mathcal{P}_1$ and $\mathcal{S}_n$. □

Proof of Lemma 4.14. Let $\mathcal{L}_n$ be a nonstretchable pseudoline arrangement and $\mathcal{S}_n$ the induced arrangement of pseudosegments. If there is a segment representation $\mathcal{G}_S$ of $\tilde{G}$, then Corollary 4.18 implies that the subset $\mathcal{P}_1$ of $\mathcal{G}_S$ representing the elements of $\mathcal{S}_n$ is isomorphic to $\mathcal{S}_n$. But as $\mathcal{S}_n$ is not stretchable, $\mathcal{P}_1 \subset \mathcal{G}_S$ yields that $\mathcal{G}_S$ is not a segment representation of $\tilde{G}$. □

4.3.3 If $\mathcal{L}_n$ is stretchable, then $\tilde{G}$ is a segment graph.

Let us reformulate the remaining implication of Theorem 4.11 as Lemma 4.19.

Lemma 4.19. If $\mathcal{L}_n$ is stretchable, then $\tilde{G}$ is a segment graph.

Proof. If $\mathcal{L}_n$ is stretchable, then there is a straight line arrangement isomorphic to $\mathcal{L}_n$. So let $\mathcal{L}_n$ be an arbitrary simple straight line arrangement, let $\mathcal{S}_n$ be the arrangement of segments induced by $\mathcal{L}_n$ and let $\bar{D}$ be the dual graph of $\mathcal{L}_n$. We construct D as in Section 4.3.1 and obtain $\tilde{G}$ from Definition 4.12. To obtain a segment representation of $\tilde{G}$, we will proceed similar to the proof of Lemma 4.13 where we showed that $\tilde{G}$ is a pseudosegment graph.

First replace each Jordan arc of $\mathcal{S}_n^D$ that is an edge e of D by a straight line segment $|_e$ with the same endpoints. This gives a straight line embedding $\mathcal{D}$ of D within $\mathcal{S}_n$. Denote the union of $\mathcal{S}_n$ and $\mathcal{D}$ embedded into $\mathcal{S}_n$ by $\mathcal{S}_n^{\mathcal{D}}$; a part of a natural straight line embedding of D within $\mathcal{S}_n$ is illustrated in Figure 4.13.

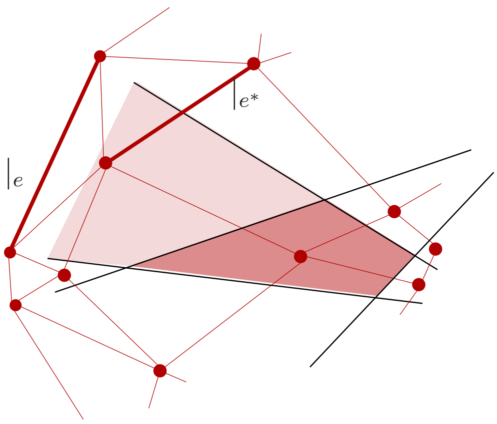

Figure 4.13: Nonadjacent edges of $\mathcal{D}$ are disjoint.

Claim. The embedding $\mathcal{D} \subset \mathcal{S}_n^{\mathcal{D}}$ of D is a natural embedding of D within $\mathcal{S}_n$.

Proof. Recall that the vertices, edges and faces of $\mathcal{L}_n$ partition the plane. This in addition with the following fact suffices to show that $\mathcal{D}$ is a natural embedding of D within $\mathcal{S}_n$, that is $\mathcal{D}$ is planar and any edge of $\mathcal{D}$ intersects an edge of $\mathcal{S}_n$ if and only if it is dual to this edge of $\mathcal{S}_n$.

Fact 1. Every face of a straight line arrangement is convex, and so is the closure of every face.

An edge of D is either dual to an edge of $\mathcal{L}_n$ or incident to an endpoint vertex. If edge e of D is incident to an endpoint vertex, we have $e = fv_{ij}$

or $e = v_{ij}v_{kl}$ such that endpoint vertices v_{ij}, v_{kl} lie on the boundary of the unbounded face f. In this case, Fact 1 and the constructive definition of D imply that $|_e \subset \bar{f}$, and $|_e$ is disjoint from any vertex or edge of $\mathcal{S}_n$.

If $e^* \in E(D)$ is dual to edge e of $\mathcal{L}_n$, there are faces f, f' of $\mathcal{L}_n$ such that $e^* = ff'$ and e is the common boundary of f and f'. Let $\bar{p}$ be the pseudoline of $\mathcal{L}_n$ supporting e. Then $F_e := f \cup e \cup f'$ is a face of $\mathcal{L}_n \backslash \{\bar{p}\}$, and is, by Fact 1, convex. Since $|_{e^*}$ connects a point of f to a point of f', it holds that $|_{e^*} \subset F_e$. This furthermore implies that $|_{e^*}$ intersects e in a single crossing point as required in a natural embedding of D within $\mathcal{S}_n$, and is disjoint from any other vertex or edge of $\mathcal{S}_n$ or face of $\mathcal{L}_n$.

To see that $\mathcal{D}$ is planar let us remind you of the partitioning of the plane given by $\mathcal{L}_n$. Then the latter analysis implies that it suffices to consider a pair of edges $e^* = ff'$ and $e = v_{ij}v_{kl}$ such that v_{ij} and v_{kl} lie on the boundary of face f; two such edges are drawn with thick lines in Figure 4.13. In this case, the definition of $\mathcal{S}_n^{\mathcal{D}}$ implies that $|_e$ and $|_{e^*}$ lie in different halfplanes with respect to the straight line $l_{ij,kl}$ that contains e_{ij} and e_{kl}. Thus, the segments of any pair of edges are either disjoint or intersect in a common endpoint. As common endpoints accord with edges of D adjacent in D, it follows that $\mathcal{D}$ is planar and is a natural embedding of D within $\mathcal{S}_n$. $\square$

This at hand we come to construct a segment representation of $\tilde{G}$. Consider $\mathcal{S}_n^{\mathcal{D}}$ and choose $\mathcal{S}_n \subset \mathcal{S}_n^{\mathcal{D}}$ as segment representation of the subgraph of $\tilde{G}$ induced by $\mathcal{S}_n$ such that each $p_i \in \mathcal{S}_n$ represents itself. To obtain a segment representation of $\tilde{G}$, we will first extend the points of $\mathcal{D}$ representing the elements of $V(D)$ to segments and obtain a segment representation of the subgraph of $\tilde{G}$ induced by $\mathcal{S}_n \cup V(D)$. In the second step we will continuously deform the segments representing the elements of $E(D)$ in $\mathcal{D}$ to segments representing the elements of $E(D)$ in a segment representation of $\tilde{G}$.

To extend the points of $\mathcal{D}$ representing the elements of $V(D)$ to segments, we will first choose a straight line for every such element; these will contain the later chosen segments. To do so note that the planar embedding $\mathcal{D}$ of D induces a cyclic ordering on the set $N_{\tilde{G}}(v)$ of neighbors of v for every $v \in V(D)$. Let us call this ordering the $\mathcal{D}$-*order* of $N_{\tilde{G}}(v)$ and set $d_f = d_{\tilde{G}}(v_f)$.

First let v_{ij} be the vertex of $\mathcal{D}$ that represents endpoint e_{ij} of segment $p_i \in \mathcal{S}_n$. Then v_{ij} is a point on $\mathcal{C}_D$ and we set l_{ij} as the tangent line of $\mathcal{C}_D$ at v_{ij}. This is done for every endpoint vertex of D. Recall that each endpoint vertex is adjacent to two other endpoint vertices v_{kl} and v_{gh}. Furthermore v_{ij} is adjacent to two vertices f, f' representing unbounded faces. Without loss of generality we assume that v_{kl} is adjacent to f and v_{gh} to f'. If $S_{(ij)(kl)}$ is the intersection point of l_{ij} and l_{kl}, then $S_{(ij)(kl)}$ lies within f by the choice of the lines l_{ij} and l_{kl}. Analogously, the intersection point $S_{(ij)(gh)}$ of l_{ij} and l_{gh} lies within f'. Let us remove $S_{(ij)(kl)}$ and $S_{(ij)(kl)}$ from l_{ij} and set s_{ij} as the resulting subset of l_{ij} that contains v_{ij}. Then we assign each v_{ij} to the respective s_{ij}. Note that no two lines l_{ij} and l_{kl} are the same and no two segments s_{ij},s_{kl} of different endpoints intersect.

Now let $(e_{ij,1}, ..., e_{ij,4})$ be a linear suborder of the cyclic $\mathcal{D}$-order of $N_{\tilde{G}}(v_{ij})$ such that $e_{ij,1}$ and $e_{ij,4}$ connect v_{ij} to endpoint vertices. Then choose four points on $s_{ij} \subset l_{ij}$ indexed by $(ij, 1), ..., (ij, 4)$ such that they are ordered on line l_{ij} as

$$(S_{(ij)(kl)}, P_{ij,1}, P_{ij,2}, e_{ij}, P_{ij,3}, P_{ij,4}, S_{(ij)(gh)}).$$

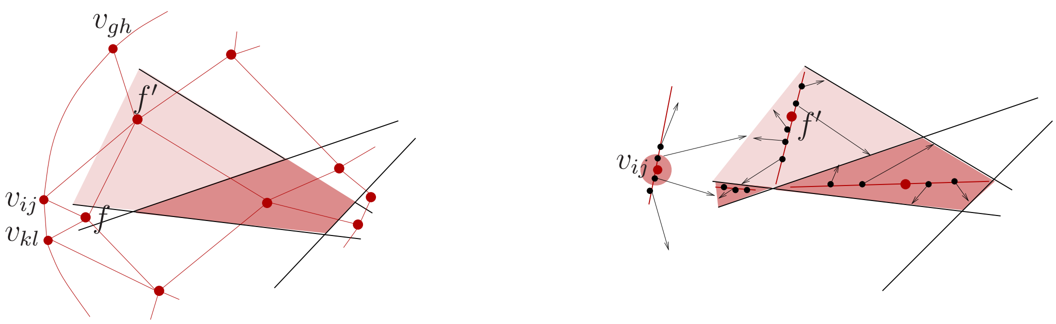

Figure 4.14: The points on a segment representing $v \in V(D)$ are assigned to the neighbors of v as indicated by the arrows.

Now let v_f be the vertex of $\mathcal{D}$ that represents face f of $\mathcal{L}_n$. Let l_f be a straight line containing v_f that is not parallel to a supporting line of any segment of $\mathcal{D}$ representing an element of $E(D)$ incident to v_f in $\mathcal{D}$.

Next let $(e_{f1}, ..., e_{fd_f})$ be a linear suborder of the cyclic $\mathcal{D}$-order of $N_{\tilde{G}}(v_f)$ such that $e_{f1}, ..., e_{ft_f-1}$ lie in one halfplane with respect to l_f and $e_{ft_f}, ..., e_{fd_f}$ in the other; thus $t_f \in \{2, ..., d_f - 1\}$. Then let $s_f \subset l_f$ be a segment with v_f as an inner point that is completely contained within f. If f is an unbounded face, we furthermore require that $s_f \subset \operatorname{conv}(\mathcal{S}_n)$. Let s_{fi} be the segment of $\mathcal{D}$ representing edge e_{fi} for $i \in \{1, ..., d_f\}$. Then we denote the endpoint of s_f that lies within $\operatorname{conv}(s_{f1}, s_{fd_f})$ by e_f^1, and the one within $\operatorname{conv}(s_{ft_f-1}, s_{ft_f})$

by e_f^2. Now choose d_f points on s_f and index them by $(f1), ..., (fd_f)$ such that they are ordered linearly on s_f as

$$(e_f^1, P_{f1}, ..., P_{ft_f-1}, v_f, P_{fd_f}, P_{fd_f-1}, ..., P_{ft_f}e_f^2).$$

This is done for every element of $V(D)$ representing a face of $\mathcal{L}_n$ such that no two lines l_f and $l_{f'}$ of different faces f, f' of $\mathcal{L}_n$ are the same. In Figure 4.14 an example of a choice of segments for elements of $V(D)$ and an assignment of the points for the elements of $E(D)$ is given.

Denote the union of the segments representing the elements of $V(D)$ as $\mathcal{S}_V$. By construction, every two segments of $\mathcal{S}_V$ are disjoint and $\mathcal{S}_V$ is disjoint from $\mathcal{S}_n$. This corresponds to the fact that elements of $V(D)$ are pairwise nonadjacent and no element of $V(D)$ is adjacent to any element of $\mathcal{S}_n$ in $\tilde{G}$. Furthermore, all segments that represent faces of $\mathcal{L}_n$ are contained within $\operatorname{conv}(\mathcal{S}_n)$.

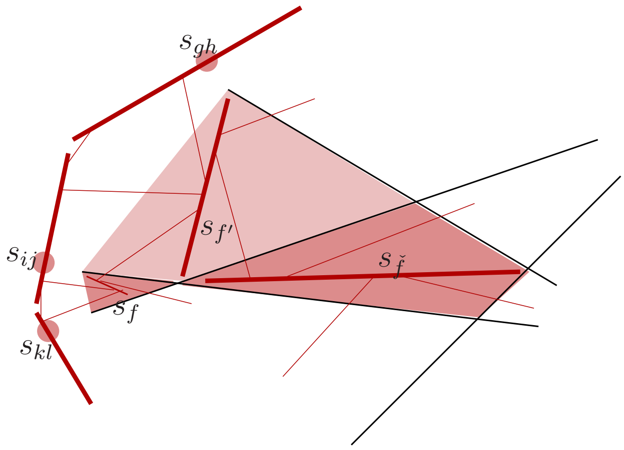

Figure 4.15: Using the points on the segments representing the elements of $V(D)$ we can exchange the segments representing the elements of $E(D)$ in $\mathcal{D}$ in order to obtain a segment representation of $\tilde{G}$.

Now we come to the second step. By the definition of $\mathcal{S}_n^{\mathcal{D}}$, every $e \in E(D)$ is represented by a segment $|_e$ that intersects exactly those elements of $\mathcal{S}_n$ and $V(D)$, the respective element of $E(D)$ is adjacent to in $\tilde{G}$. As $e = vv'$ with $v, v' \in V(D)$, e appears indexed in the two linear orders $\bar{N}_{\tilde{G}}(v)$ and $\bar{N}_{\tilde{G}}(v')$. Let us assume that $e = e_{vj}$ in $\bar{N}_{\tilde{G}}(v)$ and $e = e_{v'j'} \in \bar{N}_{\tilde{G}}(v')$ with $j \in \{1, ..., d_v\}$ and $j' \in \{1, ..., d_{v'}\}$. Then set $s_e := [P_{vj}, P_{v'j'}]$ and denote the set of all such segments representing elements of $E(D)$ bys $\mathcal{S}_E$.

By the choice of the segments of $\mathcal{S}_V$ and the points on these segments, it is possible to continuously deform segment $|_e$ to s_e without creating new intersections, see Figure 4.15 for an example of the resulting segments. Then every two segments s_e and $s_{e'}$ are disjoint. Furthermore, s_e intersects a segment of $\mathcal{S}_V \cup \mathcal{S}_n$ if and only if $|_e$ intersects this segment. This accords with the fact that the respective elements are adjacent in $\tilde{G}$.

Recalling the constructive definition of $\tilde{G}$, this implies that $\mathcal{G} = \mathcal{S}_n \cup \mathcal{S}_V \cup \mathcal{S}_E$ is a segment representation of $\tilde{G}$. Hence Lemma 4.19 holds. □

Lemma 4.14 together with Lemma 4.19 prove Theorem 4.11. An example of a segment representation resulting from this proof is given in Figure 4.16

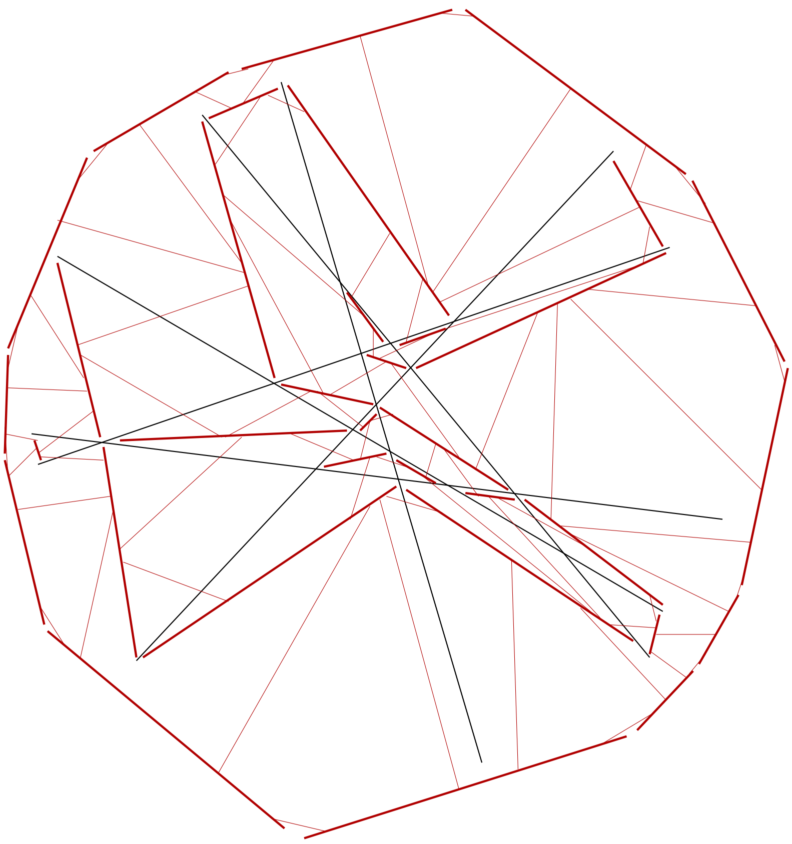

Figure 4.16: A segment representation of $\tilde{G}$ if the given arrangement $\mathcal{L}_n$ is stretchable.

4.4 Summary

One of the main open questions with respect to segment graphs has been answered by Chalopin and Gonçalves in [8] assuring that every planar graph has a segment representation. Let us point out that their result induces a proper coloring of the respective graph where the different directions of the segments are the colors. Recall that this is also the case for bipartite planar, triangle-free planar and series-parallel graphs. In each of the latter three cases the number of directions used in the respective segment representations is bounded by the chromatic number of the corresponding class. In [8] there is no bound given on the number of directions the segments lie in. Thus we are left with Conjecture 1.2.

Conjecture 1.2([68]) Every planar graph has a segment representation where the segments are of at most four directions.

Chapter 5

Chordal Graphs

A chordal graph is a graph that does not contain a chordless cycle. Already in 1972 Walter [66] showed that the class of chordal graphs is the class of tree graphs. This can be used to show that every chordal graph is a string graph. A famous subclass of chordal graphs are vertex intersection graphs of subpaths of a path, better known as interval graphs. Using the left-endpoint ordering of an interval representation one can easily construct a set of pseudosegments representing the respective interval graph. An example of such a representation is given in Figure 5.1. This raises the question whether path graphs, or even chordal graphs are intersection graphs of pseudosegments as well. Let us mention that the results of this chapter can be found in [11] and [12].

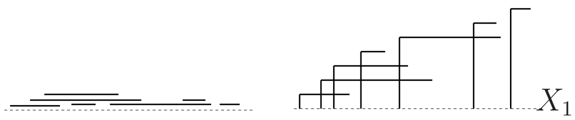

Figure 5.1: Every interval is lifted by the index it obtains from the given left-endpoint ordering; appending vertical segments of length of the respective heights gives the desired set of pseudosegment.

In the first section, we show that every path graph admits a pseudosegment representation. The proof is by induction and uses a path representation $(T, \mathcal{P})$ of the respective path graph where the set $\mathcal{P}$ consists only of *leaf-paths*.

Next, we introduce a family of chordal graphs to show that not every chordal graph is a pseudosegment graph. For every $n \in \mathbb{N}$, we define K_n^3 as the graph with vertex set $V = V_C \cup V_I$ such that $V_C = [n]$ induces a clique and $V_I = \binom{[n]}{3}$ is an independent set. The edges between V_C and V_I represent membership, that is $\{i, j, k\} \in V_I$ is adjacent to the vertices i, j and k from V_C. In every pseudosegment representation of K_n^3, the clique induced by V_C corresponds to an arrangement $\mathcal{S}_n$ of n pseudosegments. Here, the elements of V_I correspond to disjoint 3-segments of $\mathcal{S}_n$. By a planarity argument we then show that the size of a set of disjoint 3-segments in any pseudosegment representation of K_n^3 is at most $6n^2$. As $\binom{n}{3} > 6n^2$ for most $n \in \mathbb{N}$, it follows that K_n^3 is not a pseudosegment graph.

The upper bound on the number of disjoint 3-segments contained in $\mathcal{S}_n$ leads to considering arbitrary 3-segments of $\mathcal{S}_n$. One problem on bounding the number of arbitrary 3-segments contained in $\mathcal{S}_n$ is that the 3-segments can bypass the pseudosegments of the arrangement at their ends.

This is not a problem if we consider 3-segments of an arrangement $\mathcal{L}_n$ of pseudolines. Heading for an upper bound on the number of 3-segments contained in $\mathcal{L}_n$, we achieve an upper bound of $O(n^2)$ not only on the number of 3-segments but even on the number of k-segments of $\mathcal{L}_n$. This is done using the $(\leq k)$-*zone* of a pseudoline in $\mathcal{L}_n$ and a linear upper bound on the complexity of the $(\leq k)$-zone, determined at this.

Turning back to our original interest in the relation of chordal graphs and pseudosegment graphs, let us summarize what we know so far. Section 5.1 gives that every vertex intersection graph of subpaths of a tree is a pseudosegment graph. In Section 5.2 we showed that the chordal graph K_n^3 is not a pseudosegment graph for large enough n.

In order to describe the chordal graphs that are pseudosegment graphs, we then turn to a further family of chordal graphs. For every $n \in \mathbb{N}$, let S_n^3 be the graph with vertex set $V' = V_I' \cup V_C'$ such that $V_I' = [n]$ is an independent set of n vertices and $V_C' = \binom{[n]}{3}$ a clique of $\binom{n}{3}$ vertices; as before, membership accords with adjacency for elements of V_I' and V_C'. This time, we use an argument from Ramsey Theory to show that S_n^3 is not a pseudosegment graph for large enough n. Every graph S_n^3 is a vertex intersection graph of substars of a star where the substars have maximal degree three. This implies that chordal graphs that are pseudosegment graphs cannot be induced by many treelike subtrees of a tree.

5.1 Path graphs

In this section we will show that the class of path graphs, that is of vertex intersection graphs of subpaths of a tree, is a common subclass of pseudosegment and chordal graphs.

Theorem 5.1. Every path graph has a pseudosegment representation.

This result is not as trivial as it may seem at first glance. Let $G = (V, E)$ be a graph and $(T, \mathcal{P})$ a path representation of G. An intuitive attempt for converting a path representation into a pseudosegment representation would be to use a planar embedding of the tree T. The embedding of T then suggests an embedding of each of the paths corresponding to the vertices of G. These paths could be slightly perturbed into pseudosegments trying to assure that paths with common vertices intersect exactly once and are disjoint otherwise. However, Figure 5.2 gives an example of a set of three paths which cannot be perturbed locally as to give a pseudosegment representation of the corresponding subgraph.

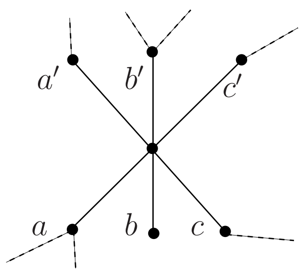

Figure 5.2: Paths $P(a, a'), P(b, b')$ and $P(c, c')$ cannot be perturbed locally into a pseudosegment representation.

5.1.1 *Preliminaries*

Let $G = (V, E)$ be an arbitrary path graph with path representation $(T, \mathcal{P})$. Without loss of generality we assume that no two paths in $\mathcal{P}$ have a common endpoint. Let P be a path in a tree T with endpoints a and b, that is $P = P(a, b)$. If both endpoints of P are leaves of T we call P a leaf-path.

Lemma 5.2. Every path graph has a path representation $(T, \mathcal{P})$ such that all paths in $\mathcal{P}$ are leaf-paths and no two vertices are represented by the same leaf-path.

Proof. Let $(T, \mathcal{P})$ be an arbitrary path representation of G and let path $P_v = P(a_v, b_v)$ represent vertex $v \in V$. Now let $\overline{T}$ be the tree obtained from T by attaching a new vertex $\overline{x}$ to every vertex x of T. Representing the vertex v by the path $\overline{P_v} = P(\overline{a_v}, \overline{b_v})$ in $\overline{T}$ yields a path representation of G using only leaf-paths. □

The definition of a path graph as an intersection graph immediately implies that every induced subgraph of a path graph is a path graph as well. Lemma 5.2 together with this observation shows that Theorem 5.1 is implied by Theorem 5.3:

Theorem 5.3. Let T be a tree and let $L = \{l_1, .., l_m\}$ be the set of leaves of T. Let G be the path graph whose vertices are in bijection with the set of all leaf-paths of T. Then graph G has a pseudosegment representation $\mathcal{G}$ with pseudosegment $s_{i,j} \in \mathcal{G}$ corresponding to path $P_{i,j} = P(l_i, l_j)$ in T. In addition, there is a collection of pairwise disjoint disks, one disk R_i associated with each leaf l_i of T, such that:

(a) $s_{i,j} \cap R_k \neq \emptyset$ if and only if $k = i$ or $k = j$. Furthermore, the intersections $s_{i,j} \cap R_i$ and $s_{i,j} \cap R_j$ are Jordan arcs.

(b) Any two pseudosegments intersecting R_i cross in the interior of R_i.

We will prove Theorem 5.3 by induction on the number of inner vertices of tree T. The construction will have multiple intersections, that is there are points where more than two pseudosegments intersect. By perturbing the pseudosegments participating in a multiple intersection locally the representation can easily be transformed into a representation without multiple intersections.

5.1.2 Proof of Theorem 5.3 for trees with one inner vertex

Let T be a tree with one inner vertex v and let $L = \{l_1, .., l_m\}$ be the set of leaves of T. Let $\mathcal{P} = \{P(l_i, l_j) \mid l_i, l_j \in L, l_i \neq l_j\}$ be and let H be the subgraph of G induced by $\mathcal{P}$. Then H is a complete graph on $\binom{m}{2}$ vertices as every path in $\mathcal{P}$ contains v.

Take a circle and choose m points $Q_1, .., Q_m$ on this circle such that the set of straight lines spanned by pairs of different points from $Q_1, .., Q_m$ contains no parallel lines. For each i choose a small disk R_i centered at Q_i such that these disks are pairwise disjoint and put them in one-to-one correspondence with the leaves of T. Let $s_{i,j}$ be the line containing Q_i and Q_j. If the disks R_k are small enough, then the arrangement has the following properties:

(a) The line $s_{i,j}$ intersects disks R_i and R_j but no further disk R_k for $k \in \{1, ..., n\} \backslash \{i, j\}$.

(b) Two lines s_I and s_J with $I \cap J = \{i\}$ contain point Q_i, hence s_I and s_J cross in the disk R_i.

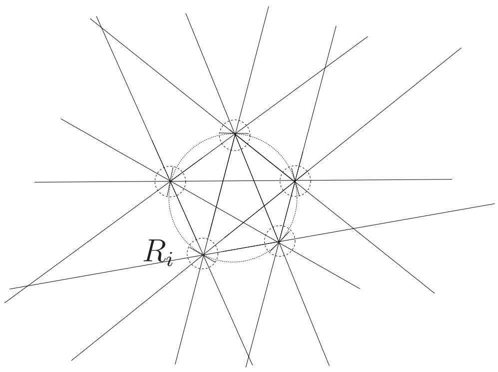

Figure 5.3: Construction of a pseudosegment representation of the vertex intersection graph of all leaf-paths of a star with five leaves.

Prune the lines such that the remaining part of each $s_{i,j}$ still contains its intersections with all the other lines and all segments have there endpoints on a circumscribing circle $\mathcal{C}$. Every pair of segments keeps its intersection, hence, we have a pseudosegment representation of H.

Add a diameter $s_{i,i}$ to every disk R_i, this segment serves as representation of the leaf-path $P_{i,i}$. Slightly perturbing multiple intersection points yields a pseudosegment representation of G with the required properties (a) and (b) of Theorem 5.3; see Figure 5.3 for an illustration.

5.1.3 Proof of Theorem 5.3 for trees with more than one inner vertex

Now let T be a tree with inner vertices $N = \{v_1, .., v_n\}$ and assume Theorem 5.3 has been proven for trees with at most $n-1$ inner vertices. Let $L = \{l_1, .., l_m\}$ be the set of leaves of T. With $L_i \subset L$ we denote the set of leaves attached to v_i. We have to construct a pseudosegment representation of the intersection graph G of $\mathcal{P} = \{P_{i,j} \mid l_i, l_j \in L\}$, that is, of the set of all leaf-paths of T. Assume that v_n is a leaf of the subtree of T induced by N. Then we define two induced subtrees of T:

- T_n is the star with inner vertex v_n and leaves $L_n = \{l_k, l_{k+1}, ..., l_m\}$.
- The tree T_0 contains all vertices of T except the leaves in L_n. The set of inner vertices of T_0 is $N_0 = N \backslash \{v_n\}$ and the set of leaves is $L_0 = L \backslash L_n \cup \{v_n\}$. For consistency we rename $l_0 := v_n$ in T_0, hence $L_0 = \{l_0, l_1, ..., l_{k-1}\}$.

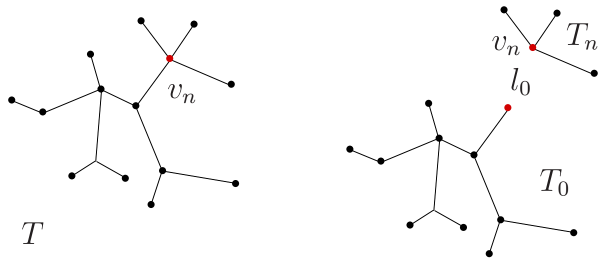

Figure 5.4: A tree T with inner vertex v_n and the two induced subtrees T_0 and T_n.

Let G_n and G_0 be the path graphs induced by all leaf-paths in T_n and T_0 respectively. Both these trees have fewer inner vertices than T. By the induction hypothesis we can assume that we have pseudosegment representations $\mathcal{G}_n$ of G_n and $\mathcal{G}_0$ of G_0. We will construct a pseudosegment representation $\mathcal{G}$ of G using $\mathcal{G}_n$ and $\mathcal{G}_0$. The idea is as follows:

1. Replace every pseudosegment of $\mathcal{G}_0$ representing a leaf-path ending in l_0 by a bundle of $|L_n|$ pseudosegments. This bundle stays within a narrow tube around the original pseudosegment of $\mathcal{G}_0$.
2. Remove all pieces of pseudosegments from the interior of the disk R_0 and patch an appropriately transformed copy of $\mathcal{G}_n$ into R_0.

3. Connect the pseudosegments from the bundles through the interior of R_0 such that the induction invariants for the transformed disks of R_r with $k \leq r \leq m$ are satisfied.

The set $\mathcal{P}$ of leaf-paths of T can be partitioned into three parts. Let $\mathcal{P}'$ be the set of leaf-paths of T that are also leaf-paths of T_0 and let $\mathcal{P}_n$ be the set of leaf-paths of T_n. Then set $\mathcal{P}^*$ as the remaining subset of $\mathcal{P}$; thus the paths in $\mathcal{P}^*$ connect leaves l_i and l_r with $1 \leq i < k \leq r \leq m$, in other words they connect a leaf l_i from T_0 through v_n with a leaf l_r in T_n. We further subdivide $\mathcal{P}^*$ into classes $\mathcal{P}^*_1, .., \mathcal{P}^*_{k-1}$ such that $\mathcal{P}^*_i$ consists of those paths in $\mathcal{P}^*$ which start in l_i. Each $\mathcal{P}^*_i$ consists of $|L_n|$ paths. In T_0, we have the pseudosegment $s_{i,0}$ which leads from l_i to l_0. Replace each such pseudosegment $s_{i,0}$ by a bundle $B_{i,0}$ of $|L_n|$ parallel pseudosegments routed in a narrow tube around the original pseudosegment $s_{i,0}$. Thus, every element of $B_{i,0}$ intersects the same elements of $\mathcal{P}'$ as $s_{i,0}$

We come to the second step of the construction. Recall that the representation $\mathcal{G}_n$ of G_n of Section 5.1.2 has the property that all long pseudosegments have their endpoints on a circle $\mathcal{C}$. Choose two arcs A_b and A_t on $\mathcal{C}$ such that every segment spanned by a point in A_b and a point in A_t intersects each long pseudosegment $s_{i,j}$ of $\mathcal{G}_n$ with $i \neq j$; this is possible by the choice of $\mathcal{C}$. We obtain a partitioning of the circle into four arcs which will be called A_b, A_l, A_t, A_r in clockwise order. The choice of A_b and A_t implies that each pseudosegment touching $\mathcal{C}$ has one endpoint in A_l and the other in A_r.

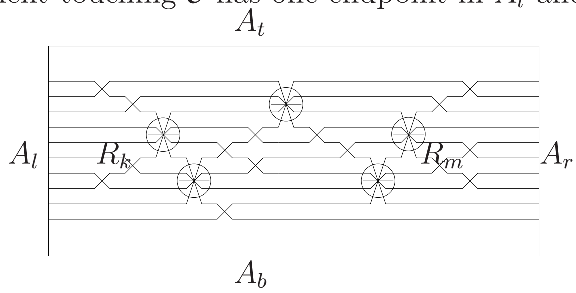

Figure 5.5: A box containing a deformed copy of the representation from Figure 5.3.

Map the interior of $\mathcal{C}$ with an homeomorphism into a wide rectangular box $\mathcal{B}$ such that A_t and A_b are mapped to the top and bottom sides of the box, A_l is the left side and A_r the right side. In this way the images of all long pseudosegments traverse the box from left to right. We may also require that the homeomorphism maps the disks R_r to disks and arranges them in a nice left to right order in the box; Figure 5.5 shows an example. The figure was generated by sweeping the representation from Figure 5.3 and converting the sweep into a wiring diagram. Then we remove every short pseudosegment $s_{r,r}$ and re-attach it horizontally such that no intersecting pairs are changed. In the box we have a left to right order of the disks R_r, $l_r \in L_n$. By possibly relabeling the leaves of L_n we can assume that the disks are ordered from left to right as $R_k, .., R_m$. We still refer to the resulting pseudosegment representation of G_n as $\mathcal{G}_n$.

To continue the construction of a pseudosegment representation of G, we remove all pieces of pseudosegments from the interior of R_0. Then place box $\mathcal{B}$ appropriately resized into the disk R_0 such that each of the pseudosegments $s_{i,0}$ from the representation of G_0 would have traversed the box from bottom to top and the sides A_l and A_r are mapped to the boundary of R_0. The boundary of R_0 is thus partitioned into four arcs which are called A_l, A'_t, A_r, A'_b in clockwise order. We assume that the remaining pieces of pseudosegments $s_{i,0}$ touch the arc A'_b in $\mathcal{G}_0$ in counterclockwise order as $s_{1,0}, .., s_{k-1,0}$, this can be achieved by renaming the leaves of T_0 appropriately.

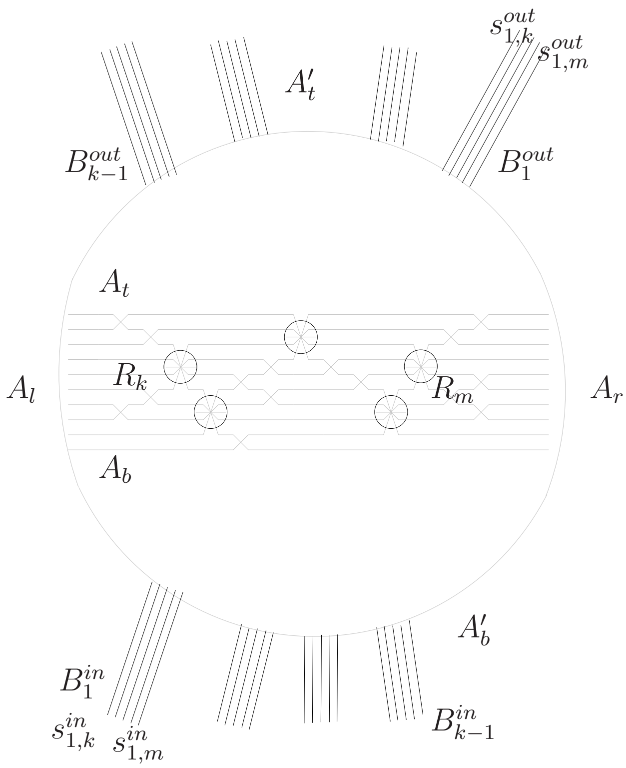

Figure 5.6: Box $\mathcal{B}$ within disk R_0 and the touching bundles.

By removing everything from the interior of R_0 we have disconnected all the pseudosegments which have been inserted in bundles replacing the original pseudosegments $s_{i,0}$. Let B_i^{in} be the half of the bundle of $s_{i,0}$ which touches A'_b and let B_i^{out} be the half which touches A'_t. By the above assumption the bundles $B_1^{in}, .., B_{k-1}^{in}$ touch A'_b in counterclockwise order, consequently, $B_1^{out}, .., B_{k-1}^{out}$ touch A'_t in counterclockwise order; see Figure 5.8 for an illustration. Within a bundle B_i^{in} we label the pseudosegments as $s_{i,k}^{in}, .., s_{i,m}^{in}$, again counterclockwise. The pseudosegment in B_i^{out} which was connected to $s_{i,r}^{in}$ is labeled $s_{i,r}^{out}$. The pieces $s_{i,r}^{in}$ and $s_{i,r}^{out}$ will be part of the pseudosegment representing the path $P_{i,r}$.

Before we connect $s_{i,r}^{in}$ and $s_{i,r}^{out}$ in order to obtain a pseudosegment representing $P_{i,r}$ recall that all paths in $\mathcal{P}_i^*$ contain leaf l_i. Thus, the respective pseudosegments have to intersect within disk R_i as required by property (b) of Theorem 5.3. To achieve this, we twist whichever of the bundles B_i^{in} or B_i^{out} traverses R_i within disk R_i thus creating a multiple intersection point; this is illustrated in Figure 5.7. Note that all elements of the respective bundle cross $s_{i,i}$ as did $s_{i,0}$ so that property (a) of Theorem 5.3 holds as well.

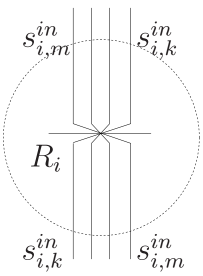

Figure 5.7: If B_i^{in} crosses R_i, we twist $s_{i,k}^{in}, \ldots, s_{i,m}^{in}$, the copies of $s_{i,0}$, within R_i.

Now we come to the third step of the construction. Due to (b) the pseudosegments representing the paths $P_{1,r}, ..., P_{k-1,r}$ have to intersect within the disk R_r that lies inside the disk R_0 for every $r \in \{k, .., m\}$. To prepare for this we take a narrow bundle of $k-1$ parallel vertical segments reaching from top to bottom of the box in R_0, intersecting the disk R_r and no other disk within R_0. This bundle is twisted in the interior of R_r. Let $\check{a}_1^r, .., \check{a}_{k-1}^r$ be the bottom endpoints of this bundle from left to right and let $\hat{a}_1^r, .., \hat{a}_{k-1}^r$ be the top endpoints from right to left. Due to the twist, the endpoints $\check{a}_j^r$ and $\hat{a}_j^r$ belong to the same pseudosegment.

Now we are ready to name the pseudosegment $s_{i,r}$ that will represent the path $P_{i,r}$ in T for $1 \leq i < k \leq r \leq m$. The first part of $s_{i,r}$ is $s_{i,r}^{in}$, this pseudosegment is part of the bundle B_i^{in} and has an endpoint on A_b'. Connect this endpoint with a straight line segment to $\check{a}_i^r$, from this point there is the connection up to $\hat{a}_i^r$. This point is again connected by a straight line segment to the endpoint of $s_{i,r}^{out}$ on the arc A_t'. The last part of $s_{i,r}$ is the pseudosegment $s_{i,r}^{out}$ in the bundle B_i^{out}. The construction is illustrated in Figure 5.8. Obviously each $s_{i,r}$ is a Jordan arc. Let the union of all these "new" Jordan arcs be $\mathcal{G}^*$.

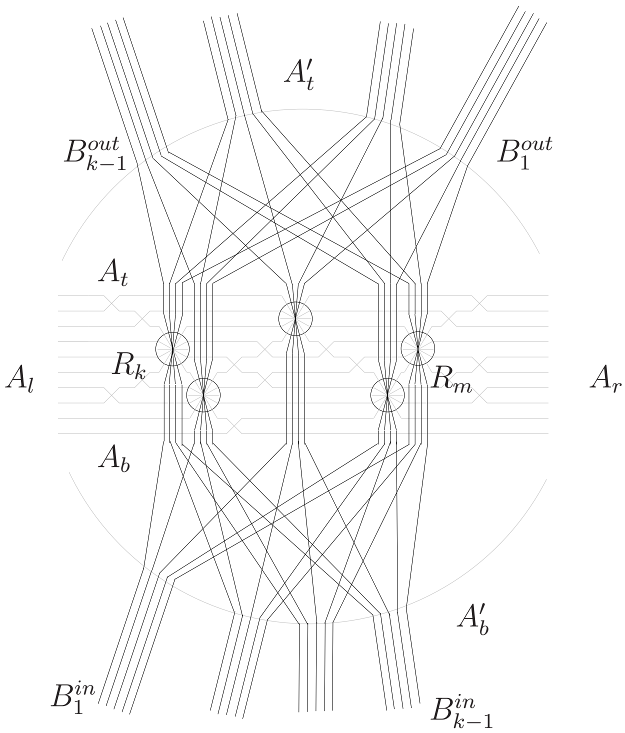

Figure 5.8: An example of the routing of pseudosegments in the disk R_0.

Observation 5.4. Let $s_{i,r}$ and $s_{i',r'}$ be two pseudosegments of $\mathcal{G}^*$ representing paths $P_{i,r}$ and $P_{i',r'}$ with $i \leq i'$. Then it follows from the construction that

(1) $s_{i,r}$ and $s_{i',r'}$ intersect between A_b' and A_b if and only if $i \neq i'$ and $r > r'$.

(2) $s_{i,r}$ and $s_{i',r'}$ intersect within box $\mathcal{B}$ if and only if $i \neq i'$ and $r' = r$.

(3) $s_{i,r}$ and $s_{i',r'}$ intersect between A_t and A'_t if and only if $i \neq i'$ and $r < r'$.

(4) $s_{i,r}$ and $s_{i',r'}$ intersect in R_i if and only if $i = i'$.

Thus, $\mathcal{G}^*$ is a pseudosegment representation of the subgraph of G induced by $\mathcal{P}^*$ fullfiling properties (a) and (b) of Theorem 5.3 by the choice of the pieces of $s_{i,r}$. Thus the construction implies that $\mathcal{G}^* \cup \mathcal{G}_n$ forms a pseudosegment representation of the subgraph of G induced by $\mathcal{P}^* \cup \mathcal{P}_n$ fulfiling properties (a) and (b) of Theorem 5.3.

Recall that every element of a bundle $B_{i,0}$ intersects the same elements of $\mathcal{P}'$ as $s_{i,0}$. By the choice of $\mathcal{G}_0$, none of these intersections takes place within R_0. Thus, the elements of $\mathcal{G}^* \cup \mathcal{G}_n \cup \mathcal{G}_0 \backslash \{s_{1,o}, ..., s_{k-1,0}\}$ forms a pseudosegment representation of G fulfiling properties (a) and (b) of Theorem 5.3.

As Theorem 5.3 implies Theorem 5.1, path graphs are pseudosegment graphs.

5.2 Nonpseudosegment graphs- a planarity argument

To show that not all chordal graphs have a pseudosegment representation, let us consider the following chordal graph.

Definition 5.5. For $n \in \mathbb{N}$ let K_n^3 be the graph whose vertices can be partitioned into two sets, $V_C = [n]$ and $V_I = \binom{[n]}{3}$. The vertices of V_C induce a clique and V_I forms an independent set. Additionally each vertex $\{i, j, k\} \in V_I$ is adjacent only to vertex $l \in V_C$ if and only if $l \in \{i, j, k\}$.

To see that these graphs are chordal, let S be a star with $\binom{n}{3}$ leaves indexed by all different triples of $[n]$. We assign $\{i, j, k\}$ to the leaf indexed $\{i, j, k\}$ and i to the substar of S connecting all leaves indexed $\{i, y, z\}$ with $y, z \in [n] \backslash \{i\}$. Figure 5.9 sketches the graph K_5^3; it is a vertex intersection graph of substars of degree $\binom{4}{2}$ of a star with $\binom{5}{3}$ leaves.

Theorem 5.6. For large enough $n \in \mathbb{N}$ there is no pseudosegment representation of K_n^3.

Proof. Assuming that there is a pseudosegment representation $\mathcal{G}$ of K_n^3, the set $\mathcal{G}$ of pseudosegments can be divided into $\mathcal{S}_n$ and $\mathcal{S}_I$, that is the pseudosegments representing the vertices from V_C and V_I respectively. The pseudosegments of $\mathcal{S}_n$ form a set of n pairwise crossing pseudosegments, that

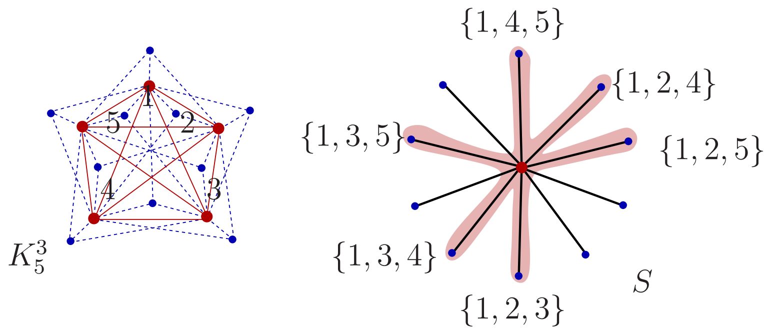

Figure 5.9: A sketch of K_5^3 and a star, hosting a tree representation of K_5^3, with a substar representing vertex 1 of K_5^3.

is an arrangement of pseudosegments. The pseudosegments of $\mathcal{S}_I$ have the following properties:

(i) any two different pseudosegments of $\mathcal{S}_I$ are disjoint, and

(ii) every pseudosegment of $\mathcal{S}_I$ has nonempty intersection with exactly three different pseudosegments from the arrangement $\mathcal{S}_n$ and no two different pseudosegments of $\mathcal{S}_I$ intersect the same three pseudosegments of $\mathcal{S}_n$.

The idea of the proof is to show that a set $\mathcal{G} = \mathcal{S}_n \cup \mathcal{S}_I$ of pseudosegments with properties (i) and (ii) can have at most $O(n^2)$ elements. Theorem 5.6 then follows as $\mathcal{S}_I$ has $\binom{n}{3}$ elements.

5.2.1 Geometric restrictions

Every pseudosegment $p \in \mathcal{S}_n$ is cut into n pieces, its edges, by the $n-1$ other pseudosegments of $\mathcal{S}_n$. Let W be the set of all edges of pseudosegments of $\mathcal{S}_n$; note that $|W| = n^2$. A pseudosegment $t \in \mathcal{S}_I$ intersects with exactly three edges of three different pseudosegments of $\mathcal{S}_n$ such that each intersection is a crossing; thus every $t \in \mathcal{S}_I$ is a 3-segment. Being a connected simple arc, every 3-segment has a unique middle and two outer intersections. Let $S(w)$ be the set of 3-segments with middle intersection on the edge $w \in W$. With this we partition the set $\mathcal{S}_I$ as $\mathcal{S}_I = \dot{\bigcup}_{w \in W} S(w)$.

Define $G_p = (W, E_p)$ as the simple graph where two elements $w, w' \in W$ are adjacent if and only if there exists a 3-segment $t \in \mathcal{S}_I$ such that t has its middle intersection on w and an outer intersection on w'.

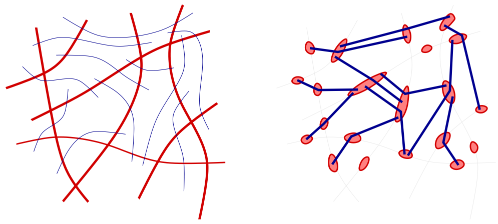

Figure 5.10: A partial arrangement with 3-segments and the corresponding graph G_p induced by them.

Lemma 5.7. The graph $G_p = (W, E_p)$ is planar.

Proof. A planar embedding of G_p is induced by $\mathcal{S}_n$ and $\mathcal{S}_I$. Contract all edges of pseudosegments of $\mathcal{S}_n$; the contracted pieces represent the vertices of G_p. The 3-segments of $\mathcal{S}_I$ are pairwise non-crossing, this property is maintained during the contraction of edges of $\mathcal{S}_n$, see Figure 5.10. If $t \in \mathcal{S}_I$ has its middle intersection on w and its outer intersections on w' and w'', then t contributes the two edges ww' and ww''. Hence, the multigraph obtained through these contractions is planar and its underlying simple graph is indeed G_p. $\square$

Let $N_{G_p}(w)$ be the set of neighbors of vertex $w \in W$ in G_p so that $d_{G_p}(w) = |N_{G_p}(w)|$.

Lemma 5.8. The size of a set $S(w)$ of 3-segments is bounded by $d_{G_p}(w) - 1$ for every $w \in W$.

Proof. For every $w \in W$ define $G[N_{G_p}(w)] = (N_{G_p}(w), E_w)$ as the graph where two vertices $u, u' \in N_{G_p}(w)$ are adjacent if and only if there is a 3-segment $t \in S(w)$ that has its outer intersections with u and u'. The number of edges of $G[N_{G_p}(w)]$ equals the number of 3-segments in $S(w)$. The idea is to contract just the pieces corresponding to elements of $N_{G_p}(w)$ to points. The 3-segments in $S(w)$ together with the vertices obtained from the contraction of the elements of $N_{G_p}(w)$ form a planar graph, see Figure 5.11. Note that the resulting graph is not a multigraph, since a multiple edge would correspond to a pair of 3-segments of $S(w)$ intersecting the same three edges of $\mathcal{S}_n$ with

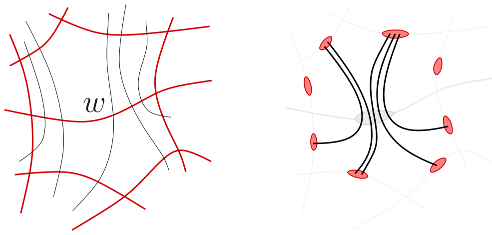

Figure 5.11: The planar graph $G[N_{G_p}(w)]$ is induced by the 3-segments with middle intersection on w.

middle intersection on w. We will show that $G[N_{G_p}(w)]$ is acyclic, hence a forest. This implies the statement of Lemma 5.8.

Assume there was a cycle $C = (w_1, .., w_k, w_1)$ in $G[N_{G_p}(w)]$ with edges $w_k w_1$ and $w_i w_{i+1}$ with $1 \leq i < k$. Let t_i be the 3-segment defining edge $w_i w_{i+1}$. Recall that t_i intersects w_i, w and w_{i+1}. A cycle in $G[N_{G_p}(w)]$ corresponds to a simple closed curve in the pseudosegment representation $\mathcal{G}$ of G as follows: Denote the part of w_i connecting its crossings with t_i and t_{i-1} by a_i. As $w_i \in W$ is an edge of $\mathcal{S}_n$ and $t_j \in S(w) \subseteq \mathcal{S}_I$, the set of edges of $\mathcal{S}_n$ and 3-segments of $S(w)$ contributing to C as vertices or edges of C does not induce more crossings than the pairs (w_i, t_j) with $j \in \{i-1, i\}$. Ignoring the pending ends of t_i, the union of the a_i and t_i, $i \in \{1, .., k\}$ corresponds to a simple closed curve $\mathcal{C}$ within the pseudosegment representation $\mathcal{G}$. The curve $\mathcal{C}$ is the concatenation of a_i and t_i in the order $a_1, t_1, a_2, .., t_{k-1}, a_k, t_k$, see Figure 5.12.

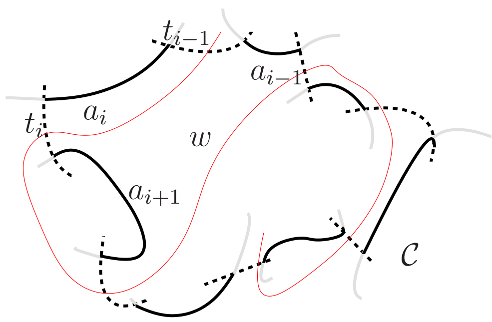

Figure 5.12: A chain of segments corresponding to a cycle C in $G[N_{G_p}(w)]$.

Note that $k \geq 3$, as $G[N_{G_p}(w)]$ is not a multigraph. Choose three 3-segments t_j, t_i, t_l from C such that they intersect w in this order and no other 3-segment of C crosses w between them. We will identify a simple closed curve $\mathcal{C}'$ separating w_i and w_{i+1}. Even more, the complete pseudosegments p and p' containing w_i respectively w_{i+1} will be separated by $\mathcal{C}'$. This is a contradiction to the fact that they both belong to the arrangement $\mathcal{S}_n$.

Such a curve $\mathcal{C}'$ can be described as follows: By possibly shifting the indices of w_i along C, we can assume $i < j < l$. Denote the part of w between its intersections with t_j and t_l by $w_{j,l}$. Let $P_{j+1,l}$ be the subpath of $C \setminus w_i$ connecting w_{j+1} and w_l, denote the corresponding part of $\mathcal{C}$ by $\mathcal{C}_{j+1,l}$. Connect $w_{j,l}$ to $\mathcal{C}_{j+1,l}$ at t_j and t_l. This gives a simple closed curve $\mathcal{C}'$. The curve $\mathcal{C}'$ consists of an arc of $\mathcal{C}$, the arc $w_{j,l}$ of w and parts of t_j and t_l. It follows that $\mathcal{C}'$ can not be crossed by a pseudosegment from $\mathcal{S}_n$. Recall that by the definition of a pseudosegment representation, an intersection of pseudosegments implies that they cross. Applied to the intersection of t_i and $w_{j,l} \subset w$ this has the consequence that w_i and w_{i+1} lie in different regions with respect to $\mathcal{C}'$, see Figure 5.13. As shown before this implies that the complete pseudosegments p containing w_i and p' containing w_{i+1} have to lie in different regions with respect to $\mathcal{C}'$. Thus, they cannot intersect, a contradiction to the choice of $\mathcal{S}_n$. Thus $G[N_{G_p}(w)]$ is acyclic and $|E_w|$ is bounded by $d_{G_p}(w) - 1$. □

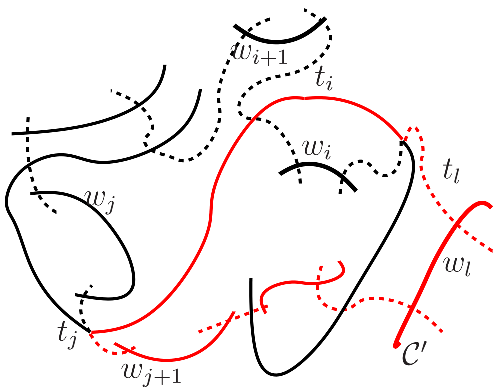

Figure 5.13: Pieces w_i and w_{i+1} are separated by the simple closed curve $\mathcal{C}'$.

As G_p is planar we have that $\sum_{w \in W} d_{G_p}(w) = 2|E_p| < 6|W|$. With this and $|W| = n^2$, Lemma 5.8 implies

$$|S| = \sum_{w \in W} |S(w)| \leq \sum_{w \in W} (d_{G_p}(w) - 1) < 6|W| = 6n^2.$$

Since $\binom{n}{3} > 6n^2$ for all $n \geq 39$, we conclude that K_n^3 does not belong to PSI for $n \geq 39$. This completes the proof of Theorem 5.6. □

5.3 Pseudoline arrangements and k-segments

In the previous section we considered the chordal graph K_n^3 in view of pseudosegment representations. For this purpose we partitioned the graph K_n^3 into its maximal independent set and its maximal clique. In any pseudosegment representation $\mathcal{G}$ of K_n^3, the clique corresponds to a set $\mathcal{S}_n \subset \mathcal{G}$ of n pairwise intersecting pseudosegments, that is an arrangement of pseudosegments. By showing that a set of disjoint 3-segments contained in $\mathcal{S}_n$ can consist of at most $6n^2$ elements, we were able to show that K_n^3 has no pseudosegment representation for $n \geq 39$.

This analysis naturally leads to ask for the size of a set of arbitrary 3-segments contained in $\mathcal{S}_n$. If we do not pose any restrictions on the intersection behavior of the 3-segments of $\mathcal{S}_n$, there are arrangements of pseudosegments that can contain $\binom{n}{3}$ 3-segments such that no two of them intersect the same three elements of the arrangement. An example of such an arrangement with a set of $\binom{n}{3}$ 3-segments is given in Figure 5.14.

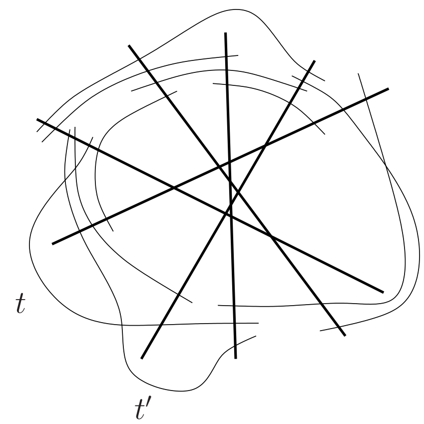

Figure 5.14: An arrangement $\mathcal{S}_5$ of five segments with a set of $\binom{5}{3}$ different 3-segments; here t and t' intersect twice.

Working on pseudosegments, it seems appropriate to require that the 3-segments of $\mathcal{S}_n$ form a set of pseudosegments themselves.

Question 5.9. Let $\mathcal{S}_n$ be an arrangement of n pseudosegments. What is the maximal size of a set $\mathcal{J}$ of different 3-segments of $\mathcal{S}_n$ such that the union of $\mathcal{S}_n \cup \mathcal{J}$ is a set of pseudosegments?

Although we conjecture that the size of $\mathcal{J}$ is $o(n^{2+\epsilon})$ for all $\epsilon > 0$ we have not even been able to show that the size of $\mathcal{J}$ is $o(n^3)$. One problem on answering this question is that the Jordan arcs of $\mathcal{J}$ can bypass the pseudosegments of $\mathcal{S}_n$ at their ends. This problem does not exist if we consider the analog question for an arrangement of pseudolines.

Question 5.10. Let $\mathcal{L}_n$ be an arrangement of n pseudolines. What is the maximal size of a set $\mathcal{J}$ of different 3-segments of $\mathcal{L}_n$?

The main result of this section is Theorem 5.11 which gives an upper bound on the maximal size of a set $\mathcal{K}$ of k-segments contained in an arrangement of n pseudolines with k fixed.

Theorem 5.11. For k fixed, the number of different k-segments contained in an arrangement of n pseudolines is $O(n^2)$, where the constant of proportionality depends on k; more precisely, it is bounded by $\frac{5}{2} \cdot k \cdot 3^{2k-3} n(n-1)$.

Observation 5.12. For $k = 1$ Theorem 5.11 obviously holds as there is one 1-segment of $\mathcal{L}_n$ for each of the n^2 edges of $\mathcal{L}_n$.

To prove Theorem 5.11 for $k = 2$ we will relate the number of k-segments contained in the pseudoline arrangement $\mathcal{L}_n$ to the number of edges of the zone of a pseudoline of $\mathcal{L}_n$. This motivates the definition of the $(\leq k)$-*zone* of a pseudoline in $\mathcal{L}_n$ generalizing the zone as defined in Section 2.1.2. In the proof of Theorem 5.11 for $k \geq 2$ we then use an upper bound on the number of edges of the $(\leq k)$-*zone*. The proof of this upper bound will follow in Section 5.3.4.

5.3.1 The zone and 2-segments of a pseudoline arrangement

Assume we are given an arbitrary arrangement $\mathcal{L}_n$ of pseudolines. Let p be an arbitrary pseudoline of $\mathcal{L}_n$ and let S_2 be a maximal set of 2-segments contained in $\mathcal{L}_n$. Every 2-segment of S_2 connects the two edges of $\mathcal{L}_n$ it intersects. Let us denote the set of 2-segments of S_2 that have an intersection with p by $S_2(p)$. With this we obtain $S_2 = \bigcup_{p \in \mathcal{L}_n} S_2(p)$ such that every 2-segment of S_2 belongs to exactly two sets of the set cover. Now every 2-segment of $S_2(p)$ connects an edge of $Z(p)$ to p, see Figure 5.15. The number of these edges contributes to the complexity of $Z(p)$, hence it is bounded by the upper bound of following theorem. This theorem is implied in the proof of Theorem 2.2 from [1].

Theorem 5.13. The complexity of the zone of a pseudoline in an arrangement of n pseudolines in the plane is $6(n-1) \in O(n)$. □

Obviously every pair of edges can be connected by at most one 2-segment of S_2. Thus, it remains to determine the number of different 2-segments that connect an arbitrary edge of $Z(p)$ to different edges of p. An upper bound on this number is given by the following claim.

Claim. Every edge of the zone $Z(p)$ can be connected to at most two different edges of p by 2-segments.

Proof. Every pseudoline of $\mathcal{L}_n$ contributes at most one edge to each face and every edge lies on the boundary of two different faces. A 2-segment of $S_2(p)$ connects an edge of $Z(p)$ to p, and these two edges lie on the same face of $Z(p)$. Hence, every edge of $Z(p)$ can be connected to at most two different edges of p by 2-segments of $\mathcal{L}_n$. □

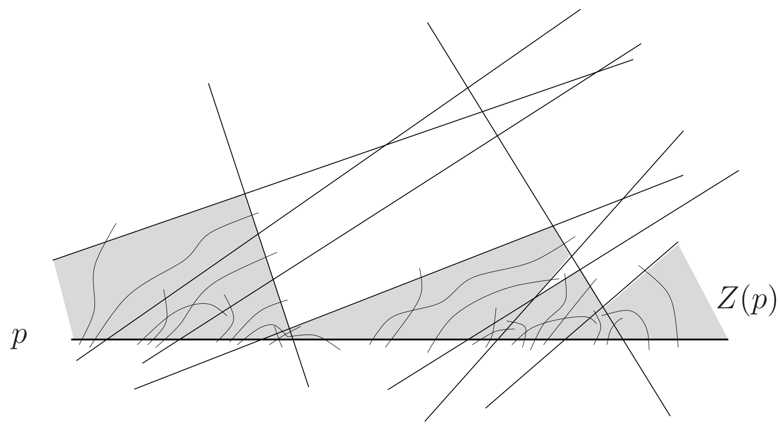

Figure 5.15: No edge of $Z(p)$ can be connected to an edge of p by more than two different 2-segments of $\mathcal{L}_n$.

With Theorem 5.13 and the previous Lemma, we obtain an upper bound of $2 \cdot 6(n-1) \in O(n)$ on the number of 2-segments in $S_2(p)$. As $\mathcal{L}_n$ contains n pseudolines, $S_2 = \bigcup_{p \in \mathcal{L}_n} S_2(p)$ and every 2-segments belongs to exactly two sets of $\bigcup_{p \in \mathcal{L}_n} S_2(p)$, we have

$$|S_2| \leq \frac{1}{2} \cdot n \cdot 2 \cdot 6(n-1) \in O(n^2).$$

5.3.2 The $(\leq k)$-zone and k-segments of a pseudoline arrangement

The relation between the number of 2-segments in $S_2(p)$ and the number of edges of $Z(p)$ motivates the following definition of the $(\leq k)$-*zone* which will be our main tool to prove Theorem 5.11 for $k \geq 2$. To define the $(\leq k)$-*zone* of a pseudoline in a pseudoline arrangement in analogy to the classical zone, note that every k-segment has two outer and $k-2$ inner intersections. We say that a k-segment connects the edges, and also the pseudolines, it has its outer intersections with. Then a k-segment connects a vertex v of $\mathcal{L}_n$ to pseudoline $p \in \mathcal{L}_n$ if there is a k-segment connecting an edge that is adjacent to v to p. We say that a k-segment connects a face f to p if it intersects two edges of the boundary of f and connects one of them to p.

Definition 5.14. Let $\mathcal{L}$ be an arrangement of pseudolines, let p be an arbitrary pseudoline of $\mathcal{L}$ and $k \geq 2$ fixed. The $(\leq k)$-*zone* $Z_{(\leq k)}(p)$ *of* p *in* $\mathcal{L}$ is the set of vertices, edges and faces of $\mathcal{L}$ that can be connected to p by l-segments of $\mathcal{L}$ for some $l \leq k$.

With respect to this definition, the classical zone $Z(p)$ corresponds to the (≤ 2)-zone $Z_{(\leq 2)}(p)$. In view of Question 5.10 we are interested in the number of edges of the $(\leq k)$-zone. A bound on this number is given in the following theorem.

Theorem 5.15. Let $k \geq 2$ fixed. Then the number of edges of the $(\leq k)$-zone is $O(n)$ with the constant of proportionality depending on k; more precisely it is bounded by $5 \cdot 3^{k-1}(n-1)$. □

We postpone the proof of Theorem 5.15 to Section 5.3.4 and proceed with the proof of Theorem 5.11.

5.3.3 Proof of Theorem 5.11 for $k \geq 2$

Let $\mathcal{L}_n$ be a pseudoline arrangement and let S_k be a maximal set of k-segments contained in $\mathcal{L}_n$ with $k \geq 2$ fixed. For every pseudoline p of $\mathcal{L}_n$ let $S_k(p)$ denote the set of k-segments of S_k that have an outer intersection on p. As before we have $S_k = \bigcup_{p \in \mathcal{L}_n} S_k(p)$ so that every k-segment of S_k belongs to two sets of $\bigcup_{p \in \mathcal{L}_n} S_k(p)$. For an example see Figure 5.16.

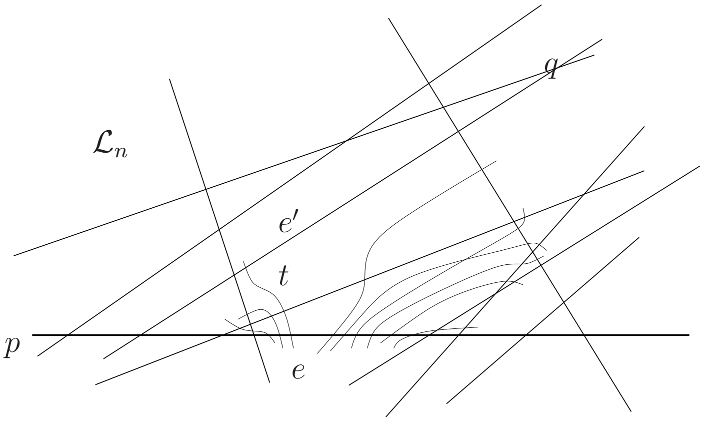

Figure 5.16: Different 3-segments of $S_3(p)$, among them t connecting edges $e \subset p$ and $e' \subset q$.

By Theorem 5.15, the number of edges of the $(\leq k)$-zone is bounded by $5 \cdot 3^{k-1}(n-1)$. Thus it remains to determine the number of k-segments of $S_k(p)$ that connect an arbitrary but fixed edge of the $(\leq k)$-zone to p.

Claim. For every pair of edges e, e' of $\mathcal{L}_n$ there are at most 3^{k-2} different k-segments of $\mathcal{L}_n$ that connect e and e'.

Proof. Let e and e' be edges of pseudolines q and p of $\mathcal{L}_n$ respectively. Assume that there is a k-segment t of $\mathcal{L}_n$ connecting e and e'. Let $\mathcal{L}(e, e')$ be the set of pseudolines of $\mathcal{L}_n$ different from p and q that are intersected by t. Assume there is a k-segment t', different from t, that connects e and e'. In this case, t, t' and the edges e and e' induce a closed curve. As e and e' are edges of $\mathcal{L}_n$, every pseudoline of $\mathcal{L}_n$ that intersects t has to intersect t' as well, and vice versa. As $\mathcal{L}(e, e') \subset \mathcal{L}_n$, $\mathcal{L}(e, e')$ forms an arrangement of $k-2$ pseudolines. With respect to this arrangement, t, and any other k-segment of S_k connecting e and e' can be seen as a possibility of adding a pseudoline $\bar{t}$ to $\mathcal{L}(e, e')$, entering at an unbounded face of $\mathcal{L}(e, e')$ and leaving at its antipodal face. The resulting set $\mathcal{L}(e, e') \cup \{\bar{t}\}$ is a pseudoline arrangement with $k-1$ pseudolines. Such a possibility is known as a *cutpath* of the arrangement. It has been investigated in [41] where, among other results, an upper bound on the number of cutpaths is given.

Lemma 5.16 ([41])**.** The number of cutpaths in an arrangement of m pseudolines is bounded by 3^m. □

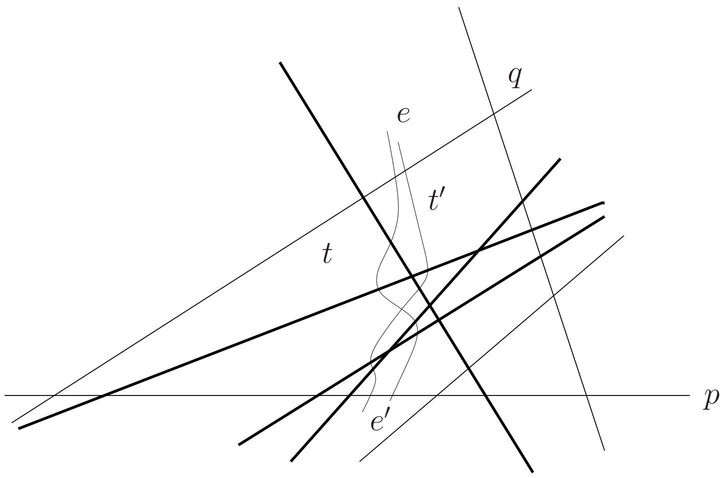

Figure 5.17: The thickly drawn pseudolines of $\mathcal{L}_n$ form an arrangement $\mathcal{L}(e, e')$ of pseudolines such that t and t' are cutpaths of $\mathcal{L}(e, e')$.

As $\mathcal{L}(e, e')$ is an arrangement of $k-2$ pseudolines, we obtain an upper bound of 3^{k-2} on the number of k-segments that connect e and e'. As e and e' were chosen arbitrarily, there are at most 3^{k-2} many different k-segments connecting a fixed pair of edges of $\mathcal{L}_n$. $\square$

Claim. Every edge of the $(\leq k)$-zone $Z_{(\leq k)}(p)$ in $\mathcal{L}_n$ can be connected to at most k different edges of p by k-segments of $\mathcal{L}_n$.

Proof. Let e be an arbitrary but fixed edge of $Z_{(\leq k)}(p)$ and let q be the pseudoline of $\mathcal{L}_n$ that contains e. We have to determine the number of different edges of p that can be connected to e by a k-segment. Let us index the edges of p with $1, ..., n$ such that e_1 and e_n are the unbounded edges of p and every pair (e_i, e_{i+1}) of consecutive edges of p has a common vertex on its boundary. Then let e_i and e_j, $i \leq j$, be the edges of p with lowest and highest index that are connected to e by k-segments and let t_i and t_j be k-segments connecting e_i and e_j respectively to e.

As before, the elements e, t_i, t_j and p induce a closed curve such that each of the $k-2$ pseudolines of $\mathcal{L}_n \backslash \{p, q\}$ intersecting t_i intersects either t_j, or p between the edges e_i and e_j. Correspondingly each of the $k-2$ pseudolines of $\mathcal{L}_n \backslash \{p, q\}$ intersecting t_j intersects either t_i, or p between the edges e_i and e_j. As q may intersect p between e_i and e_j, there are at most $2(k-2)+1$ pseudolines intersecting p between e_i and e_j, and so $j - i + 1 \leq 2k - 2$.

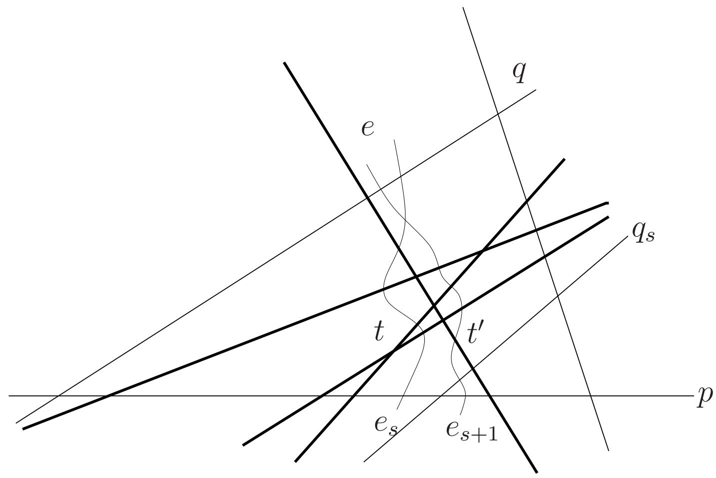

Figure 5.18: As $q \neq q_s$ and t is a 6-segment, t' is not a 6-segment.

Now consider a pair of edges e_s, e_{s+1} of p with $i \leq s < j$. Let q_s be the pseudoline of $\mathcal{L}_n$ intersecting p between e_s and e_{s+1}. Let t be a k-segment connecting e_s and e. Assume that $q \neq q_s$. Set $\mathcal{L}(e, e_s)$ as the set of pseudolines intersected by t different from p and q. If $q_s \notin \mathcal{L}(e, e_s)$, then e and e_{s+1} lie in different halfplanes with respect to q_s, see Figure 5.18. In this case, every l-segment t' of $\mathcal{L}_n$ that connects e_{s+1} and e has to intersect q_s. As t, t', e, q_s and p induce a closed curve, t' has to intersect every pseudoline of $\mathcal{L}(e, e_s)$. But then t' has $k+1$ intersections with elements of $\mathcal{L}_n$, hence t' is not a k-segment. If $q_s \in \mathcal{L}(e, e_s)$, the analog argument implies that t' has $k-1$ intersections with elements of $\mathcal{L}_n$ so that t' is not a k-segment.

Thus, except for the pair of edges of p adjacent to an edge of q no two adjacent edges of p can be connected to e by k-segments. So it follows that at most k of the at most $2k-2$ different edges of p can be connected to the same edge of $Z_{(\leq k)}(p)$. □

We conclude that any edge of the $(\leq k)$-zone $Z_{(\leq k)}(p)$ can be connected to p by at most $k \cdot 3^{k-2}$ different k-segments of $S_k(p)$. From Theorem 5.13 we know that the number of edges of $Z_{(\leq k)}(p)$ is bounded by $5 \cdot 3^{k-1}(n-1)$ for every $p \in \mathcal{L}_n$. In $S_k = \bigcup_{p \in \mathcal{L}_n} S_k(p)$ every k-segment of S_k appears twice. As there are n pseudolines in $\mathcal{L}_n$, we finish the proof of Theorem 5.11 with Observation 5.12 and the following formula for $k \geq 2$:

$$|S_k| \leq \tfrac{1}{2} n \cdot k \cdot 3^{k-2} \cdot 5 \cdot 3^{k-1}(n-1) = \tfrac{5}{2} \cdot k \cdot 3^{2k-3} \cdot n(n-1) \in O(n^2).$$

5.3.4 The $(\leq k)$-zone of a pseudoline arrangement

Theorem 5.15. Let $k \geq 2$ fixed. Then the number of edges of the $(\leq k)$-zone is $O(n)$ with the constant of proportionality depending on k; more precisely it is bounded by $5 \cdot 3^{k-1}(n-1)$.

In the following we will prove Theorem 5.15 generalizing the proof of Theorem 2.2 from [50]. So let p be a pseudoline of $\mathcal{L}_n$ and assume that p is a horizontal straight line dividing the plane into an upper and a lower half-plane, H_p^+ and H_p^- respectively. Let $E_k^+(p)$ denote the set of edges of $Z_{(\leq k)}(p)$ that lie in H_p^+ and $E_k^-(p)$ the ones that lie in H_p^-. It suffices to determine an upper bound for the number of edges in $E_k^+(p)$ as reflecting the arrangement at p gives the same upper bound for the number of edges in $E_k^-(p)$. Then Theorem 5.15 follows from Theorem 5.17.

Theorem 5.17. Let $k \geq 2$ be fixed. Then the number of edges of $E_k^+(p)$ is in $O(n)$ with the constant of proportionality depending on k; more precisely it is bounded by $\frac{5}{2} \cdot 3^{k-1}(n-1)$.

Proof. Let $\mathcal{L}_n$ be an arrangement of pseudolines and let p be a pseudoline of $\mathcal{L}_n$. For $k \geq 3$ set $D_k^+(p)$ as the set of edges of $Z_{(\leq k)}(p)$ that lie in H_p^+ and can be connected to p by k-segments but not by l-segments with $l < k$. That is $D_k^+(p) = E_k^+(p) \backslash E_{k-1}^+(p)$, hence

$$|E_k^+(p)| = |E_{k-1}^+(p)| + |D_k^+(p)|.$$

To determine an upper bound on $D_k^+(p)$, let us introduce some more notation that we illustrate in Figure 5.19. Set $v_{qq'}$ as the vertex defined by the intersection of pseudolines q and q' of $\mathcal{L}_n$. For $q \in \mathcal{L}_n \backslash \{p\}$ let q^+ be the part of q contained in H_p^+. Then orient each halfline q^+ away from v_{qp}.

Now let e be an edge of q^+ that is not adjacent to p. Let v_{qg} and v_{qs} be the vertices adjacent to e and assume that v_{qg} lies between v_{qp} and v_{qs} on q. As every edge inherits an orientation from its supporting halfline, we call v_{qg} the tail and v_{qs} the head of e. With respect to the orientation of the halfline containing the tail of e, that is g^+, e can be classified as either *left outgoing* or *right outgoing*.

Every edge adjacent to p belongs to $E_2(p)$, hence every edge of $D_k^+(p)$ is either left or right outgoing. So let $R_k^+(p)$ be the set of edges of $D_k^+(p)$ that are right outgoing and $L_k^+(p)$ the set of edges of $D_k^+(p)$ that are left outgoing.

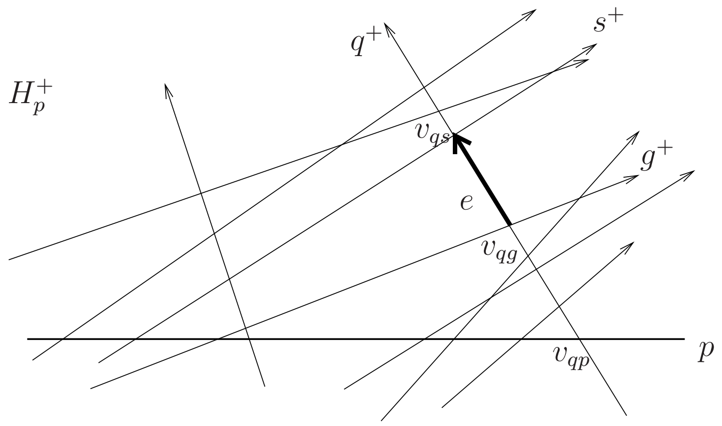

Figure 5.19: Edge e in H_p^+ is a left outgoing edge at g^+ and is bounded by vertices v_{qs} and v_{qg}.

Lemma 5.18. For every p of $\mathcal{L}_n$ it holds that $|R_k^+(p)| < (\frac{5}{2} \cdot 3^{k-2} - \frac{1}{2})(n-1)$.

Proof. Let q be a pseudoline of $\mathcal{L}_n \backslash \{p\}$ and let e_q be a right outgoing edge at q^+. Then we denote the supporting line of e_q by p_q. Next we index the edges that are right outgoing at q^+ increasingly by $e_q^1, e_q^2, ...$ such that the intersection points of the corresponding supporting halflines p_q^i and q appear along q as $(v_{qp}, v_{qp_q^1}, v_{qp_q^2}, ...)$.

As we are heading for an upper bound of $R_k^+(p)$ we can assume that the $(k-1)$st right outgoing edge at halfline q^+ of H_p^+ belongs to $R_k^+(p)$. Now assume that there is an $h \geq k$ such that the h-th right outgoing edge e_q^h at halfline q^+ belongs to $R_k^+(p)$; an example is given in Figure 5.20. As e_q^h belongs to $R_k^+(p)$, there is a k-segment t of $\mathcal{L}_n$ connecting e_q^h to an edge of p. Since $h \geq k$, the $k-1$ pseudolines $p_q^1, ..., p_q^{k-1}$ altogether prevent that t connects e_q^h to an edge of p that lies to the right of q. Thus t connects e_q^h to some edge e_p of p that lies to the left of q. But then t has an inner intersection with some edge e of q^+.

Let r^+ be the halfline containing e_q^h. Then let $\hat{e}$ be the edge of q^+ that is adjacent to v_{qr} and lies between e and v_{qr} on q. Let us construct another k-segment of $\mathcal{L}_n$ that connects e_p and e_q^h: First we take a copy of the part of t that connects e_p to e. This copy is placed next to t such that it lies completely to the left of q^+ and, still, has its last intersection on e_p. Then we take a copy of the part of q^+ that connects the intersection point of e and t to some point of $\hat{e}$. Let us join these two copies at their endpoints that are

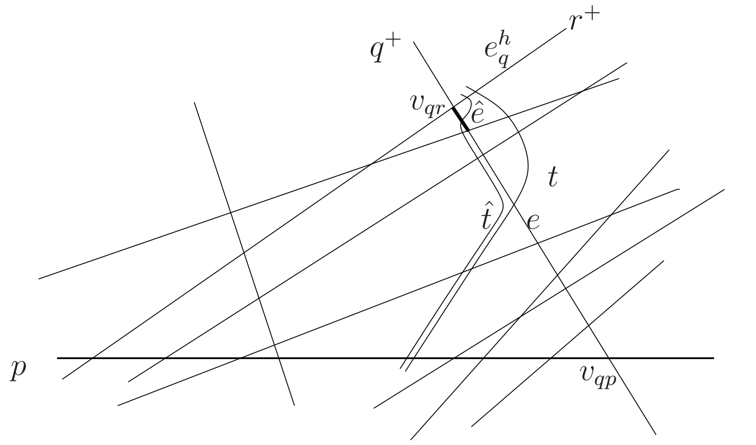

Figure 5.20: Edge $e_q^h \subset r^+$, with $h \geq k$ is right outgoing at q^+ and has a witness $\hat{e} \subset q^+$; here $\hat{e}$ lies between v_{qr} and v_{qp}.

next to e and place this union so that it lies completely to the left of q^+ and is disjoint from r^+. Finally we connect the endpoint of this arc that lies next to $\hat{e}$ by a Jordan arc to a point on e_q^h that intersects $\hat{e}$ and e_q^h and no other vertex or edge of $\mathcal{L}_n$. All this can be done in such a way that we obtain a Jordan arc $\hat{t}$ that is a k-segment of $\mathcal{L}_n$ having its first intersection with e_p, its last intersection with e_q^h and its second to last intersection with $\hat{e}$. Then we call $\hat{e}$ the *witness* of $e_q^h \in R_k^+(p) \subset D_k^+(p)$.

As $e_q^h \in D_k^+(p) = E_k^+(p) \backslash E_{k-1}^+(p)$, it holds that $\hat{e} \in D_{k-1}^+(p)$. This implies that the edges adjacent to $\hat{e}$ that lie to the left of q belong to $E_{k-1}^+(p)$. As every edge of $\mathcal{L}_n$ is adjacent to four edges of $\mathcal{L}_n$, edge $\hat{e}$ can be the witness of at most two edges of $R_k^+(p)$.

Claim. If edge $\hat{e}$, defined as before, is the witness of two edges of $R_k^+(p)$, then $\hat{e}$ belongs to $L_{k-1}^+(p)$.

Proof. Let $e_q^h \subset r^+$ and $\hat{e} \subset q^+$ be defined as before and let v_{qr} and v_{qg} be the vertices of $\mathcal{L}_n$ that bound $\hat{e}$; see Figure 5.21 for an illustration. By definition, $\hat{e}$ is the witness of e_q^h. Assume that $\hat{e}$ belongs to $R_{k-1}^+(p)$. Then the intersection v_{gp} lies to the right of q. Let e_g denote the edge of g^+ that is adjacent to v_{qg} and lies to the right of q. If $\hat{e}$ is the witness of e_g, then there is a k-segment t' having its first intersection with p, its last intersection with e_g and its second to last intersection with $\hat{e}$. This implies that t' intersects p to the left of q. But then t' has to intersect g^+ to the left of q which implies that t' has more than one intersection with g. This contradicts the assumption that t' is a k-segment of $\mathcal{L}_n$, hence $\hat{e}$ cannot be the witness of e_g, and thus, $\hat{e}$ cannot be the witness of two edges of $R_k^+(p)$. $\square$

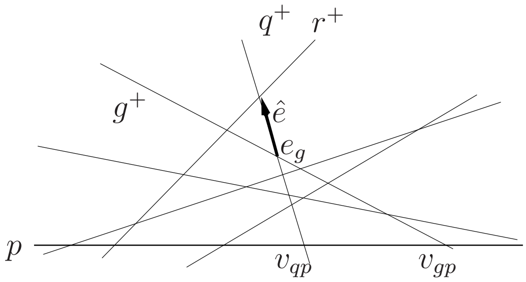

Figure 5.21: If $\hat{e}$ is in $R_{k-1}^+(p)$, then $\hat{e}$ cannot be the witness of edge e_g.

Recalling that we account for every $(k-1)$-st right outgoing edge at every halfline in H_p^+, we obtain

$$|R_k^+(p)| \leq (n-1) + |D_{k-1}^+(p)| + |L_{k-1}^+(p)|.$$

Then we obtain an upper bound $a_k \geq |R_k^+(p)|$ by solving the recurrence $a_k = (n-1) + 3a_{k-1}$. The initial condition $a_2 = 2(n-1)$ as $k \geq 2$ can be read off the proof of Theorem 2.2 from [1]. This gives the upper bound stated before, that is

$$|R_k^+(p)| \leq a_k = (\frac{5}{2} \cdot 3^{k-2} - \frac{1}{2})(n-1).$$

$\square$

Interchanging right with left outgoing edges yields the analog result for the number of left outgoing edges, thus we have $(5\cdot 3^{k-2}-1)(n-1)$ as upper bound for the number of edges of $D_k^+(p)$. Recall that $|E_k^+(p)| = |E_{k-1}^+(p)| + |D_k^+(p)|$, hence we obtain an upper bound $b_k \geq |E_k^+(p)|$ on the number of edges of $Z_{(\leq k)}(p)$ in H_p^+ by solving the recurrence $b_k = b_{k-1} + (5 \cdot 3^{k-2} - 1)(n-1)$. Again, the initial condition $b_2 = 3(n-1)$ for $k = 2$ results from the proof of Theorem 2.2. This leads to an upper bound $b_k = (\frac{5}{2} \cdot 3^{k-1} - k - \frac{5}{2})(n-1)$. Then it holds that $|E_k^+(p)| \leq \frac{5}{2} \cdot 3^{k-1}(n-1)$ as stated in Theorem 5.17. $\square$

Reflecting the arrangement at p gives the same upper bound for $E_k^-(p)$, so we obtain $5 \cdot 3^{k-1}(n-1) \in O(n)$ as upper bound on the number of edges in $Z_{(\leq k)}(p)$.

Remark: Towards the end of our work on the number of k-segments in pseudoline arrangements, we encountered the following definition in [50].

Definition 5.19. The $(\leq k)$-*zone* of an hyperplane g in an hyperplane arrangement $\mathcal{H}$ in $\mathbb{R}^d$ is defined as the set of all faces of $\mathcal{H}$ for which a point X of their relative interior can be connected to some point Y of g by the segment $s = [X, Y]$ so that s intersects at most k hyperplanes of $\mathcal{H}$.

The author suggests an upper bound of $O(n^{d-1}k)$ for the number of vertices of the $(\leq k)$-zone in $\mathbb{R}^d$ using Clarkson's Theorem on levels as stated in [50]. This result implies that the number of edges of the $(\leq k)$-zone defined in Section 5.3.2 is $O(nk)$. This together with the lately improved upper bound of $2^m(\frac{5}{2})^{\binom{m}{2}}$ on the number of cutpaths in an arrangement of m pseudolines [22] gives an upper bound of $c \cdot (nk)^2 \cdot 2^{k-2}(\frac{5}{2})^{\binom{k-2}{2}}$ on the number of k-segments in an arrangement of n pseudolines with a constant $c > 0$.

5.4 Nonpseudosegment graphs- a Ramsey argument

Recall our original interest in the relation of chordal graphs an pseudosegment graphs. In Section 5.1 we have shown that vertex intersection graphs of subpaths of a tree are pseudosegment graphs. In the subsequent section we have shown that the chordal graph K_n^3 has no pseudosegment representation if $n \geq 39$. We would like to formulate restrictions on the tree representations of chordal graphs that are pseudosegment graphs as well. It is easy to see that there is a tree representation of K_n^3 where the host tree is a caterpillar with maximal degree three though with disproportionately high diameter. To account for this, consider the following chordal graph.

Definition 5.20. For $n \in \mathbb{N}$ let S_n^3 be the graph whose vertices can be partitioned into two sets, $V_I' = [n]$ and $V_C' = \binom{[n]}{3}$. The vertices of V_I' form an independent set and V_C' induces a clique of S_n^3. Additionally each vertex $\{i, j, k\} \in V_C'$ is adjacent to vertex $l \in V_I'$ if and only if $l \in \{i, j, k\}$.

Every S_n^3 is a vertex intersection graph of substars of a star, where the substars have maximal degree three. Figure 5.22 sketches S_5^3 as a vertex intersection graph of substars of degree three of a star with 5 leaves.

Theorem 5.21. For large enough $n \in \mathbb{N}$ there is no pseudosegment representation of S_n^3.

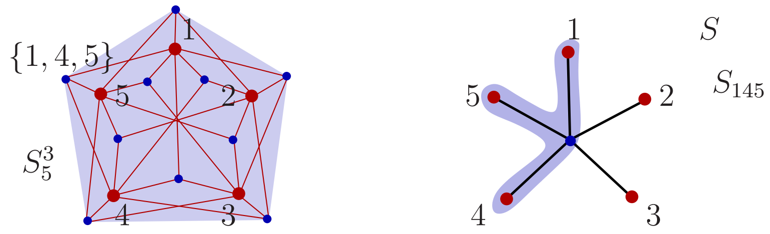

Figure 5.22: A sketch of S_5^3 and a star hosting a tree representation of S_5^3 with a substar representing vertex $\{1,4,5\}$.

Proof. Assuming that there is a pseudosegment representation $\mathcal{G}$ of S_n^3, the set $\mathcal{G}$ of pseudosegments can be divided into $\mathcal{S}_m$ and $\mathcal{S}_I$, that is the pseudosegments representing the vertices from V_C' and V_I' respectively. Any two different pseudosegments of $\mathcal{S}_I$ are disjoint. The pseudosegments of $\mathcal{S}_m$ have the following properties:

(i) $\mathcal{S}_m$ is an arrangement of $m = \binom{n}{3}$ pseudosegments, and

(ii) every pseudosegment of $\mathcal{S}_m$ has nonempty intersection with exactly three different pseudosegments $\mathcal{S}_I$ and no two different pseudosegments of $\mathcal{S}_m$ intersect the same three pseudosegments of $\mathcal{S}_I$.

To show that not every S_n^3 is a pseudosegment graph we first restrict our attention to the intersection behavior of elements of $\mathcal{S}_m$ with respect to elements of $\mathcal{S}_I$. At this we will align the elements of $\mathcal{S}_I$ along the X_1-axis. This will be used to classify subsets of $\mathcal{S}_I$ by the intersection behavior of the elements of $\mathcal{S}_m$ with respect to $\mathcal{S}_I$, and at the same time to classify elements of $\mathcal{S}_m$. Then, the application of Theorem 5.22, a Ramsey argument, will leave us with a set $Y \subset \mathcal{S}_I$ of arbitrary size such that all elements of $\mathcal{S}_m$ intersecting triples of Y behave alike. Within these elements of $\mathcal{S}_m$, we will find a pair of elements with more than one intersection if Y exceeds a certain size. Since this is not allowed in a pseudosegment representation, it follows that most of the graphs of $(S_n^3)_{n\in\mathbb{N}}$ are not pseudosegment graphs.

5.4.1 Classification of the elements of $\mathcal{S}_m$ and a Ramsey theorem

The pseudosegments of $\mathcal{S}_I \subset \mathcal{G}$ are pairwise disjoint. To simplify the picture we use an homeomorphism of the plane which aligns the pseudosegments of $\mathcal{S}_I$ as vertical segments of unit length touching the X_1-axis with their lower endpoints at positions $1, 2, \dots, n$. For ease of reference we will call these vertical segments *sticks* and index them such that p_i denotes the stick containing the point $(i, 0)$.

With every ordered triple (i, j, k), $1 \leq i < j < k \leq n$, there is a pseudosegment p_{ijk} in $\mathcal{S}_m \subset \mathcal{G}$ intersecting the sticks p_i, p_j and p_k from $\mathcal{S}_I$. This pseudosegment is disjoint from all other sticks of $\mathcal{S}_I$ and the union of all such pseudosegments forms an arrangement $\mathcal{S}_m$ of $m = \binom{n}{3}$ pseudosegments.

For every p_{ijk} of $\mathcal{S}_m$, $1 \leq i < j < k \leq n$, let ϕ_{ijk} denote the middle of the three sticks intersected by p_{ijk}. We partition the ordered triples (i, j, k) into three *classes* depending on the position of ϕ_{ijk} in the list (p_i, p_j, p_k). If $\phi_{ijk} = p_i$, that is the middle intersection of p_{ijk} is left of the other two, we assign (i, j, k) to class $[L]$. The class of (i, j, k) is $[M]$ if $\phi_{ijk} = p_j$, that is the middle intersection of p_{ijk} is between the other two. The class of (i, j, k) is $[R]$ if $\phi_{ijk} = p_k$, that is the middle intersection of p_{ijk} is to the right of the other two. We use this notation rather flexible and also write $p_{ijk} \in [X]$ or say that p_{ijk} is of class $[X]$ when the triple (i, j, k) is of class $[X]$, for $X \in \{L, M, R\}$. Examples of pseudosegments of classes $[M]$ and $[R]$ are given in Figure 5.23.

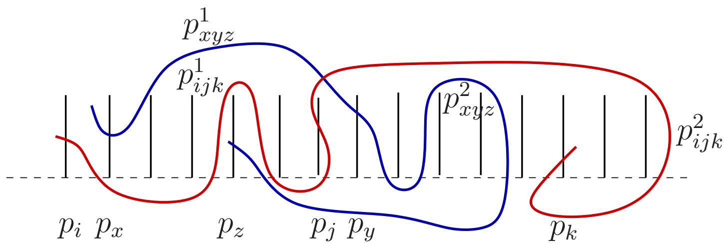

Figure 5.23: An example of a pseudosegment $p_{ijk} \in [M]$ and $p_{xyz} \in [R]$.

Cutting p_{ijk} at the intersection points with the three sticks yields two arcs p^1_{ijk} and p^2_{ijk} each connecting two sticks and up to two ends. The ends are of no further interest. For the arcs we adopt the convention that p^1_{ijk} connects ϕ_{ijk} to the stick further left and p^2_{ijk} connects ϕ_{ijk} to the stick further right. In the example of Figure 5.23, $\phi_{xyz} = p_y$ so that p^1_{xyz} is the arc connecting p_x and p_y while arc p^2_{xyz} connects p_y and p_z.

For a contradiction we will show that if n is large enough, then there are different pseudosegments p_{ijk} and p_{xyz} in a pseudosegment representation of S^3_n such that p^1_{ijk} and p^1_{xyz} intersect and p^2_{ijk} and p^2_{xyz} intersect. Hence, p_{ijk}

and p_{xyz} intersect at least twice which is not allowed in a pseudosegment representation.

To get to that contradiction we need some control over the behavior of the pseudosegments of the arrangement between the sticks. The subsequent definitions will enable us to describe the crucial relations. Let $\boldsymbol{r}_x$ be a vertical ray downwards starting at $(x, 0)$, that is the ray pointing down from the lower end of stick p_x. Let $I^s_x(ijk)$ be the number of intersections of ray $\boldsymbol{r}_x$ with p^s_{ijk} and let $J^s_x(ijk)$ be the parity of $I^s_x(ijk)$, i.e., $J^s_x(ijk) \equiv I^s_x(ijk) \pmod 2$.

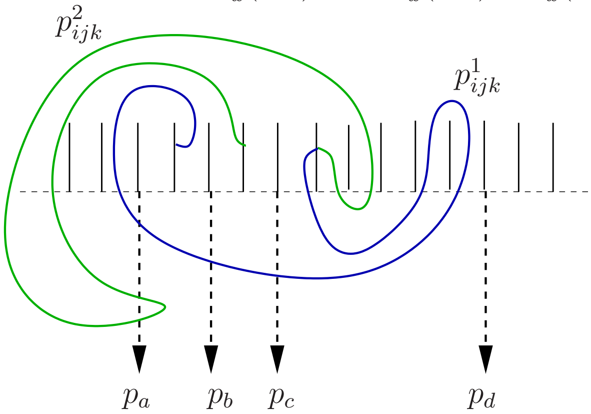

Figure 5.24: The pattern of 3-segment $p_{ijk} \in R$ is $(1, 1, 1, 0, 0, 0, 0, 0)$.

Let (a, i, b, j, c, k, d) be an ordered 7-tuple of the set $[n]$, in other words let $1 \leq a < i < b < j < c < k < d \leq n$. Then we call p_{ijk} the induced pseudosegment of this 7-tuple and set $T^s_x = J^s_x(ijk)$. The *pattern* of the 7-tuple (a, i, b, j, c, k, d) is the binary 8-tuple

$$(T^1_a, T^1_b, T^1_c, T^1_d, T^2_a, T^2_b, T^2_c, T^2_d).$$

An example of such a pattern is given in Figure 5.24. With this we define the *color* of a 7-tuple (a, i, b, j, c, k, d) as the pair consisting of the class of the induced 3-segment and the pattern. The 7-tuples of $[n]$ are thus colored with the 768 colors from the set $[3] \cdot \mathbf{2}^8$. Ordered 7-tuples and 7-element subsets of $[n]$ are in bijection. Therefore we can apply the Ramsey theorem cited next with parameters $768, 7, 13$.

Theorem 5.22. For every choice of numbers $r, p, k \in \mathbb{N}$ there exists a number $n \in \mathbb{N}$ such that whenever X is an n-element set and c is a coloring of the system of all p-element subsets of X using r colors, i.e. $c : \binom{X}{p} \to \{1, 2, .., r\}$, then there is a k-element subset $Y \subseteq X$ such that all the p-subsets in $\binom{Y}{p}$ have the same color.

5.4.2 Geometric restrictions

The application of the Ramsey theorem leaves us with an uniform configuration. We have kept only a subset Y of sticks of $\mathcal{S}_I$ such that all pseudosegments of $\mathcal{S}_m$ connecting three of them are of the same class and all 7-tuples on Y have the same pattern $T = (T_1^1, T_2^1, T_3^1, T_4^1, T_1^2, T_2^2, T_3^2, T_4^2)$. Now we need one more argument which is a direct consequence of Theorem 2.1, the Jordan Curve Theorem.

Given two curves γ and γ', closed or not, we let $X(\gamma, \gamma')$ be the number of crossing points of the two curves.

Fact 2. If γ and γ' are closed curves, then $X(\gamma, \gamma') \equiv 0 \pmod 2$.

With an arc p_{ij} connecting sticks p_i and p_j we associate a closed curve $\breve{\gamma}_{ij}$ as follows: At the intersection of p_{ij} with either of the sticks we append long vertical segments and connect the lower endpoints of these two segments horizontally. The union of the three connecting segments will be called the *bow* β_{ij} of the curve $\breve{\gamma}_{ij}$. If this construction is applied to several arcs we assume that the vertical segments of the bows are long enough as to avoid any intersection between the arcs of $\mathcal{S}_m$ and the horizontal part of the bows.

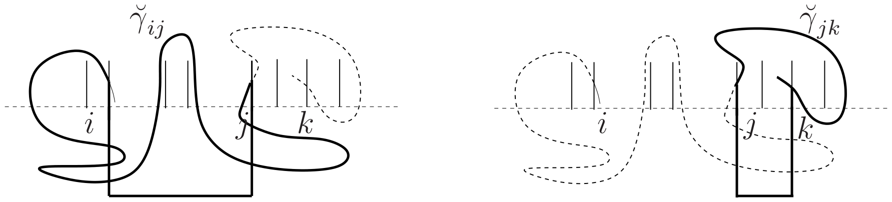

Figure 5.25: Closed curves $\breve{\gamma}_{ij}$ from p_{ij} and $\breve{\gamma}_{jk}$ from p_{jk}.

This construction ensures that we can count the crossings of two curves $\breve{\gamma}_{ij}$ and $\breve{\gamma}_{xy}$ in parts:

$$X(\breve{\gamma}_{ij}, \breve{\gamma}_{xy}) = X(p_{ij}, p_{xy}) + X(p_{ij}, \beta_{xy}) + X(\beta_{ij}, p_{xy}) + X(\beta_{ij}, \beta_{xy})$$

With Fact 2 we obtain

Fact 3. $X(p_{ij}, p_{xy}) \equiv X(p_{ij}, \beta_{xy}) + X(\beta_{ij}, p_{xy}) + X(\beta_{ij}, \beta_{xy}) \pmod 2$.

The uniformity of the colors of all 7-tuples allows us to apply Fact 3 to detect intersections of arcs of type p^s_{ijk}. Depending on the entries of the pattern T

we choose sticks p_i, p_j, p_k and p_x, p_y, p_z with appropriate pseudosegments p_{ijk} and p_{xyz} and show that they intersect twice.

So assume that the class of all those pseudosegments is $[L]$ or $[M]$, hence there is an arc connecting the two sticks with smaller indices. Let $p_{ij} = p^1_{ijk}$, and $p_{xy} = p^1_{xyz}$.

Lemma 5.23. If $T^1_1 = T^1_3$ and $i < x < j < y < k$, then there is an intersection between the arcs p_{ij} and p_{xy}.

Proof. We evaluate the right side of the congruence given in Fact 3. Here, $X(p_{ij}, \beta_{xy})$ is the number of intersections of arc p_{ij} with the bow connecting p_x and p_y. These intersections lie on the vertical part, hence on the rays $\boldsymbol{r}_x$ and $\boldsymbol{r}_y$. The parity of these intersections can be read from the pattern. The position of x between i and j implies $T^1_x = T^1_2$ and the position of y between j and k implies $T^1_y = T^1_3$. Hence, $X(p_{ij}, \beta_{xy}) \equiv T^1_2 + T^1_3 \pmod 2$.

From the positions of i left of x and of j between x and y we conclude that $X(\beta_{ij}, p_{xy}) \equiv T^1_1 + T^1_2 \pmod 2$. Since the pairs ij and xy interleave, the two bows are intersecting, i.e., $X(\beta_{ij}, \beta_{xy}) = 1$.

Together this yields $X(p_{ij}, p_{xy}) \equiv T^1_2 + T^1_3 + T^1_1 + T^1_2 + 1 \pmod 2$. With $T^1_1 = T^1_3$ we see that $X(p_{ij}, p_{xy})$ is odd, hence, there is at least one intersection between the arcs. □

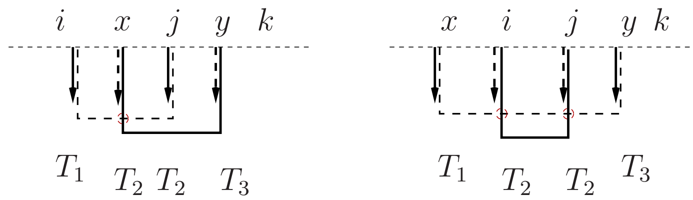

Figure 5.26: Intersections between the bows depend on the order of the sticks p_i, p_j, p_x and p_y.

Lemma 5.24. If $T^1_1 \neq T^1_3$ and $x < i < j < y < k$, then there is an intersection between the arcs p_{ij} and p_{xy}.

Proof. Since x is to the left of i and y lies between j and k, we obtain $X(p_{ij}, \beta_{xy}) \equiv T^1_1 + T^1_3 \pmod 2$. Both i and j are between x and y, thus $X(\beta_{ij}, p_{xy}) \equiv T^1_2 + T^1_2 \equiv 0 \pmod 2$. For the bows we observe that either they do not intersect or they intersect twice, in both cases $X(\beta_{ij}, \beta_{xy}) \equiv 0 \pmod 2$.

Put together, $X(p_{ij}, p_{xy}) \equiv T_1^1 + T_3^1 \pmod 2$. Since $T_1^1 \neq T_3^1$, we obtain that $X(p_{ij}, p_{xy})$ is odd, hence, there is at least one intersection between the arcs. □

In addition to the arcs p_{ij} and p_{xy} we have the arcs $p_{jk} = p^2_{ijk}$, and $p_{yz} = p^2_{xyz}$. Now we first consider the case where the class is $[M]$. The following two lemmas are counterparts to Lemmas 5.23 and 5.24; they show that depending on the parity of $T_1^2 + T_3^2$, an "alternating (alt)" or a "non-alternating (non-alt)" choice of jk and yz forces an intersection of the arcs p_{jk} and p_{yz}. For the proofs note that reflection at the X_2-axis keeps the class $[M]$ invariant but exchanges the first and the second arc; the relevant effect on the pattern is $T_1^1 \leftrightarrow T_4^2$ and $T_3^1 \leftrightarrow T_2^2$.

Lemma 5.25. If $T_2^2 = T_4^2$ and $x < j < y < k < z$, then there is an intersection between the arcs p_{jk} and p_{yz}.

Lemma 5.26. If $T_2^2 \neq T_4^2$ and $x < j < y < z < k$, then there is an intersection between the arcs p_{jk} and p_{yz}.

The table below shows that it is possible to select ijk and xyz out of six numbers such that the positions of ij and xy respectively jk and yz are any combination of alternating and non-alternating. Hence, according to the lemmas we have at least two intersections between 3-segments p_{ijk} and p_{xyz} chosen appropriately depending on the entries of pattern T. We represent elements of ijk by a box □ and elements of xyz by circles •.

□ • □ • □ •	alt / alt	$[T_1^1 = T_3^1$ and $T_2^2 = T_4^2]$
□ • □ • • □	alt / non-alt	$[T_1^1 = T_3^1$ and $T_2^2 \neq T_4^2]$
• □ □ • □ •	non-alt / alt	$[T_1^1 \neq T_3^1$ and $T_2^2 = T_4^2]$
• □ □ • • □	non-alt / non-alt	$[T_1^1 \neq T_3^1$ and $T_2^2 \neq T_4^2]$

Now consider the case where the class is $[L]$. Again we have $p_{ik} = p^2_{ijk}$ and $p_{xz} = p^2_{xyz}$ in addition to arcs p_{ij} and p_{xy}. The following two lemmas show that depending on the parity of $T_1^2 + T_3^2 + T_3^2 + T_4^2$ an alternating or a non-alternating choice of ik and xz force an intersection of the arcs p_{ik} and p_{xz}.

Lemma 5.27. If $T_1^2+T_3^2+T_3^2+T_4^2 \equiv 0 \pmod 2$ and $i < x < \{j, y\} < k < z$, then there is an intersection between the arcs p_{ik} and p_{xz}.

Proof. Since x lies between i and j and z is to the right of k, we obtain $X(p_{ik}, \beta_{xz}) \equiv T_2^2 + T_4^2 \pmod 2$. With i being left of x and k between y and z, we obtain $X(\beta_{ik}, p_{xz}) \equiv T_1^2 + T_3^2 \pmod 2$. So as the pairs ik and xz interleave, the two bows are intersecting, i.e., $X(\beta_{ik}, \beta_{xz}) = 1$.

We obtain, $X(p_{ij}, p_{xy}) \equiv T_1^2 + T_3^2 + T_3^2 + T_4^2 + 1 \pmod 2$. Hence there is at least one intersection between arcs p_{ik} and p_{xz}. ☐

Lemma 5.28. If $T_1^2+T_3^2+T_3^2+T_4^2 \equiv 1 \pmod 2$ and $i < x < \{j, y\} < z < k$, then there is an intersection between the arcs p_{ik} and p_{xz}.

Proof. Since x is between i and j and z is between j and k, we obtain $X(\gamma_{ik}, \beta_{xz}) \equiv T_2^2 + T_3^2 \pmod 2$. With i being left of x and k right of z, we obtain $X(\beta_{ik}, p_{xz}) \equiv T_1^2 + T_4^2 \pmod 2$. For the bows we observe that either they don not intersect or they intersect twice, hence $X(\beta_{ik}, \beta_{xz}) \equiv 0 \pmod 2$.

Put together $X(p_{ij}, p_{xy}) \equiv T_1^2 + T_3^2 + T_3^2 + T_4^2 \pmod 2$. Hence there is at least one intersection between the arcs. ☐

As in the previous case we provide a table showing that it is possible to select ijk and xyz out of six numbers such that the positions of ij and xy respectively ik and xz are any combination of alternating and non-alternating. We represent elements of ijk by a box ☐ and elements of xyz by circles •.

☐ • ☐ • ☐ •	alt / alt	$[T_1^1 = T_3^1$ and $T_1^2 + T_3^2 + T_3^2 + T_4^2 \equiv 0]$
☐ • ☐ • • ☐	alt / non-alt	$[T_1^1 = T_3^1$ and $T_1^2 + T_3^2 + T_3^2 + T_4^2 \equiv 1]$
• ☐ ☐ • • ☐	non-alt / alt	$[T_1^1 \neq T_3^1$ and $T_1^2 + T_3^2 + T_3^2 + T_4^2 \equiv 0]$
• ☐ ☐ • ☐ •	non-alt / non-alt	$[T_1^1 \neq T_3^1$ and $T_1^2 + T_3^2 + T_3^2 + T_4^2 \equiv 1]$

To deal with the case where the class of all pseudosegments is $[R]$ we refer to symmetry. Reflecting the picture at the X_2-axis yields a configuration where all pseudosegments are in class $[L]$.

Thus, no uniform configuration on six or more sticks can belong to a pseudosegment representation of any graph, in particular of S_n^3. Note that the definition of a pattern involves seven sticks, so let us choose 13 as the minimal size of an uniform configuration that cannot be contained within a pseudosegment representation. By Theorem 5.22 we know that there is an $\hat{n} \in \mathbb{N}$ such that every pseudosegment representation of S_n^3 with $n \geq \hat{n}$ has to contain a uniform configuration on 13 sticks, so we conclude that S_n^3 is not a pseudosegment graph for large enough n. This completes the proof of Theorem 5.21. □

5.5 Summary

In Section 5.1 we have shown that all chordal graphs that are vertex intersection graphs of subpaths of a tree have pseudosegment representations. Subsequently we have shown examples of chordal graphs that do not belong to PSI. In order to delimit the common subclass of chordal graphs and pseudosegment graphs we considered the graph S_n^3. The result of Section 5.4 then involves that the common subclass of PSI and the class of chordal graphs cannot contain graphs induced by many treelike subtrees of a tree.

Note that our smallest examples of chordal graphs that do not belong to PSI have more than 5000 vertices. Thus they are quite big in comparison to the classical examples of graphs that are not in PSI. As mentioned in Chapter 3, the complete subdivision of K_5, and by the same argument the complete subdivision of $K_{3,3}$, is not a pseudosegment graph. Each of these graphs has only 15 vertices.

Another extension of path graphs different from chordal graphs are vertex intersection graphs of subpaths of a *cactus graph*, the latter being defined as a connected graph where any two cycles have at most one vertex in common. As in the case of chordal graphs, we can use the graph K_n^3 to show that the class of vertex intersection graphs of subpaths of a cactus graph does not belong to PSI.

To see this take $\binom{n}{3}$ 4-cycles and connect them as sketched in Figure 5.27; this gives the graph G_C. Denote the vertices of G_C with maximal distance as s and t. Assign the vertices of the independent set V_I of K_n^3 to vertices of degree two, different from s and t, such that no two of them are assigned to vertices of the same 4-cycle. Assign each element of the clique V_C of K_n^3 to a path connecting s and t and containing all vertices representing its neighbors in V_I. This gives a representation of K_n^3 as vertex intersection graph of subpaths of a cactus graph.

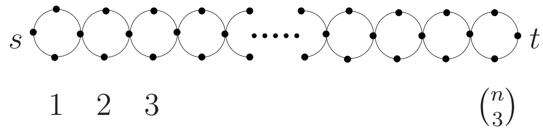

Figure 5.27: A cactus graph that can host $n+\binom{n}{3}$ paths representing K_n^3.

In Section 5.3 we considered how many combinatorially different k-segments can be contained in an arrangement of n pseudolines. Let us remind you that our original question about the number of 3-segments that can be contained in an arbitrary arrangement of pseudosegments is still open.

Question 5.9 Let $\mathcal{S}_n$ be an arrangement of n pseudosegments in the plane. What is the maximal size of a set $\mathcal{J}$ of different 3-segments of $\mathcal{S}_n$ such that the union of $\mathcal{S}_n \cup \mathcal{J}$ is a set of pseudosegments?

Chapter 6

Cocomparability Graphs

Every poset P with ground set X naturally induces two graphs on X, a comparability and a cocomparability graph. The cocomparability graph has an edge for every pair of elements of X that is incomparable in P. Recall from Chapter 3 that every cocomparability graph is a string graph. This result was obtained by embedding the linear extensions of a realizer of the respective poset onto parallel lines and connecting points on consecutive lines that corresponded to the same element of X. This operation, applied to a poset of dimension two, yields a pseudosegment representation of the respective cocomparability graph, a permutation graph.

A natural extension of a linear order is an interval order, yielding the notion of the interval dimension of a poset. The cocomparability graphs of posets of interval dimension one are the interval graphs. As every interval graph is a path graph, it is a pseudosegment graph as shown in Chapter 5. Using a minimal interval realizer of the poset corresponding to an interval graph, we obtain a pseudosegment representation of the respective interval graph different from the one obtained in Chapter 5. This leads to considering cocomparability graphs of posets of interval dimension two. These graph are known as trapezoid graphs.

In the following sections we will present different subclasses of trapezoid graphs as point-interval graph and PI*-graphs and show that they belong to PSI. In every case we will construct a pseudosegment representation of the respective graph by embedding a minimal realizer of the respective poset onto the plane. Note that we will always use finite intersection models as we are working on finite graphs.

6.1 Interval graphs

An interval graph is classically known as intersection graph of a set of non-degenerate intervals of the real line [38]. Such a set of intervals is then called an interval representation of the respective interval graph. In the context of cocomparability graphs, every interval graph G is the cocomparability graph of a poset P of interval dimension one and every interval representation of G is an interval realizer of poset P. It is easy to see that interval graphs are pseudosegment graphs.

Proposition 6.1. Every interval graph has a pseudosegment representation.

Proof. Let $G = (X, E)$ be an interval graph and let $\mathcal{I}$ be an interval representation of G. To construct a pseudosegment representation of G, embed $\mathcal{I}$ onto the plane by mapping $\mathcal{I}$ onto the X_1-axis. This is done in such a way that the embedded intervals have the same intersection relations as their counterparts in the realizer and no two different intervals share an endpoint. Every interval $I \in \mathcal{I}$ can then be denoted by $I = [(l, 0), (r, 0)]$.

Assume that the intervals of $\mathcal{I}$ are ordered according to the order of their left endpoints; that is $\mathcal{I} = \{I_1, .., I_n\}$ with $l_i < l_j$ if and only if $i < j$. Now replace interval I_j by the L-shaped curve p_j consisting of the vertical segment $v_j = [(l_j, 0), (l_j, j)]$ and the horizontal segment $h_j = [(l_j, j)(r_j, j)]$ for every $j \in \{1, ..., n\}$. See Figure 6.1 for an illustration. Obviously each p_i is a Jordan arc as it consists of a vertical and a horizontal segment that share an endpoint.

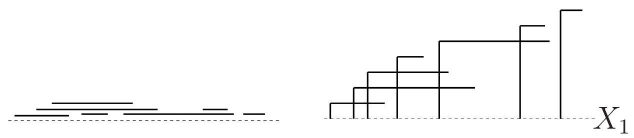

Figure 6.1: A pseudosegment representation of an interval graph using the left-endpoint ordering of an appropriate interval representation.

It is easy to see that $\mathcal{G} := \{p_1, .., p_n\}$ is a pseudosegment representation of G. Assume that $i < j$. Vertices i and j of G are not adjacent if and only if intervals I_i and I_j are disjoint. Then Jordan arcs p_i and p_j lie in different halfplanes with respect to the vertical line $l_{ij} := \{(r_i + \epsilon, x) \mid x \in \mathbb{R}\}$ for an adequate real number $\epsilon > 0$. If i and j are adjacent, then Jordan arcs p_i

and p_j intersect in the horizontal segment h_i and the vertical segment v_j. Obviously there is no further point of intersection. Thus, $\mathcal{G}$ is a pseudosegment representation of G. □

6.1.1 Circular-arc graphs

Before we proceed with a further subclass of trapezoid graphs let us consider *circular-arc graphs*. They are the intersection graphs of arcs of a circle [31] and form a generalization of interval graphs, different from the one by co-comparability graphs.

Proposition 6.2. Every circular-arc graph has a pseudosegment representation.

Proof. Let G_c be an arbitrary circular-arc graph. Let $\mathcal{G}_c$ be a set of arcs of a circle $\mathcal{C}_c$ in the plane such that $G_c \cong \Omega(\mathcal{G}_c)$. Assume that no two endpoints of different arcs of $\mathcal{G}_c$ are the same and let Q be a point on $\mathcal{C}_c$ that is not an endpoint of any arc of $\mathcal{G}_c$.

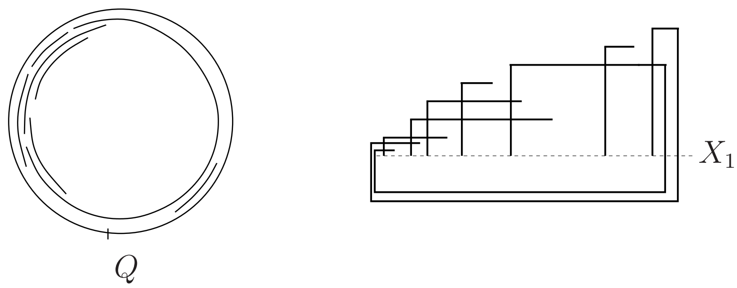

Figure 6.2: A pseudosegment representation of a circular arc graph obtained from a pseudosegment representation of an interval graph.

Set A_Q as the set of arcs containing Q and A as the remaining arcs. Remove Q from $\mathcal{C}_c$ and embed the resulting Jordan arc with all arcs of A onto the X_1-axis without changing the intersection relation or order of the arcs of A. Every arc of A_Q is cut into two pieces. First we add the pieces that intersect the rightmost arcs of A as intervals onto the X_1-axis. This is done in such a way that the intersection relations between the elements of A and these pieces of A_Q correspond to their intersection relations in $\mathcal{G}_c$. The resulting embedding represents an interval graph which is a subgraph of G_c;

let $\mathcal{G}'$ be a pseudosegment representation of this graph constructed as in Section 6.1. It remains to add the intersections between the arcs of A_Q and the leftmost arcs of A. This is done by adding disjoint arcs to the pseudosegments representing the arcs of A_Q such that each of them crosses the vertical part of the pseudosegments of A that are intersected by the corresponding arc in $\mathcal{G}_c$. This can be done as sketched in Figure 6.2. The resulting set of Jordan arcs is obviously a pseudosegment representation of G_c. As G_c was chosen arbitrarily, it follows that every circular-arc graph is a pseudosegment graph. $\square$

6.2 Point-interval graphs

Point-interval graphs were introduced in [10] as an extension of permutation and interval graphs and a restriction of trapezoid graphs. Recall that a permutation graph is a cocomparability graph of a poset that has a realizer consisting of two linear orders. A trapezoid graph is a cocomparability graph of a poset that has a realizer consisting of two interval orders. Then, a *point-interval graph* is a cocomparability graph of a poset that has a realizer consisting of a linear and an interval order. If we embed the orders of such a realizer onto two parallel lines, we obtain a representation of the respective point-interval graph as intersection graph of triangles spanned between two parallel lines, see Figure 6.3 for an example. Such a representation is also used to define point-interval graphs.

That is, let H and L be a pair of parallel lines in the Euclidean plane and let $\mathcal{T}$ be a set of triangles such that two corners of each triangle lie on line H and one corner of each triangle lies on line L. Then the intersection graph $\Omega(\mathcal{T})$ is a *point-interval graph*, for short a PI-graph, and $\mathcal{T}$ is called a *point-interval representation* of $\Omega(\mathcal{T})$.

Proposition 6.3. Every point-interval graph has a pseudosegment representation.

Proof. Consider an arbitrary point-interval graph $G = (X, E)$ and let $\mathcal{T}$ be a point-interval representation of G such that the triangles of $\mathcal{T}$ are spanned between lines $H_0 := \{(x, 0) \mid x \in \mathbb{R}\}$ and $H_1 = \{(x, 1) \mid x \in \mathbb{R}\}$. We furthermore require that no two corners of different triangles have the same

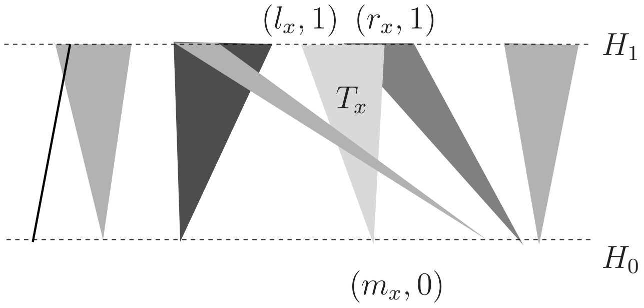

Figure 6.3: A representation of a point-interval graph as intersection graph of triangles spanned between two parallel lines $H = H_1$ and $L = H_0$.

X_1-coordinate. For vertex $x \in X$ let T_x be the triangle in $\mathcal{T}$ representing x. Let $(m_x, 0)$ denote the point T_x shares with H_0, and let $I_x = [(l_x, 1), (r_x, 1)]$ denote the interval T_x shares with H_1. Then we refer to $b_x = [(l_x, 1), (m_x, 0)]$ as the left boundary segment of T_x.

If we restrict the point-interval representation $\mathcal{T}$ to the left boundary segments of the triangles, then we obtain a permutation representation and, thus, a pseudosegment representation $\mathcal{G}_P$ of some subgraph G_P of G. If we restrict $\mathcal{T}$ to the union of the intervals on H_1, we obtain an interval representation of some subgraph G_I of G. A pseudosegment representation $\mathcal{G}_I$ of this subgraph is obtained by the construction of Section 6.1.

If G_P and G_I do not have any common edge, we simply join every pair of Jordan arcs of $\mathcal{G}_P$ and $\mathcal{G}_I$, that represent the same element of G, at their common endpoint $(l_x, 1)$. By this we obtain a Jordan arc p_x for every element x of G. Recall the definition of a permutation graph and the analysis of Section 6.1. Thus it holds that Jordan arcs $p_x, p_y \in \mathcal{G}_I \cup \mathcal{G}_P$ cross exactly once if and only if x and y are adjacent in G, and are disjoint otherwise.

If G_P and G_I have a common edge, let E_{PI} be the set of common edges of G_P and G_I. In this case G will be represented by the pseudosegment representation of G_P and a certain pseudosegment representation $\mathcal{G}_I^-$ of the subgraph $G_I - E_{PI}$ of G obtained as follows.

Observation 6.4. For every edge $e = uw \in E_{PI}$, it holds that T_u and T_w intersect in their left boundary segments and share a point on H_1, see Figure 6.4.

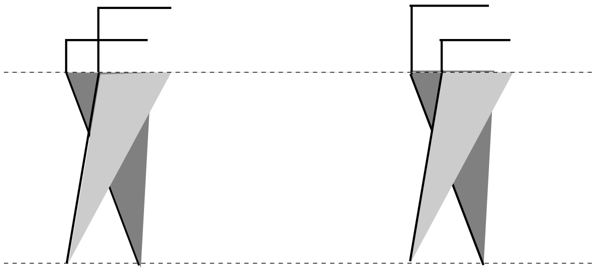

Figure 6.4: To the left, triangles corresponding to an edge $e = uw \in E_{PI}$, and to the right, a representation of the two elements in the pseudosegment representation $\mathcal{G} = \mathcal{G}_P \cup \mathcal{G}_I^-$.

Assuming that $l_u < l_w$, Observation 6.4 implies that $m_w < m_u$ if $uw \in E_{PI}$. Recall that, given a pseudosegment representation of an interval graph, the length of a vertical segment v_x of the respective Jordan arc p_x depends on the position of I_x in the left endpoint ordering $(I_1, ..., I_n)$. So let us order the intervals on H_1 depending on the order of the "tips" $\{(m_x, 0) \mid x \in X\}$ on H_0. Using this ordering in the pseudosegment construction of Section 6.1 obviously yields a pseudosegment representation of $G_I - E_{PI}$.

Now we can join every pair of Jordan arcs of $\mathcal{G}_P$ and $\mathcal{G}_I^-$, that represent the same element of G. This gives the following Jordan arc for vertex $i \in \{1, ..., n\}$ of G as the joined Jordan arcs have $(l_i, 1)$ as common endpoint:

$$p_i := [(l_i, 1+i), (r_i, 1+i)] \cup [(l_i, 1), (l_i, 1+i)] \cup [(l_i, 1), (m_i, 0)].$$

Thus, the union of $\mathcal{G} = \mathcal{G}_I^- \cup \mathcal{G}_P$ contains a Jordan arc p_x for every element x of G so that p_x and p_y cross exactly once if and only if x and y are adjacent in G. An example of a pseudosegment representation obtained by the latter construction is given in Figure 6.5.

□

6.3 PI*-GRAPHS

To obtain a pseudosegment representation of a point-interval graph, we considered a representation of the respective point-interval graph as intersection graph of triangles spanned between two parallel lines H and L such that two corners of the triangles lie on H and one corner of each triangle lies on L. If we relax this condition in such a way that all corners of the triangles lie

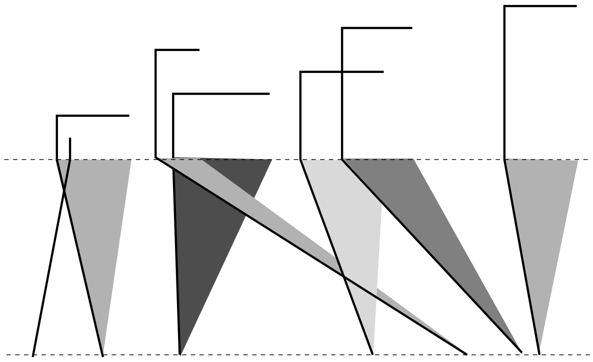

Figure 6.5: A representation of a point-interval graph as intersection graph of triangles spanned between two parallel lines $H = H_1$ and $L = H_0$.

on H and L and not all three on the same line, we obtain a further subclass of trapezoid graphs, the class of *PI*-graph* [51], sketched in Figure 6.6. A PI*-representation consists of a set of triangles such that all corners of the triangles lie on two parallel lines and not all three corners of any triangle on the same line.

Proposition 6.5. Every PI*- graph has a pseudosegment representation.

We will see that every PI*-graph G has two subgraphs that are point-interval graphs and cover G. By Proposition 6.3 we can represent these subgraphs as pseudosegment graphs. In the following we will show how to choose these subgraphs such that we can combine the respective pseudosegment representations in order to obtain a pseudosegment representation of the given PI*-graph.

Proof. Consider an arbitrary PI*-graph $G = (X, E)$ and let $\mathcal{T}$ be a PI*-representation of G. Again we assume that $\mathcal{T}$ is embedded in the plane such that the triangles of $\mathcal{T}$ are spanned between lines $H_0 := \{(x, 0) \mid x \in \mathbb{R}\}$ and $H_1 = \{(x, 1) \mid x \in \mathbb{R}\}$. Furthermore we require that no two corners of different triangles have the same X_1-coordinate.

We intend to choose two subgraphs of G, say $G(U)$ and $G(D)$, such that the union of $G(U)$ and $G(D)$ is G and both subgraphs are point-interval graphs. Note that the set of triangles of $\mathcal{T}$ that share a point with H_0 induces a point-interval graph; let this set be $\mathcal{U}'$ and set U' as the set of vertices of G corresponding to $\mathcal{U}'$. The remaining triangles are denoted as $\mathcal{D}'$, the corresponding vertices of G as D'; they induce a point-interval graph as well.

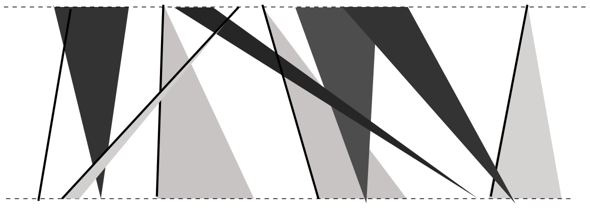

Figure 6.6: The triangles of $\mathcal{U}'$ and the left boundary segments of the triangles of $\mathcal{D}'$ induce subgraph $G(U)$ of G; the analog gives subgraph $G(D)$.

Now consider two triangles T_u, T_d with $T_u \in \mathcal{U}'$ and $T_d \in \mathcal{D}'$. Let T_u be the triangle with corners $(m_u, 0)$, $(l_u, 1)$ and $(r_u, 1)$ and T_d the triangle with corners $(m_d, 1)$, $(l_d, 0)$ and $(r_d, 0)$. If T_u and T_d intersect, at least one of the triangles contains a point of the left boundary segment of the other, as sketched in Figure 6.7. To account for these intersections let $\mathcal{U}$ be the set of triangles of $\mathcal{U}'$ and all left boundary segments of triangles of $\mathcal{D}'$. Analogously set $\mathcal{D}$ as the set of triangles of $\mathcal{D}'$ and all left boundary segments of triangles of $\mathcal{U}'$. In $\mathcal{U}$ we consider the boundary segments of elements of $\mathcal{D}'$ as degenerated triangles with the respective notations, in $\mathcal{D}$ analogously. Then $\mathcal{U}$ and $\mathcal{D}$ are point-interval representations of certain subgraphs of G. Let $G(U)$ and $G(D)$ denote the corresponding subgraphs of G.

Observation 6.6. By definition $G(U)$, as well as $G(D)$, contains all vertices of G. Note that every edge of G is contained in at least one of the subgraphs. More precisely, if xy is an edge of G we distinguish two types of intersections between the respective triangles T_x and T_y, that is

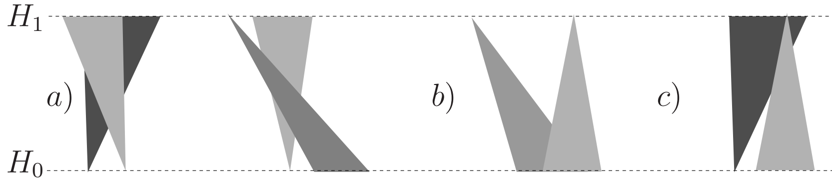

Figure 6.7: An intersection between two triangles of $\mathcal{T}$ can be an edge (a) of $G(U)$ and $G(D)$, (b) of $G(D)$ and not of $G(U)$ or (c) of $G(U)$ and not of $G(D)$.

- triangles T_x and T_y intersect in their left boundary segments. In this case, xy is an edge of $G(U)$ and $G(D)$ as both boundary segments are contained in $\mathcal{U}$ and also in $\mathcal{D}$; an example of such an intersection is given in part (a) of Figure 6.7.

- the left boundary segments of T_x and T_y are disjoint. Then T_u and T_d either share a point on H_1 or on H_0 but not on both lines, hence xy is either an edge of $G(D)$ but not of $G(U)$, see part (b) of Figure 6.7, or an edge of $G(U)$ and not of $G(D)$, see part (c) of Figure 6.7.

Observation 6.6 and the analysis of the proof of Proposition 6.3 motivate the following choice of Jordan arcs for a pseudosegment representation of G. Let $\mathcal{G}_U$ and $\mathcal{G}_D$ be pseudosegment representations of $G(U)$ and $G(D)$ obtained as in the proof of Proposition 6.3. Let u_x be the pseudosegment of $\mathcal{G}_U$ and d_x the pseudosegment of $\mathcal{G}_D$ that represent vertex $x \in X$. Then the left boundary segment b_x of triangle T_x is a part of u_x and d_x. The endpoint $(m_x, 0)$ of b_x is an endpoint of u_x and the endpoint $(m_x, 1)$ of b_x is an endpoint of d_x. By construction, u_x and d_x are disjoint above H_1 and below H_0, and b_x is the only common part of u_x and d_x. Thus, we obtain a Jordan arc p_x if we join u_x and d_x by identifying $b_x \subset u_x$ with $b_x \subset d_x$ for every $x \in X$.

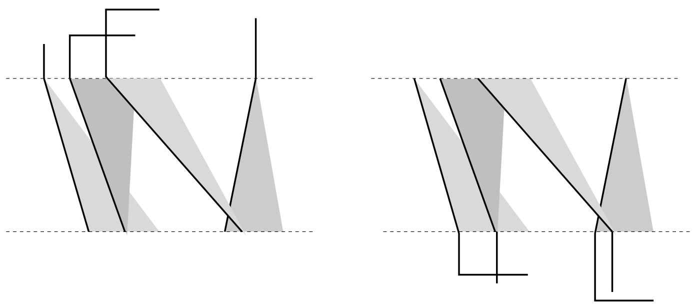

Figure 6.8: Pseudosegments representing triangles of $\mathcal{T}$ in $\mathcal{G}_U$ to the left and in $\mathcal{G}_D$ to the right.

To see that $\mathcal{G} := \{p_x \mid x \in X\}$ is a pseudosegment representation of G we first consider a pair of non-adjacent vertices x, y of G. In this case, the corresponding pseudosegments of $\mathcal{G}(U)$ and $\mathcal{G}(D)$ are disjoint. Then the choice of p_x and p_y implies that they are also disjoint in $\mathcal{G}$.

Now let xy be an edge of G that belongs to $G(U)$ and not to $G(D)$. Let i_x be the index of triangle $T_x \in \mathcal{U}$ according to the tip ordering on H_0, that is the ordering of the points $\{(m_x, 0) \mid x \in U\}$ and assume that $m_x < m_y$. Then, as in the proof of Proposition 6.5, u_x and u_y intersect in $\mathcal{G}_U$ in the horizontal part $[(l_x, 1+i_x), (r_x, 1+i_x)]$ of u_x and the vertical part $[(l_y, 1), (l_y, 1+i_y)]$ of u_y. As $\mathcal{G}_U$ is a pseudosegment representation of $G(U)$, there is no further intersection between u_x and u_y of $\mathcal{G}_U$. Thus $p_x = u_x \cup d_x$ and $p_y = u_y \cup d_y$ intersect exactly once.

If xy be an edge of G that belongs to $G(D)$ and not to $G(U)$, we consider the indices of the triangles of $\mathcal{U}$ according to the tip ordering on H_1, that is the ordering of the points $\{(m_x, 1) \mid x \in D\}$ and do the analog analysis.

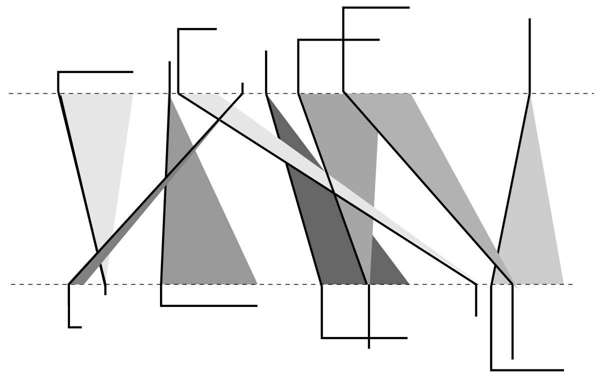

Figure 6.9: The thickly drawn lines form the pseudosegments representing the vertices of PI*-graph G given by a PI*-representation

Finally consider an edge xy of G that is an edge of $G(U)$ and $G(D)$. In this case, the Jordan arcs u_x and u_y, representing x and y in $\mathcal{G}_U$, intersect in $b_x \subset u_x$ and $b_y \subset u_y$. Recall that b_x and b_y are the common parts of u_x and d_x, and of u_y and d_y respectively. Hence, the Jordan arcs d_x and d_y, representing x and y in $\mathcal{G}_D$ intersect in the same point of $b_x \subset d_x$ and $b_y \subset d_y$. As $\mathcal{G}_U$ and $\mathcal{G}_D$ are pseudosegment representations, there is no further intersection of the corresponding arcs within each pseudosegment representation. Thus, $p_x = u_x \cup d_x$ and $p_y = u_y \cup d_y$ intersect exactly once in $b_x \cap b_y$ and have no further intersections.

Hence the set $\mathcal{G} := \{p_x \mid x \in X\}$ is a pseudosegment representation of G; an example of such a pseudosegment representation is given in Figure 6.9. $\square$

6.4 Trapezoid graphs and II_1-graphs

Finally we come to considering trapezoid graphs, that are cocomparability graphs of posets of interval dimension two. Formally, let H and L be two parallel lines such that $\{I_{01}, ..., I_{0n}\}$ and $\{I_{11}, ..., I_{1n}\}$ are families of intervals of H and L respectively. Each $i \in \{1, ..., n\}$ corresponds to a trapezoid R_i with parallel sides I_{0i} and I_{1i}. Then the intersection graph of such a family of trapezoids is a *trapezoid graph* [51].

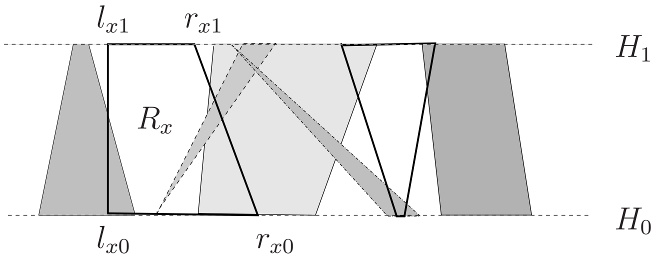

Figure 6.10: The elements of X that are comparable to x in P lie strictly to the left or to the right of R_x.

6.4.1 A failed attempt

In the previous section we combined pseudosegment representations of permutation and interval graphs to represent point-interval and PI*-graphs, generalizations of the latter two graphs, as pseudosegment graphs. As trapezoid graphs generalize PI*-graphs, it is tempting to look for a modification of the pseudosegment representations of PI*-graphs to construct pseudosegment representations of trapezoid graphs. Such a modification could be as follows:

Let $G = (X, E)$ be an arbitrary trapezoid graph. Then we can choose a minimal realizer $\mathcal{R} = \{\mathcal{I}_0, \mathcal{I}_1\}$ of the corresponding poset and embed $\mathcal{I}_0$ onto H_0 and $\mathcal{I}_1$ onto H_1 such that $I_{x0} := [(l_{x0}, 0), (r_{x0}, 0)]$ and $I_{x1} := [(l_{x1}, 1), (r_{x1}, 1)]$ denote the intervals of $x \in X$ on H_0 and H_1 respectively. This is done without changing the intersection relations. Furthermore we require that no two different endpoints of intervals on H_0 and H_1 are the same.

Similarly to the previous construction we choose two orders of the elements of X. Both result from the linear order of the left endpoints of the intervals on H_0 and H_1. That is for every element $x \in X$ there is a pair of indices (i_{x0}, i_{x1}) resulting from the position of I_{x0} and I_{x1} in the respective left endpoint orderings on H_0 and H_1 respectively; then $i_{xj} < i_{yj}$ if and only if $l_{xj} < l_{yj}$ for $j \in \{0, 1\}$. Recall the use of the tip ordering from the previous section. With this in mind we define a Jordan arc p_x for every $x \in X$ as follows

$$\begin{aligned} p_x &:= [(l_{x0}, -i_{x1}), (r_{x0}, -i_{x1})] \cup [(l_{x0}, -i_{x1}), (l_{x0}, 0)] \\ &\cup [(l_{x0}, 0), (l_{x1}, 1)] \\ &\cup [(l_{x1}, 1), (l_{x1}, 1 + i_{x0})] \cup [(l_{x1}, 1 + i_{x0}), (r_{x1}, 1 + i_{x0})]. \end{aligned}$$

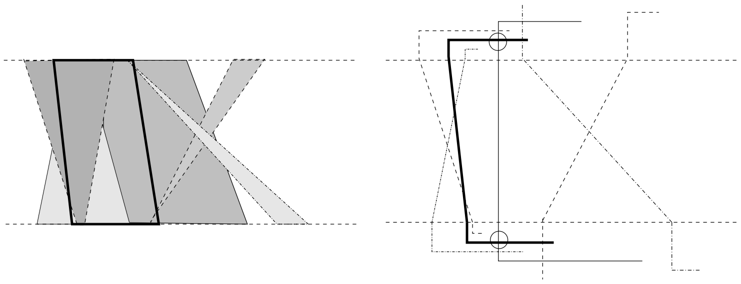

Figure 6.11: Jordan arcs obtained from the trapezoids on the left-hand side contain a pair of elements with more than one crossing point.

Note that i_{x0} is used for the part of pseudosegment p_x that lies above H_1 and i_{x1} for the part below H_0. It is easy to see that every intersection of two such Jordan arcs is a crossing as no two corners of the trapezoids are the same; see Figure 6.11 for an example.

Unfortunately this does not yield a pseudosegment representation from an arbitrary trapezoid representation. Figure 6.11 shows an example of a set of trapezoids for which the latter modification generates multiple intersections between the Jordan arcs defined as above. Nevertheless this set of trapezoids motivates to consider the following subset of trapezoid graphs.

Definition 6.7. Let H and L be two parallel lines such that $\{I_{01}, ..., I_{0n}\}$ and $\{I_{11}, ..., I_{1n}\}$ are families of intervals of H and L respectively. If it holds for every pair of elements $i, j \in \{1, ..., n\}, i \neq j$ that either $I_{0i} \cap I_{0j} = \emptyset$ or $I_{1i} \cap I_{1j} = \emptyset$, then the intersection graph G of the respective family of trapezoids $\{R_1, ..., R_n\}$ is an II_1-*graph*, and $\{R_1, ..., R_n\}$ is an II_1-*representation.*

6.4.2 II$_1$-graphs are pseudosegment graphs

Proposition 6.8. Every II$_1$-graph has a pseudosegment representation.

Proof. Let $G = (X, E)$ be an arbitrary II$_1$-graph. To prove Proposition 6.8 set $\mathcal{G} := \{p_x \mid x \in X\}$ where every p_x is obtained from an II$_1$-representation as defined in Section 6.4.1. To show that $\mathcal{G}$ is a pseudosegment representation of G consider an arbitrary pair of vertices x, y of X and the corresponding Jordan arcs p_x and p_y. Without loss of generality we assume that $l_{x1} < l_{y1}$.

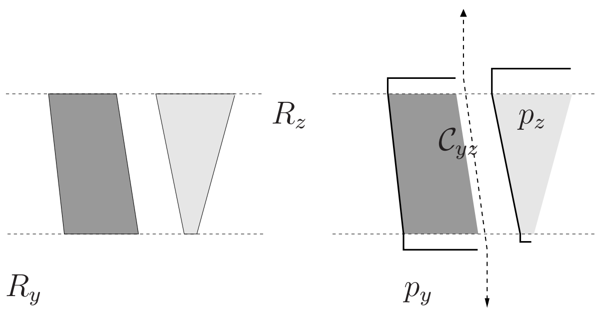

Figure 6.12: Jordan arcs representing comparable elements of X can be separated.

If x and y are not adjacent in G, then they are comparable in P. In this case, trapezoids R_x and R_y are disjoint, so it holds that $r_{x0} < l_{y0}$ and $r_{x1} < l_{y1}$. Then arcs p_x and p_y lie on different sides of the curve

$$\mathcal{C}_{xy} = \big((r_{x1}+\epsilon, \infty), (r_{x1}+\epsilon, 1)]\cup[(r_{x1}+\epsilon, 1), (r_{x0}+\epsilon, 0)]\cup[(r_{x0}+\epsilon, 0), (r_{x0}+\epsilon, \infty)\big).$$

for some small real number $\epsilon > 0$. Thus p_x and p_y are disjoint. Figure 6.13 illustrates the case where p_y is separated from p_z by the dotted curve $\mathcal{C}_{yz}$.

Now assume that x and y are adjacent in G. If $l_{y0} < l_{x0}$, then p_x and p_y intersect between H_0 and H_1 as $l_{x1} < l_{y1}$; this is illustrated by the Jordan arcs p_z and p_w on the right-hand side of Figure 6.13. In this case it holds that $i_{y0} < i_{x0}$ and $i_{x1} < i_{y1}$. Thus the definition of the arcs p_x and p_y implies that there is no further intersection between p_x and p_y as in the proof of Proposition 6.5.

Now assume that $l_{x0} < l_{y0}$. Since $l_{x1} < l_{y1}$, Jordan arcs p_x and p_y do not intersect between H_0 and H_1. As x and y are adjacent in G, the corresponding trapezoids R_x and R_y of the given II$_1$-representation intersect. Without loss

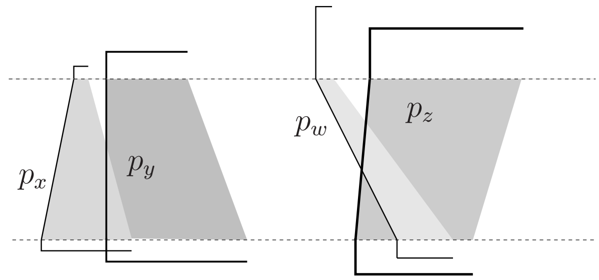

Figure 6.13: Intersections of Jordan arcs representing adjacent elements x and y, and w and z of G.

of generality assume that $[l_{x1}, r_{x1}] \cap [l_{y1}, r_{y1}] \neq \emptyset$ on H_1, that is $l_{x1} < l_{y1} < r_{x1}$. As G is an II_1-graph, it follows that $[l_{x0}, r_{x0}] \cap [l_{y0}, r_{y0}] = \emptyset$. In this case we easily calculate $(l_{y1}, 1 + i_{x0})$ as point of intersection of p_x and p_y. Again the definition of the Jordan arcs p_x and p_y, and the analysis of the proof of Proposition 6.5 imply that there is no intersection of p_x and p_y below H_1 as $r_{x0} < l_{y0}$ on H_0.

Thus the set $\mathcal{G} = \{p_x \mid x \in X\}$ is a pseudosegment representation of G. As G was chosen arbitrarily, it follows that every II_1-graph has a pseudosegment representation. $\square$

6.4.3 PI-graphs and II_1-graphs*

The definition of II_1-graphs may give rise to the question about the relation of PI^*-and II_1-graphs. In the following we will show that these graphs constitute different classes, neither containing the other. A possibility of illustrating the differences between PI^*-graphs and II_1-graphs is by *box embeddings* of the corresponding posets. Let $P = (X, <_P)$ be a poset and let $\mathcal{I} = \{\mathcal{I}_1, ..., \mathcal{I}_t\}$ be an interval realizer of P with $I_{xj} = [l_{xj}, r_{xj}] \in \mathcal{I}_j$ for all $j \in \{1, ..., t\}$. Assign each element $x \in X$ to the box $B_x = \Pi_{j=1}^{t}[l_{xj}, r_{xj}]$. The resulting set of boxes is a *box embedding* of P [23]. Every box of such a box embedding is uniquely determined by its lower left corner $(l_{x1}, ..., l_{xt})$ and its upper right corner $(r_{x1}, ..., r_{xt})$ so that $x <_P y$ if and only if $(r_{x1}, ..., r_{xt})$ is smaller than $(l_{y1}, ..., l_{yt})$ in every component.

Observation 6.9. *P has a box embedding consisting of horizontal segments, vertical segments and points if and only if the cocomparability graph of P is a PI^*-graph.*

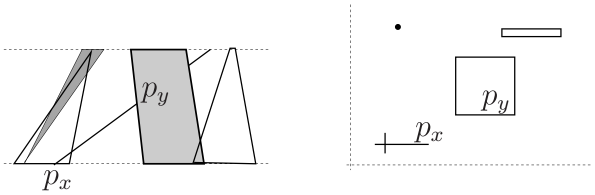

Figure 6.14: A box representation of a poset P of interval dimension two and a trapezoid representation of the cocomparability graph of P.

P has a box embedding consisting of disjoint boxes if and only if the cocomparability graph of P is an II_1-graph.

With this in mind we will construct an II_1-graph that is not a PI^*-graph and a PI^*-graph that is not an II_1-graph. First we will construct a box embedding of some poset $P[k]$ so that the cocomparability graph $H[k]$ of $P[k]$ requires a "grid-like" trapezoid representation. Then we will choose an II_1-graph and a PI^*-graph, each containing $H[k]$ as subgraph. By this, we can describe the placement of any trapezoid representing an element not in $H[k]$ with respect to the grid induced by $H[k]$. The resulting conditions on the trapezoids will then imply that each of the two graphs chosen belongs to one of the classes but not to both.

A trapezoid graph $H[k]$ with a "grid-like" trapezoid representation

Let $k \in \mathbb{N}$, $k \geq 3$ and let $X[k] = \{a_1, ..., a_k, c_1, ..., c_k, b_1, ..., b_k, d_1, ..., d_k\}$. Then we define $P[k] = (X[k], <_P)$ as the poset on $X[k]$ with the following comparabilities, illustrated in Figure 6.15:

- $a_1 <_P a_2 <_P ... <_P a_k <_P c_1 <_P c_2 <_P ... <_P c_k <_P d_k$,
- $a_1 <_P b_1 <_P b_2 <_P ... <_P b_k <_P d_1 <_P d_2 <_P ... <_P d_k$,
- $b_i <_P c_j$ with $j \in \{i+1, ..., k\}$ for every $i \in \{1, ..., k-1\}$, and
- $a_r <_P d_s$ with $r \in \{1, ..., s+1\}$ for every $s \in \{1, ..., k-1\}$.

Let $H[k]$ denote the cocomparability graph of $P[k]$ and consider an arbitrary trapezoid representation $\mathcal{H}_k$ of $H[k]$. We can assume that $\mathcal{H}_k$ is embedded between lines H_0 and H_1 such that no two trapezoids share a corner.

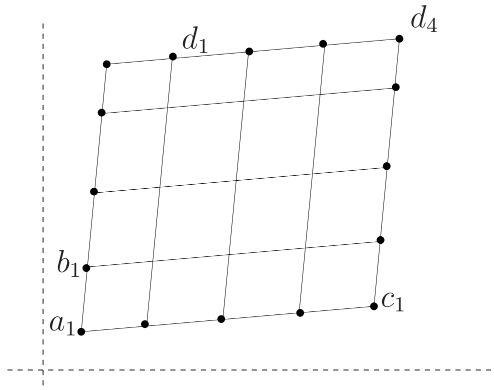

Figure 6.15: A diagram illustrating the comparabilities in $P[4]$.

Let R_x denote the trapezoid of x in $\mathcal{H}_k$ and let $I_{x0} = [(l_{x0}, 0), (r_{x0}, 0)]$ and $I_{x1} = [(l_{x1}, 1), (r_{x1}, 1)]$ denote the intersections of R_x with H_0 and H_1 respectively. Then, the trapezoids corresponding to $a_1, ..., a_k, c_1, ..., c_k, d_k$ are disjoint trapezoids that appear along H_0 in the order of the chain $(a_1, ..., a_k, c_1)$, $(c_1, ..., c_k, d_k)$. With respect to these trapezoids we can describe the placement of the trapezoids representing elements $b_1, ..., b_k$ and $d_1, ..., d_{k-1}$.

Claim. For every $i \in \{2, ..., k-1\}$ one of the two statements is true

- $I_{b_i0} \subset [(l_{c_{i-1}0}, 0), (l_{c_{i+1}0}, 0)]$ and $I_{b_i1} \subset [(r_{a_11}, 1), (r_{a_21}, 1)]$,
- $I_{b_i0} \subset [(r_{a_10}, 0), (r_{a_20}, 0)]$ and $I_{b_i1} \subset [(l_{c_{i-1}1}, 1), (l_{c_{i+1}1}, 1)]$.

For every $j \in \{2, ..., k-1\}$ set $c_1 := a_{k+1}$ and $c_2 := a_{k+2}$, then one of the two statements is true

- $I_{d_j0} \subset [(l_{c_k0}, 0), (l_{d_k0}, 0)]$ and $I_{d_j1} \subset [(r_{a_{j+1}1}, 1), (r_{a_{j+3}1}, 1)]$,
- $I_{d_j0} \subset [(r_{a_{j+1}0}, 0), (r_{a_{j+3}0}, 0)]$ and $I_{d_j1} \subset [(l_{c_k1}, 1), (l_{d_k1}, 1)]$.

Proof. Consider an arbitrary trapezoid representation $\mathcal{H}_k$ of $H[k]$. Here, the trapezoids of $\mathcal{H}_k$ representing the elements $a_1, ..., a_k$,$c_1, ..., c_k, d_k$ are disjoint as $(a_1, ..., a_k$,$c_1, ..., c_k, d_k)$ is a chain of P; they appear along H_0 and H_1 in the order of the chain. We will now analyze the placement of the trapezoid representing b_i with $i \in \{2, ..., k-1\}$. The analog analysis gives the stated conditions on intervals I_{d_j0} and I_{d_j1} for $j \in \{2, ..., k-1\}$.

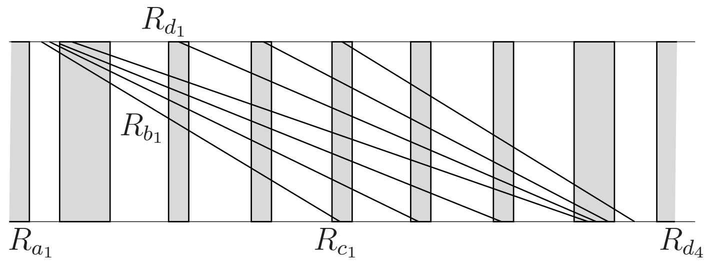

Figure 6.16: A "grid-like" trapezoid representation of the graph $H[4]$.

Recall that b_j is incomparable to $a_2, ..., a_k$ for every $j \in \{1, ..., k\}$. Hence, the trapezoid representing b_i has to intersect each of the trapezoids representing the elements $a_2, ..., a_k$. Thus it holds that either $l_{b_{i+1}0} < r_{a_2 0}$ or $l_{b_{i+1}1} < r_{a_2 1}$. In either case we can reflect the trapezoid representation $\mathcal{H}_k$ of $H[k]$ at line $H_{0.5} = \{(x, 0.5) | x \in \mathbb{R}\}$ and obtain the respective other case, so let us assume that $l_{b_{i+1}1} < r_{a_2 1}$.

Since every $b_i <_P b_{i+1}$, the trapezoid of $\mathcal{H}_k$ representing b_i has to lie to the left of the trapezoid representing b_{i+1}, hence $r_{b_i 1} < l_{b_{i+1}1} < r_{a_2 1}$. As $a_1,_P b_j$ for all $j \in \{1, ..., k\}$, it holds that

$$I_{b_i 1} = [(l_{b_i 1}, 1), (r_{b_i 1}, 1)] \subset [(r_{a_1 1}, 1), (r_{a_2 1}, 1)].$$

In addition, b_j is incomparable to $c_1, ..., c_j$ for all $j \in \{1, ..., k\}$. Thus, it follows that $l_{c_j 0} < r_{b_j 0}$.

Since $b_{i-1} <_P b_i <_P b_{i+1}$, the trapezoid representing b_i has to lie to the right of the trapezoid representing b_{i-1} and to the left of the trapezoid representing b_{i+1}. This implies that $l_{c_{i-1}0} < l_{b_i 0} < r_{b_i 0}$. Since $b_i <_P c_{i+1}$, we have $r_{b_i 0} < l_{c_{i+1}0}$, and it holds that

$$I_{b_i 0} = [(l_{b_i 0}, 0), (r_{b_i 0}, 0)] \subset [(l_{c_{i-1}0}, 0), (l_{c_{i+1}0}, 0)].$$

A trapezoid representation of $H[4]$ is given in Figure 6.15. □

Geometric restrictions on trapezoid representations of a II_1-graph

Now we come to presenting a II_1-graph that is not a PI^*-graph. To do so let $P_1 = (X_1, <_1)$ be the poset on ground set $X_1 := X[4] \cup \{B\}$ such that the comparabilities of P_1 with respect to $X[4]$ are the same as in $P[4]$ and, in addition,

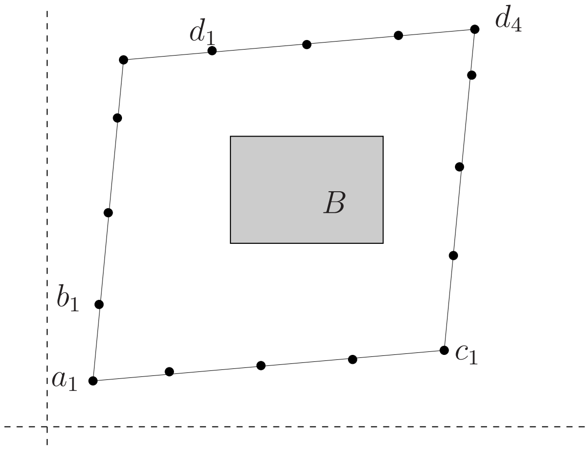

Figure 6.17: A box embedding of a poset corresponding to the II_1-graph G_1.

- $a_2 <_1 B <_1 d_3$ and $b_1 <_1 B <_1 c_4$.

A box embedding of P_1 is given in Figure 6.17. As it consists of disjoint boxes, the cocomparability graph G_1 of P_1 is an II_1-graph.

Proposition 6.10. The II_1-graph G_1 is not a PI^*-graph.

Proof. Consider an arbitrary trapezoid representation $\mathcal{R}_1$ of G_1. By construction, $H[4] \subset G_1$, so that the set of trapezoids of $\mathcal{R}_1$ representing $H[4]$ fulfills the conditions of the previous claim. As in the proof of this claim, let us assume that $l_{b_4 1} < r_{a_2 1}$.

Since $a_2 <_1 B <_1 d_3$, it holds that $r_{a_2 1} < l_{B1} < r_{B1} < l_{d_3 1}$; as $b_1 <_1 B <_1 c_4$ it follows that $r_{b_1 0} < l_{B0} < r_{B0} < l_{c_4 0}$.

As B is incomparable to a_3 and d_2, it follows that $l_{B1} < r_{a_3 1}$ and $r_{B1} > l_{d_2 1}$. As $a_3 <_1 d_2$, it holds that $r_{a_3 1} < l_{d_2 1}$, hence, $[(r_{a_3 1}, 1), (l_{d_2 1}, 1)] \subset [(l_{B1}, 1), (r_{B1}, 1)] = I_{B1}$.Thus, interval I_{B1} is nondegenerate, that is I_{B1} is not a point.

As B is incomparable to b_2 and c_3, it follows that $l_{B0} < r_{b_2 0}$ and $r_{B0} > l_{c_3 0}$. As $b_2 <_1 c_3$, it holds that $r_{b_2 0} < l_{c_3 0}$, hence, $[(r_{b_2 0}, 0), (l_{c_3 0}, 0)] \subset [(l_{B0}, 0), (r_{B0}, 0)] = I_{B0}$. Thus, interval I_{B0} is nondegenerate.

Thus, the trapezoid representing B is not a triangle. As $\mathcal{R}_1$ was chosen arbitrarily it follows that G_1 is not a PI^*-graph. $\square$

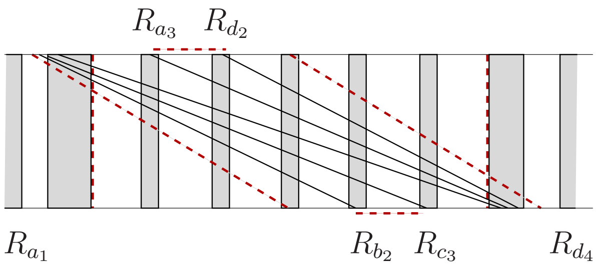

Figure 6.18: The trapezoids of elements of $X[4]$ restrict the placement of a trapezoid representing B in $\mathcal{R}_1$.

Geometric restrictions on trapezoid representations of a PI-graph*

Similar to the construction of G_1 we will construct a PI*-graph that is not a II_1-graph. Let $P_2 = (X_2, <_2)$ be the poset on ground set $X_2 := X[4] \cup \{V, H\}$ such that the comparabilities of P_2 with respect to $X[4]$ are the same as in $P[4]$ and, in addition,

(1) $a_3 <_2 V <_2 d_2$ and $b_1 <_2 V <_2 c_4$, and

(2) $a_2 <_2 H <_2 d_3$ and $b_2 <_2 H <_2 c_3$.

A box embedding of P_2 is given in Figure 6.19; here all boxes except for V and H are points, V is a vertical and H an horizontal segment. Thus, the cocomparability graph G_2 of P_2 is a PI*-graph.

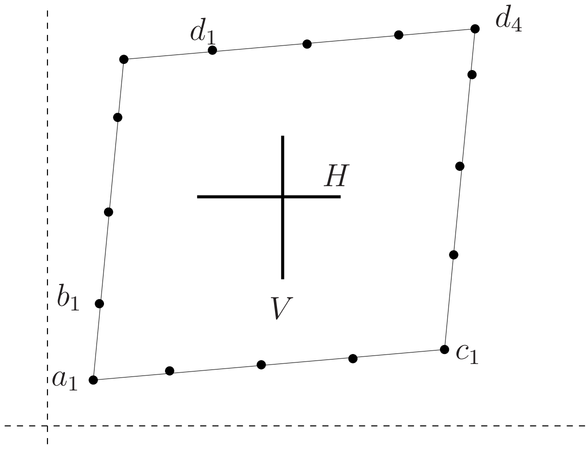

Figure 6.19: A box embedding of a poset corresponding to the PI*-graph G_2.

Proposition 6.11. The PI*-graph G_2 is not a II_1-graph.

Proof. Consider an arbitrary trapezoid representation $\mathcal{R}_2$ of G_2. Again, graph $H[4]$ is a subgraph of G_2, so that the set of trapezoids of $\mathcal{R}_2$ representing $H[4]$ fulfills the conditions of the previous claim. As in the proof of this claim, let us assume that $l_{b_4 1} < r_{a_2 1}$.

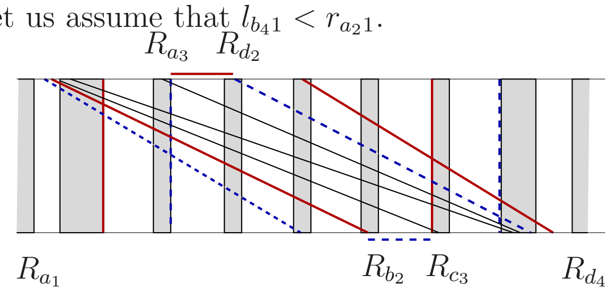

Figure 6.20: The thick and thick dotted lines restrict the placement of the trapezoids representing H and V, respectively, in $\mathcal{R}_2$.

As before we deduce from (1) that $r_{a_3 1} < l_{V1} < r_{V1} < l_{d_2 1}$ and $r_{b_1 0} < l_{V0} < r_{V0} < l_{c_4 0}$. And (2) implies that $r_{a_2 1} < l_{H1} < r_{H1} < l_{d_3 1}$ and $r_{b_2 0} < l_{H0} < r_{H0} < l_{c_3 0}$.

Since V is incomparable to b_2 and c_3, it follows that $l_{V0} < r_{b_2 0}$ and $r_{V0} > l_{c_3 0}$. As $b_2 <_2 H <_2 c_3$, we have that $I_{H0} \subset I_{V0}$.

Since H is incomparable to a_3 and d_2, it follows that $l_{H1} < l_{d_2 1}$ and $r_{H1} > r_{a_3 1}$. As $a_3 <_2 L_V <_2 d_2$, we have that $I_{V1} \subset I_{H1}$.

Thus, the trapezoids representing V and H intersect on H_0 and also on H_1. As $\mathcal{R}_2$ was chosen arbitrarily it follows that G_2 is not an II_1-graph. $\square$

6.5 Summary

Starting with interval graphs we successively built pseudosegment representations of point-interval graphs, PI*-graphs and II_1-graphs. As sketched at the beginning of Section 6.4, the method used at this cannot be extended directly to represent arbitrary trapezoid graphs as pseudosegment graphs. Thus, we are left with the following question.

Question 6.12. Does every cocomparability graph of a poset of interval dimension two have a pseudosegment representation?

Symbol Index

Index

Bibliography

[1] P. Agarwal and J. Pach, *Combinatorial geometry*, Wiley-Interscience, 1995.

[2] M. Aigner, *Graphentheorie- Eine Entwicklung aus dem 4-Farben Problem*, Teubner Studienbücher: Mathematik, Teubner, 1984.

[3] C. Berge, *Graphs and hypergraphs*, North-Holland, Amsterdam, 1973, ch. 16.

[4] M. Bodirsky, C. Dangelmayr, and J. Kára, *Representing series-parallel graphs as intersection graphs of line segments in three directions*, in Proc. of the 3rd Asian Applied Comput. Conference, 2007.

[5] J. Boland and C. Lekkerkerker, *Representation of finite graphs by a set of intervals on the real line*, Fund. Math. **51**, no. 51 (1962), pp. 45–64.

[6] K. Booth and G. Leuker, *Linear algorithms to recognize interval graphs and test for the consecutive ones property*, in Proc. of the 7th ACM Symp. Theory of Comput., 1975, pp. 255–265.

[7] A. Brandstädt, V. Le, and J. Spinrad, *Graph classes: a survey*, SIAM Monographs on Discrete Mathematics and Applications, 1999.

[8] J. Chalopin and D. Gonçalves, *Every planar graph is the intersecion graph of segments in the plane.* accepted to STOC, 2009.

[9] J. Chalopin, D. Gonçalves, and P. Ochem, *Planar graphs are in* 1-*string*, in Proc. of the 18th annual ACM-SIAM Symp. on Discr. Alg., SODA, 2007, pp. 609–617.

[10] D. Corneil and P. Kamula, *Extensions of permutation and interval graphs*, Congres. Numer. , no. 58 (1987), pp. 267–275.

[11] C. Dangelmayr and S. Felsner, *Chordal graphs as intersection graphs of pseudosegments*, in Proc. of Graph Drawing 2006, lncs 4372, Springer Verlag, 2006.

[12] C. Dangelmayr, S. Felsner, and W. Trotter, *Intersection graphs of pseudosegments: Chordal graphs.* submitted.

[13] N. de Castro, F. J. Cobos, J. C. Dana, A. Márquez, and M. Noy, *Triangle-free planar graphs as segment intersection graphs*, J. Graph Alg. and Appl. (2002).

[14] H. de Fraysseix and P. O. de Mendez, *Contact and intersection representations*, Lecture Notes in Computer Science **3383** (2005), pp. 217–227.

[15] H. de Fraysseix, P. O. de Mendez, and J. Pach, *Representations of planar graphs by segments*, Coll. Math. Soc. János Bolyai, Intuitive Geom., Szeged (Hungary) (1991).

[16] R. Diestel, *Graph theory*, Springer, 2000.

[17] P. Duchet, *Classical perfect graphs. an introduction with emphasis on triangulated and interval graphs*, Ann. Discr. Math. **21** (1984), pp. 67–96.

[18] R. Duffin, *Topology of series-parallel networks*, J. Math. Analys. Appl. **10** (1965), pp. 303–318.

[19] B. Dushnik and E. Miller, *Partially ordered sets*, Am. J. Math. (1941).

[20] G. Ehrlich, S. Even, and R. E. Tarjan, *Intersection graphs of curves in the plane*, J. Combin. Theory Ser. B (1976).

[21] S. Even, A. Lempl, and A. Pnueli, *Transitive orientations of graphs and identification of permutation graphs*, Canad. J. Math. (1971).

[22] S. Felsner, *personal communication.* September 2009.

[23] S. Felsner, *Interval orders: Combinatorial structure and algorithms*, PhD thesis, Technische Universität, Berlin, 1992.

[24] S. Felsner, *Geometric graphs and arrangements*, Vieweg, 2004.

[25] S. Felsner and H. Weil, *Sweeps, arrangements and signotopes*, Discr. Appl. Math. **109** (2001), pp. 67–94.

[26] D. Fulkerson and O. Gross, *Incidences matrices and interval graphs*, Pacif. J. Math. **15** (1965), pp. 835–855.

[27] M. Garey and D. Johnson, *Computers and intractability: A guide to the theory of NP-completeness*, Series of Books in the Math. Sci., W.H.Freeman, 1979.

[28] F. Gavril, *The intersection graphs of subtrees in trees are exactly the chordal graphs*, J. Combin. Theory Ser. B (1974).

[29] F. Gavril, *A recognition algorithm for the intersection graphs of paths in trees*, Discr. Math. (1978).

[30] P. Gilmore and A. Hoffman, *A characterization of comparability graphs and interval graphs*, Canad. J. Math. (1964).

[31] M. Golumbic, *Algorithmic graph theory and perfect graphs*, Academic Press, 1980.

[32] M. Golumbic, *Algorithmic graph theory and perfect graphs*, Annals of Discr. Math., second edition ed., 2004.

[33] M. Golumbic, D. Rotem, and J. Urrutia, *Comparability graphs and intersection graphs*, Discr. Math. (1983).

[34] J. Goodman, *Proof of a conjecture of Burr, Grünbaum and Sloane*, Discr. Math **32** (1980), pp. 27–35.

[35] J. Goodman and J. O'Rourke, *Handbook of discrete and computational geometry*, Chapman and Hall,CRC, 2004.

[36] R. L. Graham, *Problem 1*, in In Open Problems at 5th Hungarian Coll. on Combin., 1976.

[37] B. Grünbaum, *Arrangements and spreads*, no. 10 in Regional Conference Series in Mathematics, Amer. Math. Soc., 1972.

[38] G. Hajós, *Über eine Art von Graphen*, Intern. Math. Nachr. (1957). Problem 65.

[39] I. B.-A. Hartman, I. Newman, and R. Ziv, *On grid intersection graphs*, Discr. Math. **87** (1991), pp. 41–52.

[40] J.Kleinberg and E. Tardos, *Algorithm design*, Pearson International Edition, 2006.

[41] D. E. Knuth, *Axioms and hulls*, Lecture Notes Comput. Sci. 606, Springer-Verlag, 1992.

[42] P. Koebe, *Kontakprobleme der konformen Abbildungen*, Berichte über die Verhandlungen der Sächsischen Akademie der Wissenschaften 88, Math.-Physikal. Klasse, Leipzig, 1936.

[43] J. Kratochvíl, *Independent set and clique problem in intersection defined classes of graphs*, Comment. Math. Univ. Carolin **31** (1990), pp. 85–93.

[44] J. Kratochvíl, *String graphs II: recognizing string graphs is NP-hard*, J. Combin. Theory Ser. B **52** (1991), pp. 67–78.

[45] J. Kratochvíl, *A special planar satisfiability problem and a consequence of its NP-completeness*, Discr. Appl. Math. **52** (1994), pp. 233–252.

[46] J. Kratochvíl and J. Matoušek, *NP-hardness results for intersection graphs*, Comment. Math. Univ. Carolin **30** (1989), pp. 761–773.

[47] J. Kratochvíl and J. Matoušek, *Intersection graphs of segments*, J. Combin. Theory Ser. B **62** (1994), pp. 289–315.

[48] F. Levi, *Die Teilung der projektiven Ebene durch Geraden oder Pseudogeraden*, Ber. Math. Phys. Kl. Sächs. Akad. Wiss. **78** (1926), pp. 256–267.

[49] E. Marczewski, *Sur deux propriètés des classes d'ensembles*, Fund. Math. , no. 33 (1945), pp. 303–307.

[50] J. Matoušek, *Lectures on discrete geometry*, Graduate Texts in Mathematics 212, Springer-Verlag, 2002.

[51] T. McKee and F. McMorris, *Topics in intersection graph theory*, SIAM Monographs on Discr. Math. and Appl., 1999.

[52] M.Middendorf and F.Pfeiffer, *The max clique problem in classes of string graphs*, Discr. Math. **108**, no. 108 (1992), pp. 365–372.

[53] B. Mohar and C. Thomassen, *Graphs on surfaces*, Johns Hopkins University Press, 2001.

[54] C. Monma and V. K. Wei, *Intersection graphs of paths in a tree*, J. Combin. Theory Ser. B (1986).

[55] J. Pach and G. Tóth, *Recognizing string graphs is decidable*, Discr. and Comput. Geom. **28** (2002), pp. 593–606.

[56] G. Ringel, *Teilung der Ebene durch Geraden oder topologische Geraden*, Math. Z. **64** (1956), pp. 79–102.

[57] F. Roberts, *Discrete mathematical models, with applications to social, biological and environmental problems*, Prentice-Hall, Englewood Cliffs, NJ., 1976.

[58] M. Schaefer, E. Sedgwick, and D. Štefankovič, *Recognizing string graphs in NP*, J. Comput. Syst. Sci **2** (2003), pp. 365–380.

[59] M. Schaefer and D. Štefankovič, *Decidability of string graphs*, J. Comput. Syst. Sci **68** (2004), pp. 319–334.

[60] L. Scharf and M. Scherfenberg, *Inducing polygons of line arrangements*, in Proc. of the 19th Internat. Symp. on Alg. and Comput. (ISAAC 2008), S.-H. Hong, H. Nagamochi, and T. Fukunaga, eds., Lecture Notes in Computer Science 5369, 2008, pp. 508–520.

[61] E. R. Scheinerman, *Intersection classes and multiple intersection parameters of graphs*, PhD thesis, Princeton University, 1984.

[62] A. Schrijver, *Combinatorial optimization- polyhedra and efficiency*, Springer, 2003.

[63] F. W. Sinden, *Topology of thin RC-circuits*, Bell System Tech. J. (1966).

[64] R. Tarjan and M. Yannakis, *Simple linear-time algorithms to test chordality of graphs, test acyclicity of hypergraphs, and selectively reduce acyclic hypergraphs*, SIAM J. Comput. **13** (1984), pp. 566–579.

[65] O. Veblen, *Theory on plane curves in non-metrical analysis situs*, Transactions of the Amer. Math. Soc. **6**, no. 2(1) (1905), pp. 83–98.

[66] J. R. Walter, *Representations of rigid cycle graphs*, PhD thesis, Wayne State University, Detroit, 1972.

[67] G. Wegner, *Eigenschaften der Nerven homologisch-einfacher Familien im n-dimensionalen euklidischen Raum*, PhD thesis, Universität Göttingen, 1967.

[68] D. West, *Open problems*, SIAM J. Discr. Math. Newsletter **2**, no. 1 (1991), pp. 10–12.

[69] D. West, *Introduction to graph theory*, Prentice Hall, 2001.

Lebenslauf

Aus Gründen des Datenschutzes ist in der Online-Version der Arbeit kein Lebenslauf enthalten.

Eidestattliche Erklärung

Hiermit erkläre ich an Eides statt, die vorliegende Arbeit selbstständig verfasst zu haben. Alle verwendeten Hilfsmittel sind aufgeführt. Des Weiteren versichere ich, dass diese Arbeit nicht in dieser oder ähnlicher Form an einer weiteren Universität im Rahmen eines Prüfungsverfahrens eingereicht wurde.

Cornelia Dangelmayr

Zusammenfassung

In der vorliegenden Arbeit werden graphentheoretische Eigenschaften von Durchschnittsgraphen von Pseudosegmenten, auch Pseudosegmentgraphen genannt, bestimmt. Dabei verstehen wir unter einer Menge von Pseudosegmenten eine endliche Menge von Jordankurven in der Euklidischen Ebene, für die gilt, dass sich je zwei Kurven in höchstens einem Punkt treffen, der entweder ein Kreuzungspunkt oder ein Endpunkt einer Kurve ist.

Pseudosegmentgraphen gehören zur Klasse der Kurvengraphen, die 1966 von Sinden eingeführt wurden [63]. Bekannte Beispiele von Kurvengraphen sind chordale und planare Graphen, Unvergleichbarkeitsgraphen und Segmentgraphen.

Im Jahre 1984 stellte Scheinerman die Vermutung auf, dass jeder planare Graph ein Segmentgraph ist [61]. Diese Vermutung erregte das Interesse vieler Forscher [13, 14, 15, 39], konnte aber erst im Jahr 2009 bestätigt werden [8]. Eine weitergehende Vermutung von West aus dem Jahre 1991 besagt, dass jeder planare Graph eine Segmentdarstellung besizt, in der die Segmente in höchstens vier Richtungen liegen [68]. Dies ist weiterhin offen.

Diese Vermutungen veranlassten uns, Teilklassen von planaren Graphen, insbesondere serien-parallele Graphen, zu betrachten. Unser Ergebnis zeigt, dass jeder serien-parallele Graph eine Segmentdarstellung besitzt, in der die Segmente in höchstens drei Richtungen liegen.

Zur Unterscheidung von Pseudosegment- und Segmentdarstellungen betrachten wir streckbare und nichtstreckbare Arrangements von Pseudogeraden. Darauf aufbauend leiten wir eine Konstruktion her, die Pseudosegmentgraphen erzeugt, die keine Segmentgraphen sind.

Im Anschluss beschäftigen wir uns mit der Beziehung von chordalen und Pseudosegmentgraphen. Zum einen zeigen wir, dass Pfadgraphen Pseudosegmentgraphen sind. Und zum anderen stellen wir chordale Graphen vor, die keine Pseudosegmentgraphen sind; diese lassen sich zudem zur Beschränkung der gemeinsame Teilklasse von chordalen und Pseudosegmentgraphen verwenden.

Im letzten Teil der Arbeit werden wir Trapezgraphen, eine Teilklasse von Unvergleichbarkeitsgraphen, betrachten und Pseudosegmentdarstellungen von Intervalgraphen, Punkt-Interval-Graphen und zwei weiteren Typen von Trapezgraphen konstruieren.